Electronic Theses and Dissertations   Theses, Dissertations, and Major Papers

1992

Bending stress concentration for spur gears.

SyedShoeb I. Nagamiyan
University of Windsor

NOTICE

AVIS

The quality of this microform is heavily dependent upon the quality of the original thesis submitted for microfilming. Every effort has been made to ensure the highest quality of reproduction possible.

La qualité de cette microforme dépend grandement de la qualité de la thèse soumise au microfilmage. Nous avons tout fait pour assurer une qualité supérieure de reproduction.

If pages are missing, contact the university which granted the degree.

S'il manque des pages, veuillez communiquer avec l'université qui a conféré le grade.

Some pages may have indistinct print especially if the original pages were typed with a poor typewriter ribbon or if the university sent us an inferior photocopy.

La qualité d'impression de certaines pages peut laisser à désirer, surtout si les pages originales ont été dactylographiées à l'aide d'un ruban usé ou si l'université nous a fait parvenir une photocopie de qualité inférieure.

Reproduction in full or in part of this microform is governed by the Canadian Copyright Act, R.S.C. 1970, c. C-30, and subsequent amendments.

La reproduction, même partielle, de cette microforme est soumise à la Loi canadienne sur le droit d'auteur, SRC 1970, c. C-30, et ses amendements subséquents.

Canada

BENDING STPESS CONCENTRATION FCR SPUR GEARS

A Thesis Submitted To The

Faculty Of Graduate Studies And Research

Through The Department Of

Mechanical Engineering In Partial Fulfilment

Of The Requirements For The Degree Of

Master Of Applied Science At The

University Of Windsor

By

SyedShoeb I. Nagamiyan

Windsor, Ontario

1992

The author has granted an irrevocable non-exclusive licence allowing the National Library of Canada to reproduce, loan, distribute or sell copies of his/her thesis by any means and in any form or format, making this thesis available to interested persons.

L'auteur a accordé une licence irrévocable et non exclusive permettant à la Bibliothèque nationale du Canada de reproduire, prêter, distribuer ou vendre des copies de sa thèse de quelque manière et sous quelque forme que ce soit pour mettre des exemplaires de cette thèse à la disposition des personnes intéressées.

The author retains ownership of the copyright in his/her thesis. Neither the thesis nor substantial extracts from it may be printed or otherwise reproduced without his/her permission.

L'auteur conserve la propriété du droit d'auteur qui protège sa thèse. Ni la thèse ni des extraits substantiels de celle-ci ne doivent être imprimés ou autrement reproduits sans son autorisation.

ABSTRACT

The main purpose of this study was to use localised tooth dimensions to determine the magnitude and location of the maximum tensile stress for the spur gear teeth.

Log linear equations using Broghamer and Dolan data for stress concentration were developed and compared with the existing equations. It was found that these log linear equations improved the accuracy and decreased the deviation.

By comparing tooth geometry and Lewis factor with that given by AGMA, by graphical construction, and by Broghamer and Dolan for involute spur gear teeth, it is shown that FIGS.EXT software accurately generates teeth.

Dimensions such as the load height, tooth thickness and radius of the trochoid contour, determined at the various locations of the trochoid contour, were used to determine maximum nominal tensile stress and its location in FIGS.EXT software for involute spur gear teeth. This location defined as the theoretical weakest location, and its corresponding dimensions were recorded as the localised dimensions. As a function of these localised dimensions, a single log linear equation is developed for stress concentration factor. This equation is independent of pressure angle and manufacturing process.

The single equation of the gear tooth stress concentration was also used to predict the maximum tensile stress and its location as a general solution for

i

proportionate cantilever beams. This general solution was compared with that obtained by FEA and it was found that this single equation overestimates the maximum tensile stress.

ACKNOWLEDGEMENTS

TABLE OF CONTENTS

LIST OF TABLES

LIST OF FIGURES

xiv

NOMENCLATURE

a	Length of addendum of the tooth.
B	Backlash in gear tooth.
b	Length of dedendum of the tooth.
b_c	Distance of load position from fixed end of the cantilever beam.
C	Distance between the location of the theoretical weakest section and the Lewis weakest section.
C_i	Tooth thickness constant.
D_B	Broghamer & Dolan value of the dimensions of the Lewis weakest section.
D_c	Maximum thickness of the cantilever beam.
D_F	FIGS.EXT value of dimensions of the Lewis weakest section.
d_c	Minimum thickness of the cantilever beam.
F	Face width of the gear.
h	Load height above the Lewis weakest section.
h_1	Load height above the theoretical weakest section.
K	Bending stress concentration factor for tensile fillet = S_t/σ_t
K_c	Bending stress concentration factor for compressive fillet = S_c/σ_c
K_d	Stress concentration factor contributed to only axial load.

K_c Stress concentration factor contributed to only tangential load.

K_b Stress concentration factor obtained from machine design text for cantilever beam either in tension or in bending load.

L   Location of the maximum tensile stress from addendum circle.

l_c Length of the cantilever beam.

m   Module of gear tooth = 1 / P_d

M_{bs} Maximum tensile stress of the gear teeth as determined by equation 7.1

N   Number of teeth.

P   Load applied perpendicular to the tooth surface.

P_a Axil load on the gear tooth.

P_c Circular pitch of the gear.

P_d Diametral pitch

P_{ds} Difference in per cent for location of the maximum tensile stress as determined by Finite Elements with respect to that determined by equation 7.1.

P_h Error in per cent for load height as determined by Broghamer and Dolan with respect to that determined by FIGS.EXT software.

P_r Difference in localised radius of the trochoid with respect to minimum trochoid radius.

P_s	Tensile load or bending load applied to cantilever beam.
P_t	Error in per cent for tooth thickness as determined by Broghamer and Dolan with respect to that determined by FIGS.EXT software.
P_{ta}	Tangential Load on the gear tooth.
P_{tl}	Difference in tooth thickness measured at theoretical weakest section with respect to that measured at Lewis weakest section.
P_{st}	Error in estimating the maximum tensile stress for gear teeth and cantilever beam.
P_x	Error in per cent for Lewis x-factor as determined by Broghamer and Dolan with respect to that determined by FIGS.EXT software.
r_a	Radius of the addendum circle.
r_b	Base radius of the gear tooth.
r_c	Fillet radius of the cantilever beam.
r_d	Radius of the dedendum circle.
r_f	Minimum trochoid radius of the generated fillet.
r_l	Radius of the trochoid contour.
r_p	Pitch radius of the gear tooth.
r_t	Radius of the cutter tip.
S_a	Direct compressive stress
S_c	Experimental maximum compressive stress
S_l	Lewis bending stress calculated at the

Lewis weakest section

S_o Maximum tensile stress produced in gear tooth subjected to only tangential load.

S_t Experimental maximum tensile stress

S_{te} Maximum tensile stress determined from the equation of bending stress concentration factor.

T_p Tooth thickness measured along the pitch circle.

T_b Base tooth thickness.

T_r Involute tooth thickness at radius "r".

T_t Tip tooth thickness.

T_1 Pitch tooth thickness of the pinion.

T_2 Pitch tooth thickness of the gear.

TRATIO   Tooth thickness ratio = T_1 / T_2

t   Tooth thickness measured at the Lewis weakest section.

t_c Width of the cantilever beam.

t_1 Tooth thickness at the theoretical weakest section.

Y   Distance from pitch circle to intersection of the load line and the tooth axis.

Y_f Form factor for gear design = $2 * X * P_d / 3$

X   X-factor = $(t/2)^2 / h$

ω Angular velocity of the gear.

β Half tooth thickness angle of tooth.

ϕ Pressure angle of the cutter.

ϕ_i Load angle between line of action of the applied force and perpendicular to the tooth axis.

θ Roll angle.

μ Average error obtained in determining the maximum tensile stress.

σ Standard deviation of the error obtained in determining the maximum tensile stress.

$\text{Inv}(\phi)$ Involute of the pressure angle

σ_t Nominal tensile stress $= S_1 - S_a$

σ_c Nominal Compressive stress $= S_1 + S_a$

$c_1, c_2 \& c_3$ Constants used to model the equation of the bending stress concentration.

Exp K   Experimental stress concentration factor $= S_t / \sigma_t$., Where σ_t is determined at the Lewis weakest section.

1.INTRODUCTION

Gears are among the oldest machine elements in the history of machine design. Gears are not only used in automobiles but also in delicate devices such as computers and printers. Almost every machine in modern industry depends on gears for its basic function. Therefore, it is not an exaggeration to say that the annual dollar volume of all geared devices sold in the world runs into billions of dollars. Though gears are part of the machine, gear design and its level of design are extremely important for successful and smooth function of the machine. In order to understand gear geometry and its design, it is helpful to know what gears are and why they are used in a machine.

A gear is defined as a toothed wheel that is usually round. Teeth, which carry the load and transmit the uniform motion from one shaft to another to run machines, are found on the periphery of wheel. They are as essential to the gear as the heart is to the human body.

1.1 Involute Gear Tooth Geometry And Its Role In Stress Concentration:

A gear tooth is described by two kinds of profiles, as shown in **Figure 1.1**. The first part is the contacting profile where contact of two mating gears takes place. This profile lies between the addendum circle and the base circle of a
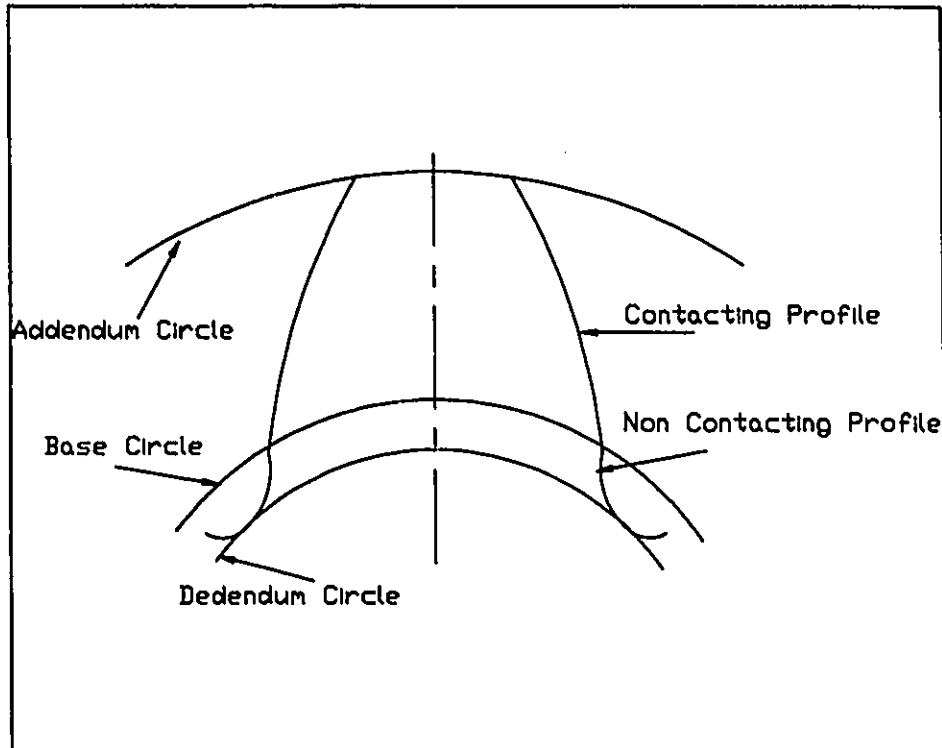
FIGURE 1.1: GEAR TOOTH AND ITS PROFILE

gear. It could be of any conjugate form such as involute of a circle or cycloidal. The involute profile is the most common form of all tooth forms. Straight tooth gears with involute tooth form and connecting parallel shafts are called involute spur gears. These are the most basic gears which are widely used in industry. Although there exist numerous processes to manufacture involute gears, most of them are based on two basic methods, generating and forming. Both methods produce involute form in a gear tooth.

The second part, called the root profile, is below the involute profile. This profile is significantly different in a generated gear tooth and a formed gear tooth. This difference in the profile of the generated gear tooth and formed gear tooth is illustrated in **Figure 1.2**. In a formed gear tooth, this profile is of constant radius of curvature. While in case of the generated gear tooth, it is of gradually increasing curvature with minimum trochoid radius occurring at the intersection of the root profile and the dedendum circle. This type of root profile is called a trochoid root profile.

It should be noted that stress concentration increases as this radius decreases.
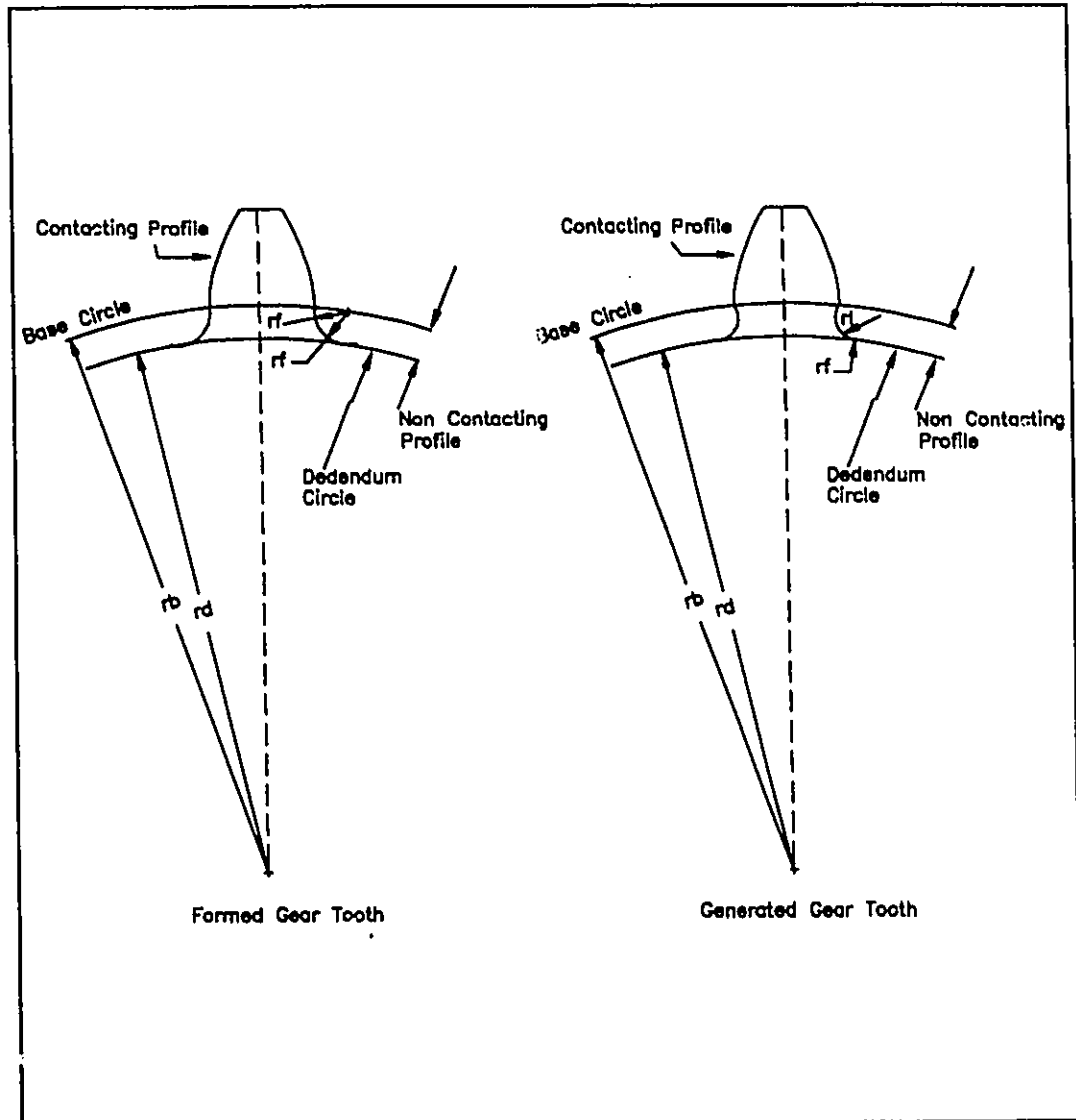
FIGURE 1.2: FORMED AND GENERATED GEAR TOOTH PROFILE

1.2 Bending Stress Concentration Factor Of A Gear Tooth:

In 1942, Broghamer and Dolan(2) conducted photoelasticity experiments on several generated and formed gear tooth models, while changing variables such as pressure angle of the tooth, addendum, dedendum, cutter tip radius, number of teeth and load height to determine maximum tensile stress(S_t) and its location in the root profile. It was found that the maximum tensile stress is always greater than nominal tensile stress(σ_t) as determined at the nominal weakest section. It was also observed that the position of maximum tensile stress is lower than the nominal weakest section, but not as low as the intersection of the root profile and dedendum circle. They defined the stress concentration as the ratio of the maximum tensile stress found in the root profile to the nominal tensile stress as determined at the " Lewis " weakest section. It was concluded that the minimum radius of the trochoid, the tooth thickness, the load height and the pressure angle of cutter were the principal variables and the addendum, dedendum, number of teeth and the method of manufacturing were the secondary variables of the stress concentration factor of a gear tooth. Therefore, two equations of stress concentration factor based on these principal variables were developed - one for 14.5° and the other for 20° pressure angle gear teeth.

Stress concentration is a highly localised and geometry dependent phenomenon. It is also very sensitive to small

5

changes of section. Therefore, it is logical to infer that stress concentration of a gear tooth is dependent only on the localised geometry of the root profile where the position of the maximum tensile stress is found.

At this point, it is important to cite the drawbacks of present equations of stress concentration factor for a gear tooth. The Lewis weakest section theory neglects the direct compressive stress produced by the axial component of a load. Perhaps this is the reason why the position of the Lewis weakest section is found to be higher than the position located in the photoelastic analysis. In spite of this position discrepancy, present equations are based on the Lewis weakest section and its location. Furthermore, these equations utilize the minimum trochoid radius as the principal variable, even though the maximum stress is never found at the intersection of the root profile and the dedendum circle.

Knowing these drawbacks of bending stress concentration analysis for the gear teeth, it will be of great interest to know

(i)   The accurate localised dimensions of the gear teeth and its corresponding equation for bending stress concentration.

(ii) The maximum tensile stress and its location in the gear tooth.

1.3 Involutometry And Its Important Properties :

It is useful to know the involute profile, its important properties and involutometry equations since they are used in the FIGS.EXT software to generate the involute tooth models.

An involute curve can be defined as the locus of a point (I) on a line rolling out on its base circle, as shown in **Figure 1.3**. Consider an instantaneous point (I) on the involute curve at the radius (r) from the centre of the base circle of radius(r_b) as shown in **Figure 1.4** to define the following involute properties.

(i) Line Of Action

A line such as IF, tangent to the base circle at F, is defined as the line of action. The line of action, being tangent to base radius at point F, is always perpendicular to that base radius(CF).

(ii) Pressure Angle (ϕ) :

An angle ICF is defined as the pressure angle in the involute gear geometry corresponding to the point I of the involute profile. Though this pressure angle varies all along the involute profile, it is used as a definable variable when referred at the pitch point to identify the group of involute gears. The most common groups of gears based on the pressure angle are 14.5° involute spur gears and 20° involute spur gears. It can be determined corresponding to any point at

7
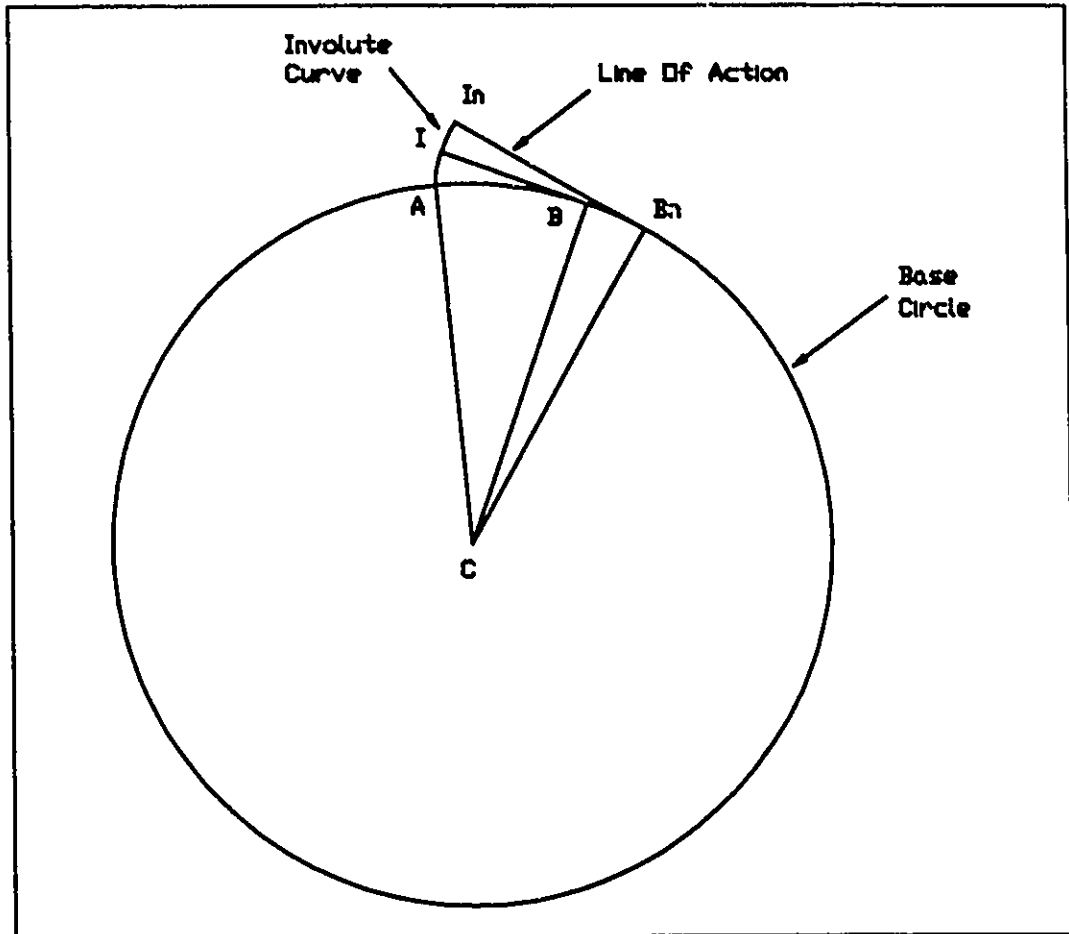
FIGURE 1.3: INVOLUTE CURVE
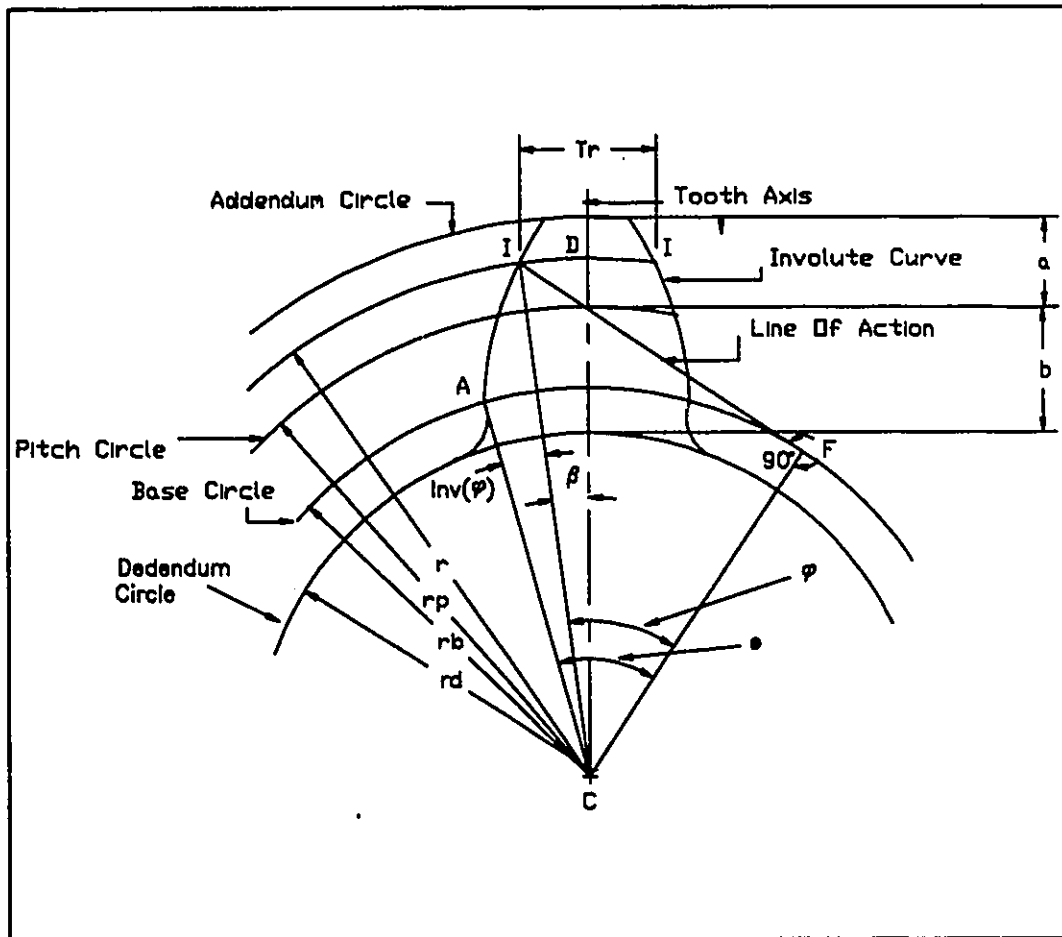
FIGURE 1.4: BASIC DIMENSIONS OF AN INVOLUTE TOOTH

radius "r" on the involute profile by the following equation.

$$\phi = \arccos\left(\frac{r_b}{r}\right)$$

(iii)   Roll Angle (θ) :

An angle ACF is called the roll angle and is used to define an important involute function in the involutometry.

$$\theta = \frac{AF}{r_b} = \frac{IF}{r_b} = \tan(\phi) = \frac{(r^2 - r_b^2)^{.5}}{r_b}$$

(iv) Involute Of The Pressure Angle (Inv(ϕ)) :

An involute of the pressure angle is defined as the difference between the roll angle and the pressure angle. It is frequently used in the FIGS.EXT software to generate the involute profile.

$$Inv(\phi) = \theta - \phi$$

$$\therefore Inv(\phi) = \tan(\phi) - (\phi)$$

(v)   Half tooth thickness angle (β) :

An angle ICD defined as follows is called the half tooth thickness angle.

$$\beta = \frac{T_r}{2*r}$$

(vi) Tooth Thickness Constant(C_i):

The sum of the half tooth thickness angle and involute of pressure angle [inv(ϕ)] at any point on the involute profile is always constant, no matter where it is on the involute profile. It is determined by the following equation.

10

$$C_i = Inv(\phi) + \frac{T_r}{2*r}$$

(vii) **Addendum (a)** : It is the radial distance between the addendum circle and the pitch circle. It is used to determine the addendum radius of the gear(r_a).

$$r_a = r_p + a$$

(viii) **Dedendum (b)** : It is the radial distance between the dedendum circle and pitch circle. It is used to determine the dedendum radius of the gear(r_d).

$$r_d = r_p - b$$

2. LITERATURE SURVEY

Since 1892, the Lewis theory of gear analysis has remained the basis for the design of spur gear teeth. But there has been improvement and continuous research [4], [5], [6], [7], [8], [9] and [10] in this area in the subsequent years. The most important improvement made by Broghamer and Dolan [2] in 1942, was the addition of the stress concentration factor in the design of the gear teeth.

Before proceeding with an analysis of Broghamer and Dolan stress concentration factors for the gear teeth, it is useful to know the Lewis theory of gear design in brief.

The Lewis theory considers a parabola, drawn from the intersection of the line of action and the tooth axis, and defines the "Lewis weakest section" in the root profile where this parabola becomes tangent to the root profile as shown in **Figure 2.1**. The Lewis theory assumes a tooth load acting at the apex of this parabola. The gear tooth is then assumed as the short cantilever beam of a section similar to the Lewis weakest section (F*t) of a gear tooth, subjected to only uniformly distributed load (P_{ta}) across its width. The Lewis theory finally determines a bending stress of this cantilever beam. The Lewis bending stress equation [1] is

$$S_1 = \frac{6 * P_{ta} * h}{F * t^2} \quad ----------(2.1)$$
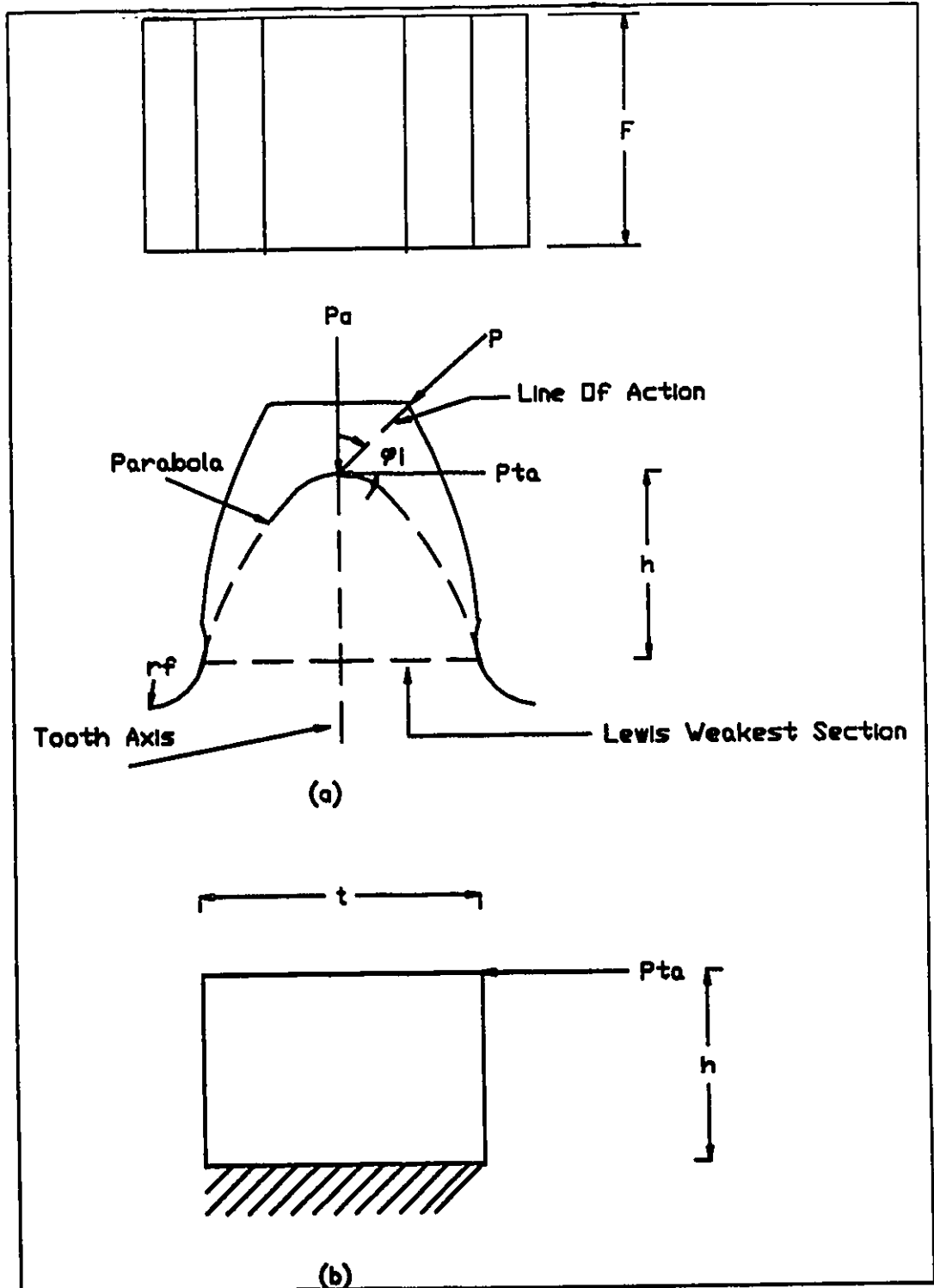
FIGURE 2.1: LEWIS THEORY OF GEAR DESIGN
(a) GEAR TOOTH AND ITS FORCE ANALYSIS
(b) CANTILEVER BEAM FOR LEWIS EQUATION

2.1 Broghamer And Dolan Stress Concentration Factors:

Broghamer and Dolan discovered that the Lewis equation determines the bending stress at an assumed (Lewis) weakest section and does not consider the stress concentration produced in the section of the stressed root profile of a gear tooth. In order to consider this stress concentration in the gear tooth design, they performed photoelastic experiments on eleven kinds of the gear tooth models to determine magnitude and location of the maximum stress developed in the root profile and its variables. The dimensions of gear tooth models are given in **Table A-5.1.** These gear tooth models are then grouped according to variables such as loading condition, pressure angle of the tooth and the manufacturing method (**Table A-5.2**). The effects of the variation in each of these variables on the stress concentration were analyzed. Each gear tooth model was tested a number of times to obtain the consistent pattern of photoelastic fringes. The fringe stress value of each of these patterns was obtained from the calibration of beams loaded in pure bending. The stress value for each model was then converted to equivalent stress for a model of unit width and unit load. These values of maximum tensile stress (S_t) and maximum compressive stress (S_c) with the values of load angle (ϕ_1), load height (h) and tooth thickness (t) for each case of the tooth models are tabulated in **Table A-5.1.**

14

Broghamer and Dolan also determined the position of the "actual weakest section", corresponding to the maximum stress developed in the root profile and then compared it with the position of the Lewis weakest section.

The maximum stress obtained in the test for each model was 30% to 120% greater than the Lewis bending stress determined at the Lewis weakest section by using the equation 2.1. These maximum stresses were expressed in the form of dimensionless factors called " Bending stress concentration factors(K and Kc) ", which were defined as the ratio of the maximum stress developed in the root profile to the nominal stress. Broghamer and Dolan used the following equations [2.1] to calculate the nominal stresses and bending stress concentration factors for tensile fillet and compressive fillet of a gear tooth.

$$S_a = \frac{P_a}{F * t} \quad \text{------------} (2.2)$$

$$\sigma_t = S_1 - S_a = \frac{6 * P_{ta} * h}{F * t^2} - \frac{P_a}{F * t} \quad \text{------------} (2.3)$$

$$K_c = \frac{S_c}{S_1} \quad \text{------------} (2.4)$$

$$K = \frac{S_t}{\sigma_t} = \frac{S_t}{S_1 - S_a} \quad \text{------------} (2.5)$$

2.1.1 Gear Tooth Stress Concentration And Its Variables:

The maximum stress - S_t and S_c for tensile and compressive fillets respectively, were identical for all nine cases of the tooth model 1 of the group A as shown in **Figure 2.2(a)**. While for all six cases of the tooth model 2 of the group B, the effect of direct compressive stress produced by the axial component was observed in the form of smaller maximum tensile stress at the tensile fillet, and larger maximum compressive stress at the compressive fillet as shown in **Figure 2.2(b)**.

The slight increase in the bending stress was obtained for a only few cases of the sharp fillet radius in group C, when the addendum was increased by 35% and 4.5% in model 4 and model 5 respectively. While in cases with larger minimum trochoid radius, no remarkable change in these factors was noted.

Broghamer and Dolan determined, for 14.5° and 20° pressure angle tooth models of group D and group E, that bending stress concentration factors decreased with the increase in the load height and a pronounced increase with a decrease in the minimum trochoid radius. Furthermore, the pressure angle was also considered as a dominant variable of stress concentration since stress concentration factors, for 14.5° pressure angle teeth, were 3% to 10% greater than those of 20° pressure angle teeth. It was noted that the bending stress concentration factors decreased with the increase in the number of teeth.

16
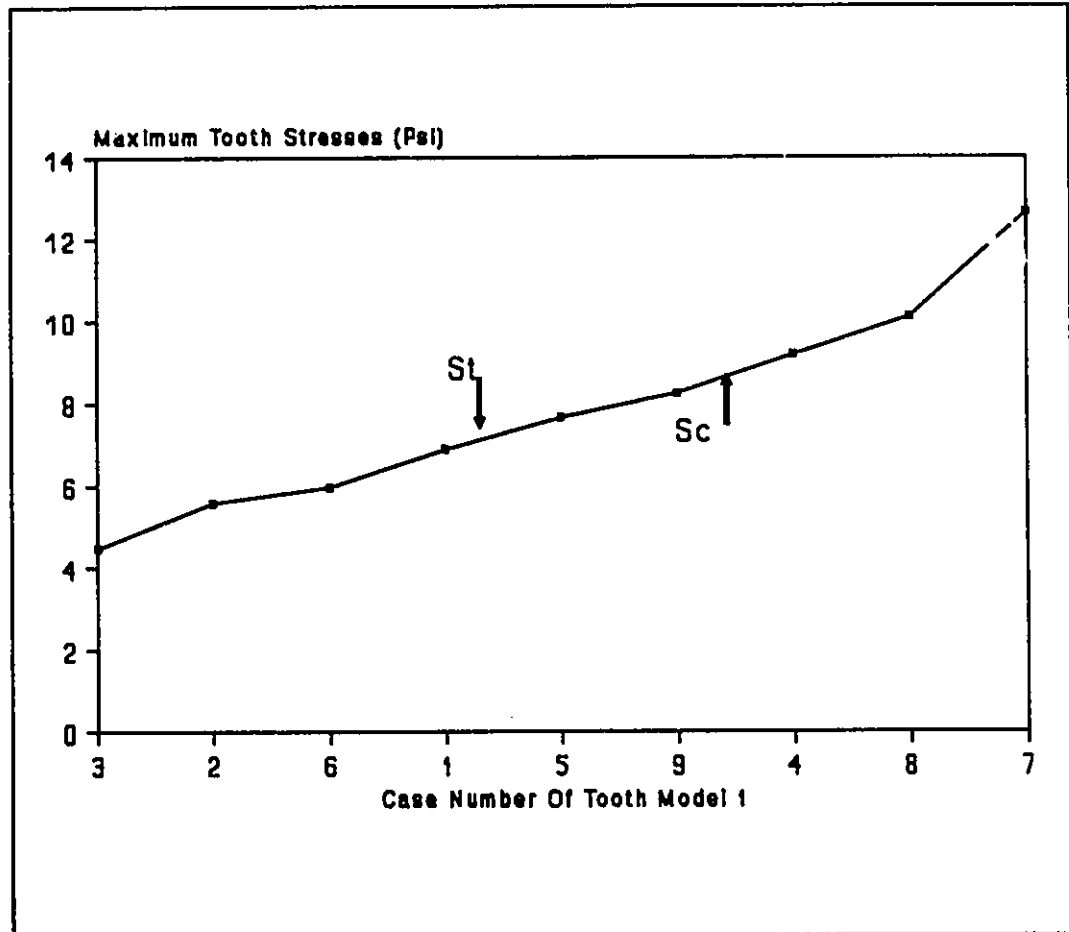
FIGURE 2.2(a): MAXIMUM STRESS FOR CASES OF TOOTH MODEL 1 (GROUP A)
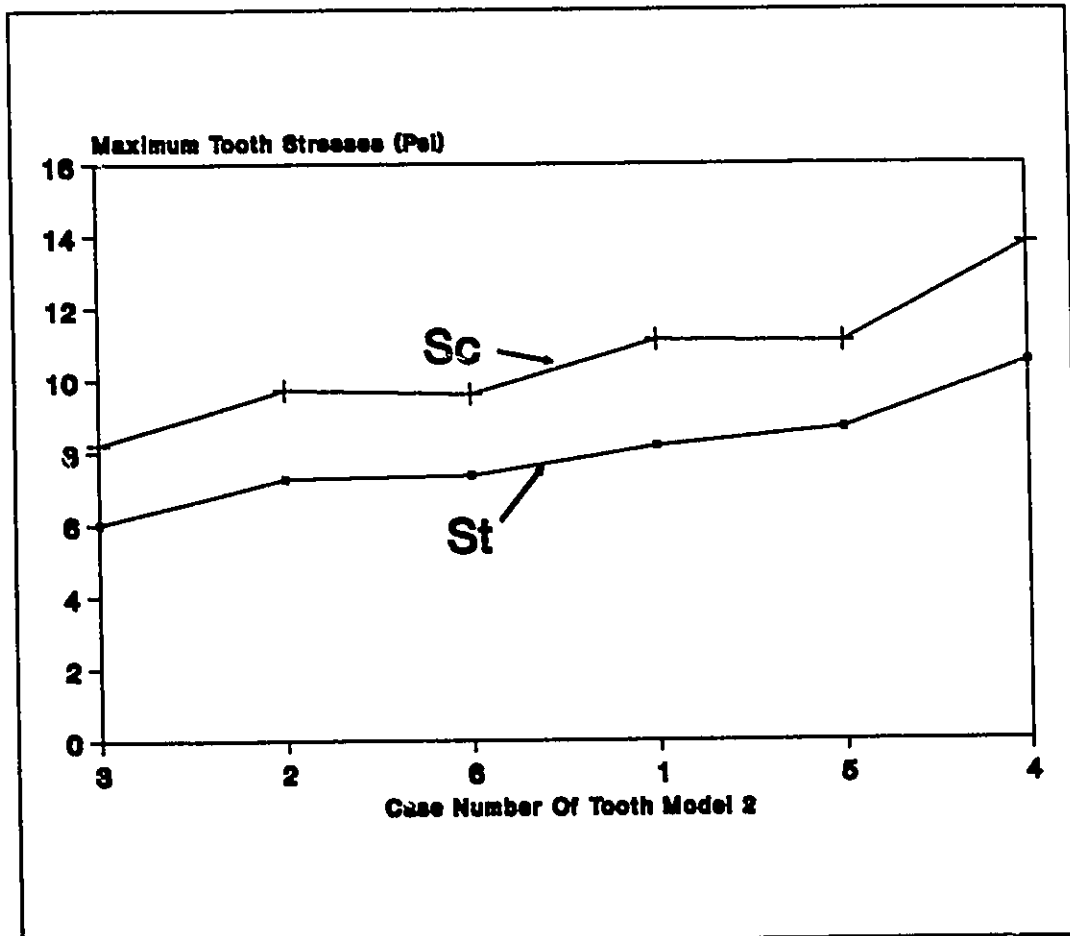
FIGURE 2.2(b): MAXIMUM STRESS FOR CASES OF TOOTH MODEL 2 (GROUP B)

The conventionalized gear tooth models, as mentioned in group F, were short cantilever beams having circular fillet. These gear tooth models were tested to determine the effects produced by varying only one variable at a time during the experiment on stress concentration. These models were similar to formed tooth models. In comparing the stress results of these models with those of standard gear tooth models, Broghamer & Dolan drew the two following important conclusions.

(1) Maximum tensile stress developed in the conventionalised tooth models was <u>only slightly larger</u> than that for the standard gear tooth models of similar proportions if the effect of direct compressive stress produced by an axial load is considered in the nominal stress for stress concentration analysis.

(2) Bending stress concentration factors for generated tooth models were smaller than those for conventionalised tooth models of similar proportion. The reason for these smaller bending stress concentration factors was mentioned as the effective radius which acts as a stress raiser in the root profile of the generated models is <u>larger</u> than the minimum trochoid radius of the root profile.

In the final analysis, Broghamer and Dolan concluded that the principal factors affecting the stress concentration were the minimum trochoid radius, the pressure angle, the tooth thickness and load height and the secondary variables were the

length of addendum & dedendum, number of teeth and the manufacturing method of producing the tooth profile.

2.1.2   Location Of Stress Concentration :

The actual weakest section was not located at the position where Lewis defined the weakest section, but was slightly lower towards the dedendum circle. The maximum distance between the Lewis weakest section and the actual weakest section, was so small that they used the Lewis weakest section for the analysis of the gear tooth stress concentration.

In order to compute the bending stress concentration factors based on tooth dimensions, Broghamer and Dolan developed the following two equations [2.2] in terms of the principal variables - One for 14.5° and the other for 20° pressure angle generated teeth.

For 14.5° pressure angle teeth

$$K=0.22+(\frac{t}{r_f})^{0.2}(\frac{t}{h})^{0.4} \text{ ----------(2.6)}$$

For 20° pressure angle teeth

$$K=0.18+(\frac{t}{r_f})^{0.15}(\frac{t}{h})^{0.45} \text{ ----------(2.7)}$$

20

It has been claimed that these equations determine the bending stress concentration factors with an accuracy of 3% for the following range of t/r_f and t/h ratio.

$$1.9 < t/r_f < 12.60$$
$$0.94 < t/h < 3.24$$

2.1.3   Disadvantages Of Broghamer Stress Concentration Factors:

Broghamer and Dolan used the identical stress concentration factor for the Lewis bending stress and the direct compression stress, as realised from the following derivation.

$$K = \frac{S_t}{S_l - S_a}$$

$$S_t = K(S_l) - K(S_a)$$

$$\therefore S_t = K(\frac{6 * P_{ta} * h}{F * t^2}) - K(\frac{P_a}{F * t}) \quad -----------(2.8)$$

Generally stress concentration factor varies with the change in the geometry and loading condition of machine elements. Therefore, the stress concentration factor for the tangential load and the axial load cannot be identical as used in the definition of the stress concentration of a gear tooth.

It is discovered from the reported Broghamer and Dolan experimental data that the load angle is erroneous for each

21

case of the experiments. In general, the value of load angle decreases as load moves from the tip down on the tooth profile towards pitch circle and is equal to the pressure angle of the tooth, when the load is at the pitch circle. This value further decreases as load moves down towards the base circle. In the experimental data, the value of the load angle is never equal to the pressure angle in any case having load position at the pitch circle (Except model 11). While in model 11, the value of the load angle is equal, instead of smaller, to the tooth pressure angle for each case having the load position below the pitch circle. Since these values of the load angles are in error for most of the cases, the values of the nominal stresses calculated using these load angles are incorrect and hence the present bending stress concentration factors are wrong.

Since the value of the maximum compressive stress obtained from the test results includes the effect of direct compressive stress produced by an axial component of the load, stress concentration factor for compressive fillet should not only consider the Lewis stress, but also the direct compressive stress. Compressive stress concentration factor should be defined as follows.

$$K_c = \frac{S_c}{S_l + S_a} \qquad --------- (2.9)$$

Bending stress concentration factors increased only in the cases of smaller minimum trochoid radius with the increase

22

of addendum.

The reason for higher bending stress for 14.5° pressure angle tooth models is due to their smaller tooth thickness at the Lewis weakest section than that of the 20° pressure angle tooth models. Therefore geometric change of the root profile, instead of the pressure angle, was responsible for this increase in bending stress.

The Broghamer and Dolan equations of stress concentration factors are dependent on the minimum trochoid radius of the generated root profile or the constant radius of the formed root profile (r_f) depending upon the manufacturing method used to produce the gear teeth. Since the location of maximum stress for generated gear models was never found at the minimum trochoid radius, they should be dependent on the localised radius of the trochoid contour corresponding to the theoretical weakest section. It was also identified that bending stress concentration factors were smaller for generated tooth models than those for formed tooth models because of the larger effective radius(localised radius of the trochoid contour) of the former models, than that of the latter tooth models. Broghamer and Dolan could not incorporate this decrease of bending stress concentration factors in their equations by using the localised radius of the trochoid contour as a variable. Furthermore the Broghamer & Dolan equations are applicable to the cases of the models in which a value of the ratio of t/rf ranges from 1.9 to 12.60. This

23

.

range is determined from the dimensions of the tooth models used in the experiments. Since a case in model 8 has the value of 12.66 for t/rf ratio as shown in **Table 2.1**, therefore this case should not be considered in tooth stress analysis.

TABLE 2.1:   **DIMENSIONS OF A CASE 12 OF THE MODEL 8. [2.3]**

Model	Case	Y in.	ϕ_1 deg.	t in.	r_t in.	h in.	t/r_t
8	12	-0.15	20	1.14	0.09	0.448	12.66

3. OBJECTIVE OF RESEARCH

From the analysis of Broghamer and Dolan for gear tooth stress concentration, it is clear that the variation in the tooth dimensions produces the change in the localised variables of the root profile and hence the bending stress concentration is either increased or decreased accordingly. If the bending stress concentration factor is expressed as a function of only localised variables where the position of the maximum nominal tensile stress is found, it is possible to develop an equation which is dependent only on the localised geometry and independent of the other non localised tooth variables such as the minimum trochoid radius, addendum, dedendum, pressure angle of cutter, type of tooth form and manufacturing method of a gear tooth. Since the nominal tensile stress includes the direct compressive stress produced by the axial component of a load, the position of the weakest section corresponding to maximum nominal tensile stress may be more accurately located than the one determined by the Lewis theory. Thus a general solution for the bending stress concentration factor can be obtained by determining the maximum tensile stress and its location. Furthermore this equation can also be used to estimate the maximum tensile stress and its location for the typically loaded proportionate cantilever beam.

The objectives of the research are summarised in the following order.

3.1   To analyze the Broghamer and Dolan experimental data for
      bending stress and to determine the equations which fit
      the test data better in comparison with the Broghamer and
      Dolan equations.

3.2   To use FIGS.EXT software to generate the Broghamer and
      Dolan gear tooth models, to confirm the correctness of
      the software by comparing the Lewis factors of these
      models determined by this software with those obtained by
      graphical methods as well as gear design references, and
      to demonstrate that this software correctly determines
      the tooth thickness, load height and localised radius of
      the trochoid contour of the gear tooth models.

3.3   To determine the bending stress concentration factors
      dependent on the dimensions of the theoretical weakest
      section for 14.5° and 20° pressure angle teeth and then
      to determine the bending stress concentration factors
      independent of the pressure angle using a single
      equation.

3.4   To determine the magnitude and the location of the
      maximum tensile stress for a gear tooth.

3.5   To test the applicability of a single equation of the
      bending stress concentration factor to determine the
      general solution of stress concentration for beam
      bending.

4. ANALYSIS OF THE EQUATIONS FOR GEAR TOOTH STRESS CONCENTRATION:

4.1 Purpose:

The purpose of analyzing the Broghamer and Dolan equations - 2.6 and 2.7 is

(1) To verify the claim that these equations are accurate to 3% to determine the bending stress concentration for 20° and 14.5° pressure angle teeth.

(2) To determine a better statistical fit of the data for the equations.

4.2 Methodology:

4.2.1 Accuracy Of The Broghamer and Dolan Equations:

The accuracy of Broghamer and Dolan equations is defined as the absolute maximum error in per cent that occurs between the values of the maximum tensile stress determined by these equations and the experimentally measured maximum tensile stress. The maximum tensile stress (S_{te}) is calculated by multiplying the nominal tensile stress with the bending stress concentration factor(K) obtained by using equations 2.6 and 2.7 for each case of the 14.5° and 20° pressure angle tooth models. The error in this value of the maximum tensile stress

in comparison with the experimental maximum tensile stress is determined by using the equation 4.1.

$$P_{st} = \left(\frac{S_{c\theta} - S_t}{S_t} \right) *100 \quad ----------(4.1)$$

4.2.2   Log Linear Equations And Their Accuracy:

Log linear equations for 20° and 14.5° pressure angle teeth were developed using the computer program **GETSCO20** and **GETSCO14.5** respectively. These programs determine values of a matrix A(3,3), and arrays C(3) and B(3) defined as below.

$$K = c_1 \left(\frac{t}{r_f} \right)^{c_2} \left(\frac{t}{h} \right)^{c_3} \quad -----------(4.2)$$

Taking log of both sides of the equation 4.2

$$Log(k) = Log(c_1) + c_2 * \log\left(\frac{t}{r_f} \right) + c_3 * \log\left(\frac{t}{h} \right)$$

Determining the error term

$$e = \log(K) - Log(c_1) - c_2 * Log\left(\frac{t}{r_f} \right) - c_3 * Log\left(\frac{t}{h} \right)$$

Squaring this error term, taking derivative with respect to constants c_1, c_2 and c_3, and rearranging the terms, the result is expressed as matrix A(3,3), C(3) and B(3), and then solved using the Gaussian Elimination to determine the constants of the equations in both computer programs.

$$A(3,3) \;*\; C(3) \;=\; B(3)$$

29

$$
\begin{vmatrix}
N & \sum_{i=1}^{N} LOG(t/rf) & \sum_{i=1}^{N} LOG(t/h) \\[2ex]
\sum_{i=1}^{N} LOG(t/rf) & \sum_{i=1}^{N} LOG(t/rf)^2 & \sum_{i=1}^{N} \{LOG(t/rf)*LOG(t/h)\} \\[2ex]
\sum_{i=1}^{N} LOG(t/h) & \sum_{i=1}^{N} \{LOG(t/rf)*LOG(t/h)\} & \sum_{i=1}^{N} LOG(t/h)^2
\end{vmatrix} *
$$

$$
\begin{vmatrix}
LOG(C_1) \\[2ex]
C_2 \\[2ex]
C_3
\end{vmatrix}
=
\begin{vmatrix}
\sum_{i=1}^{N} LOG(K) \\[2ex]
\sum_{i=1}^{N} LOG(K)*LOG(t/rf) \\[2ex]
\sum_{i=1}^{N} LOG(K)*LOG(t/h)
\end{vmatrix}
$$

Where N = 35 for 20° pressure angle teeth.

N = 54 for 14.5° pressure angle teeth.

The equations 4.3 and 4.4 are the log linear equations as

30

obtained from the computer program for 20° and 14.5° pressure angle teeth respectively. The accuracy of these equations is determined in the same fashion as previously.

For 20° pressure angle teeth

$$K = 1.16 \left(\frac{t}{rf}\right)^{0.15} \left(\frac{t}{h}\right)^{0.39} \text{----------} (4.3)$$

For 14.5° pressure angle teeth

$$K = 1.15 \left(\frac{t}{rf}\right)^{0.20} \left(\frac{t}{h}\right)^{0.38} \text{----------} (4.4)$$

4.2.3 Comparison Of Broghamer And Dolan, With The Log Linear Equations.

In order to compare the equations, statistical parameters such as average error(μ), standard deviation(σ), accuracy and range for 3σ limits of error of Broghamer and Dolan, and log linear equations are determined for 14.5° and 20° pressure angle teeth. The formulae for average error(μ) and standard deviation (σ) are:

$$\mu = \sum_{i=1}^{n} \frac{P_{sti}}{n} \text{----------} (4.5)$$

$$\sigma = \sqrt{\frac{\sum_{i=1}^{n} (P_{st_i} - \mu)^2}{n-1}} \text{----------} (4.6)$$

4.3   Results/Discussion:

4.3.1   Accuracy:

The error in determining the maximum tensile stress by using Broghamer and Dolan, and Log linear equations is listed in **Table B-1** for each case of the tooth models. 20 per cent of 14.5° pressure angle tooth cases and 18.5 per cent of 20° pressure angle tooth cases have 3 per cent or greater error. The maximum error (accuracy) of the Broghamer and Dolan equation for 20° and 14.5° pressure angle teeth is about 6%.

In the case of log linear equations, the accuracy is 5% and 4.4% for 20° and 14.5° pressure angle teeth respectively.

4.3.2   Statistical Analysis Of Broghamer and Dolan, And Log Linear Equations.

Table 4.1 indicates the statistical parameters such as average error, standard deviation, accuracy and range for 3σ limits obtained in determining the maximum tensile stress by using Broghamer and Dolan, and Log linear equations for 14.5° and 20° pressure angle teeth models. Average error for both sets of the equations do not change significantly. But the decreased standard deviation and smaller range of 3σ limits in case of log linear equations for 20° and 14.5° pressure angle

32

TABLE 4.1: **STATISTICAL PARAMETERS FOR EQUATIONS OF BENDING STRESS CONCENTRATION FACTOR BASED ON MINIMUM TROCHOID RADIUS.**

Equations	ϕ deg.	μ per cent	σ per cent	Accuracy per cent	Range-3σ per cent
Broghamer & Dolan	14.5	-0.11	2.22	5.42	-6.77 to 6.55
	20	-0.49	2.25	5.78	-7.24 to 6.26
Log Linear	14.5	0.32	1.98	4.39	-5.62 to 6.26
	20	0.66	2.14	4.98	-5.76 to 7.08

teeth indicate that error of these equations are reduced compared to Broghamer and Dolan equations. The accuracy of the log linear equations for 20° and 14.5° pressure angle teeth is also increased compared to Broghamer and Dolan equations.

SOFTWARE FOR GENERATED INVOLUTE SPUR GEAR TEETH TO DETERMINE ITS LOCALISED VARIABLES.

5.1 Purpose:

Two methods are used to generate the gear tooth models. The first one is graphical and the second one is analytical. The procedure to generate the tooth model is the same in the graphical as well as the analytical method. In the analytical method, this procedure is programmed in FIGS.EXT software. The purpose of generating the tooth layout is as follows.

(1)   The layout for a standard proportion AGMA tooth model is generated by both the graphical method and FIGS.EXT software to determine the Lewis form factor. This value of the Lewis form factor is then compared with that given by AGMA to determine the reliability of the methods to generate the tooth layout and to determine the dimensions of the Lewis weakest section giving load height(h) and tooth thickness(t) for a known load position.

(2)   Layouts for tooth models 3 to 11 were generated by FIGS.EXT software to determine the Lewis x-factor and the dimensions of the Lewis weakest section. These values of the Lewis x-factor and the dimensions of the Lewis weakest section for each tooth model are then compared with those recorded by

Broghamer and Dolan.

(3)   To show the capabilities of FIGS.EXT software, for example:

    (i)   To generate the gear tooth models with varying design parameters such as tooth thickness, tooth pitch, addendum, dedendum and number of teeth.

    (ii) To accurately determine the load angle.

(4)   To determine the dimensions of the theoretical weakest section including the radius of the trochoid contour(r_1), tooth thickness(t_1) and the load height(h_1).

5.2   Methodology:

5.2.1   Determination Of The Lewis Form Factor For AGMA Tooth Model.

5.2.1.1   By Using Graphical Methods:

The graphical method to generate the layout for the AGMA tooth model and to determine its Lewis form factor is explained in **Appendix C.**

5.2.1.2   By Using FIGS.EXT Software:

FIGS.EXT software determines the Lewis form factor for

36

AGMA tooth models in the following manner.

(i) Computing The Gear Geometry:

In the beginning of the software, values of the dimensions required to construct the gear tooth, are provided. The software uses the fundamental involute gear geometry equations to calculate the rest of the dimensions of the gear tooth geometry.

(ii) Generating The Tooth Layout:

The procedure that is used in FIGS software to generate the tooth model is exactly same as the graphical method. The graphical version of this software called FIGS.BAS(copyrighted) produces the tooth layout as shown in **Figure 5.1**. This software determines the co-ordinates of various points, defining the contour of the cutting edge of the cutter, for various locations where pitch line of the cutter is tangent to pitch circle of the gear tooth. These co-ordinates are determined by using the analytical equations of gear tooth geometry. Thus plotting these points, the full layout of the gear tooth is generated. In order to compare the similarity of the tooth layouts generated by the graphical method and FIGS.EXT software, the tooth thickness at the tip and the base circle of these tooth layouts is compared.

37
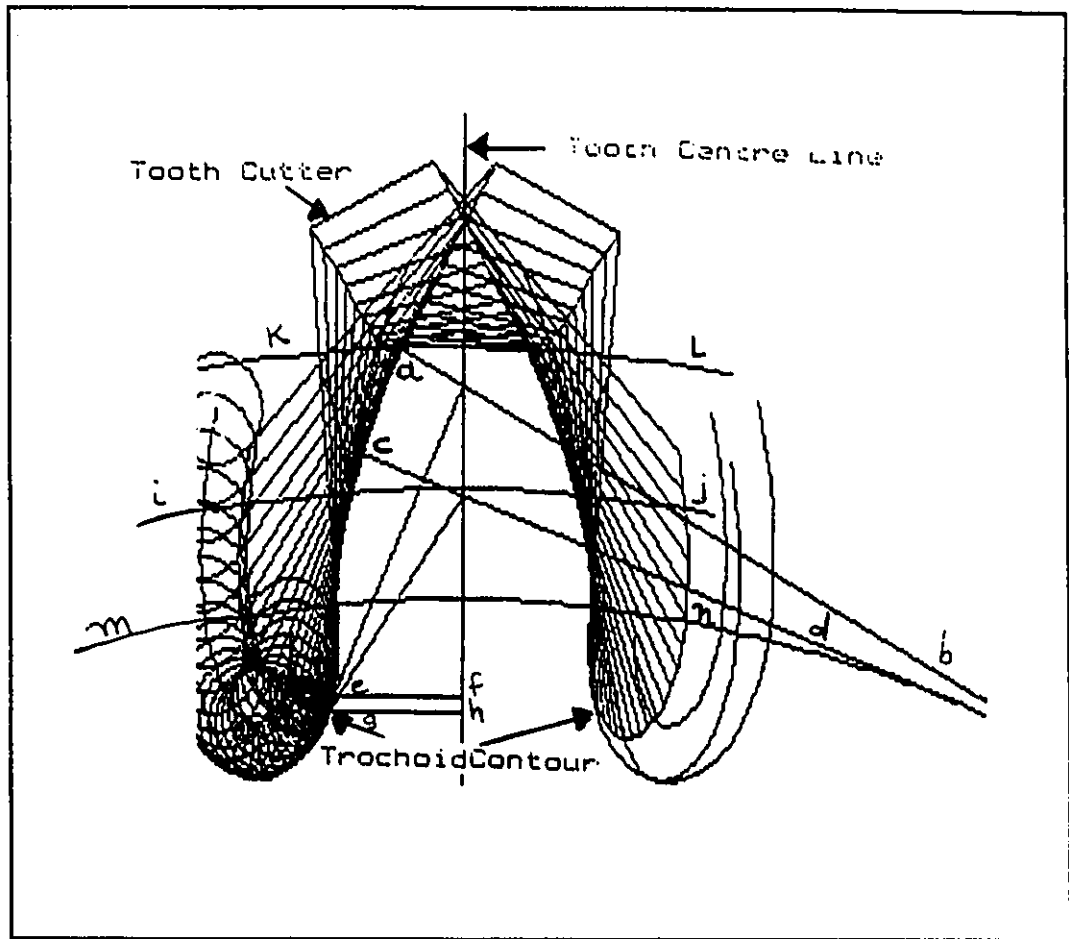
FIGURE 5.1: TOOTH LAYOUT AS GENERATED BY FIGS SOFTWARE

---

[1] ab: Load line for tip loaded tooth model
cd: Load line for Broghamer & Dolan tooth model
ef: Tooth thickness for tip loaded tooth model
gh: Tooth thickness for Broghamer & Dolan tooth model
ij: Pitch circle
kl: Addendum circle
mn: Base circle

(iii) Lewis Form Factor For AGMA Tooth Model:

The Lewis form factor is calculated from Lewis x-factor as explained in the graphical method by using the equation C-4 in FIGS.EXT software and then this value of the Lewis form factor is compared with that obtained from the graphical method and AGMA [1.2].

5.2.2   Determination Of The Lewis x-Factor And Dimensions Of The Lewis Weakest Section For Tooth Models.

The Lewis x-factor and the dimensions of the Lewis weakest section for generated tooth models 3 to 11 are determined by FIGS.EXT software. In order to compare these values of the dimensions with those recorded by Broghamer and Dolan, the error(P_h, P_t and P_x) in the values of the load height, tooth thickness and the Lewis x-factor for each case of the tooth model is determined by using the equation 5.1. These errors are recorded in **Table A-5.1**.

$$P_h \text{ or } P_t \text{ or } P_x = (D_B - D_F) * 100 / D_F \text{ ------------} (5.1)$$

where D_B = Broghamer & Dolan value of dimensions

D_F = FIGS.EXT software value of dimensions

39

5.2.2.1   By Graphical Methods For Model 3, 6 And 10.

The purpose of generating three tooth models such as model 3 (Non standard), model 6 (20° pressure angle tooth) and model 10 (14.5° pressure angle tooth) by the graphical method is to determine the Lewis x-factor and dimensions of the Lewis weakest section and then to compare them with those obtained by FIGS.EXT software and recorded by Broghamer and Dolan[2]. This comparison determines contiguity of three methods (Graphical, FIGS.EXT software and Broghamer And Dolan) for these results.

The procedure of the graphical method to generate these models is similar in every manner to that used to generate the AGMA tooth model except in the construction of the load line because the load position varies depending upon the given value of Y for the respective cases of the models. The load line is constructed by locating the point B, as the intersection of load line and the tooth axis, at the distance Y either above or below the point R on the tooth axis as shown in **Figure C-5**. Then load line B_1B_2 passing through the point B and tangent to the base circle of the tooth is drawn.

In order to determine how accurately these layouts for models 3, 6 and 10 are produced by the graphical method, tooth thickness at the tip and at the base is measured and compared with those obtained from the analytical tooth thickness relation of gear geometry and FIGS.EXT software. The

analytical method to determine the tooth thickness at the tip and the base is described in **Appendix D**.

The Lewis x-factor with the dimensions of the Lewis weakest section is determined from the graphical layout for these models. Then the values of Lewis x-factor with dimensions of the Lewis weakest section determined by the graphical method and Broghamer and Dolan are compared with those obtained by FIGS.EXT software. In addition to this comparison of the dimensions of the Lewis weakest section, the values of the tooth thickness and the load height for model 3 and 6 are plotted against the distance Y to determine the variation of these dimensions determined by these three methods.

5.2.3   Capabilities Of FIGS.EXT Software:

The following are the important features of FIGS.EXT software to generate the layout of the variety of the tooth models.

(1)   Generates Standard As Well As Non Standard Proportion Gear Teeth:

The determination of Lewis x-factor with 10 per cent accuracy for 94 per cent of tooth models shows that FIGS.EXT can be used for standard proportion gear tooth. The scope of the FIGS.EXT software is not only limited to standard proportion teeth but also it works for non standard proportion

41

gear teeth. Consider an example of generating the layout for tooth model 4 having non standard pitch tooth thickness - 0.883" and the length of addendum - 0.675". The procedure to use this software for this model is similar to that used for standard proportion teeth except for a few changes. These changes are:

(1)   Assume the value of cutter space equal to that of the non standard pitch tooth thickness.

(2)   Determine a value of the TRATIO in the following manner.

$$T_2 = (P_c - B) - T_1$$

$$TRATIO = \frac{T_1}{T_2} = \frac{P_c - B}{T_2} - 1 \ ----------(5.2)$$

A Value of this ratio for model 4 and model 5 is 1.2838 and 1.4063 respectively.

(3)   Since the value of the addendum is provided to FIGS.EXT software, this value can easily be varied according to the requirement. Set the value of addendum equal to 0.675" for this model.

(ii) Generates Tooth Models With Varying Number Of Teeth:

The standard proportion teeth having number of teeth in range of 12 to 300 are generated by the FIGS.EXT software to determine their Lewis form factor. These form factors are then compared with those given by AGMA [1.2]. Thus the capacity of FIGS.EXT to generate the tooth models with varying number of

42

teeth is determined.

(iii)   **Determines Load Angle:**

Load angle is defined as the angle B_3BB_2 between the load line and the perpendicular to the tooth axis as shown in **Figure C-5.** This angle is analytically determined in FIGS.EXT software as follows.

$$m\angle B_3BB_2 + m\angle\alpha = m\angle\alpha + m\angle BOB_1 = 90°$$

$$\therefore \phi_1 = m\angle B_3BB_2 = m\angle BOB_1 \ ----------(5.3)$$

The value of the load angle for each case of the tooth models 4 to 11 is calculated by the equation 5.4 and recorded in **Table A-5.1.**

$$\phi_1 = \arccos\left(\frac{r_b}{r_p + Y}\right) \ ----------(5.4)$$

5.2.4   **Determination Of Tooth Thickness(t_1), Load Height(h_1) And Radius Of The Trochoid Contour(r_1) For Tooth Models:**

Before describing the method used in FIGS.EXT software to determine the tooth thickness, load height and radius of the trochoid contour corresponding to the theoretical weakest section, it is important to understand the trochoid contour.

The contour, produced by a point of the cutter tip, when the cutter rolls down on the pitch circle of the tooth, is known as trochoid contour. Based on this concept of trochoid

43

contour, the trochoid contour produced by the cutter tip can be defined, if the location of a point on the cutter tip, corresponding to every tangential location of the pitch line of the tooth cutter and the pitch circle of the tooth, is determined, while the generating rack rolls on the pitch circle of the tooth to produce the tooth layout. This location is determined by analytical equations of the gear tooth geometry. Consider an instantaneous location such as a point 14 on the tip of the cutter as well as on the trochoid contour of the tooth layout, to describe the method used to determine the tooth thickness, load height and the radius of the trochoid contour as shown in **Figure 5.2**. This method is briefly described as follows.

(i) Tooth Thickness:

It should be noted that the horizontal distance between the point 14 and the gear center 0 is the half tooth thickness corresponding to the point 14 of the trochoid contour. This distance is determined in the following manner.

Determine the angle beta12 as shown in **Figure 5.2**

$$\beta_{12} = \arctan\left(\frac{DR}{R(2) - \frac{TR}{2}}\right) \quad \text{----------} (5.5)$$
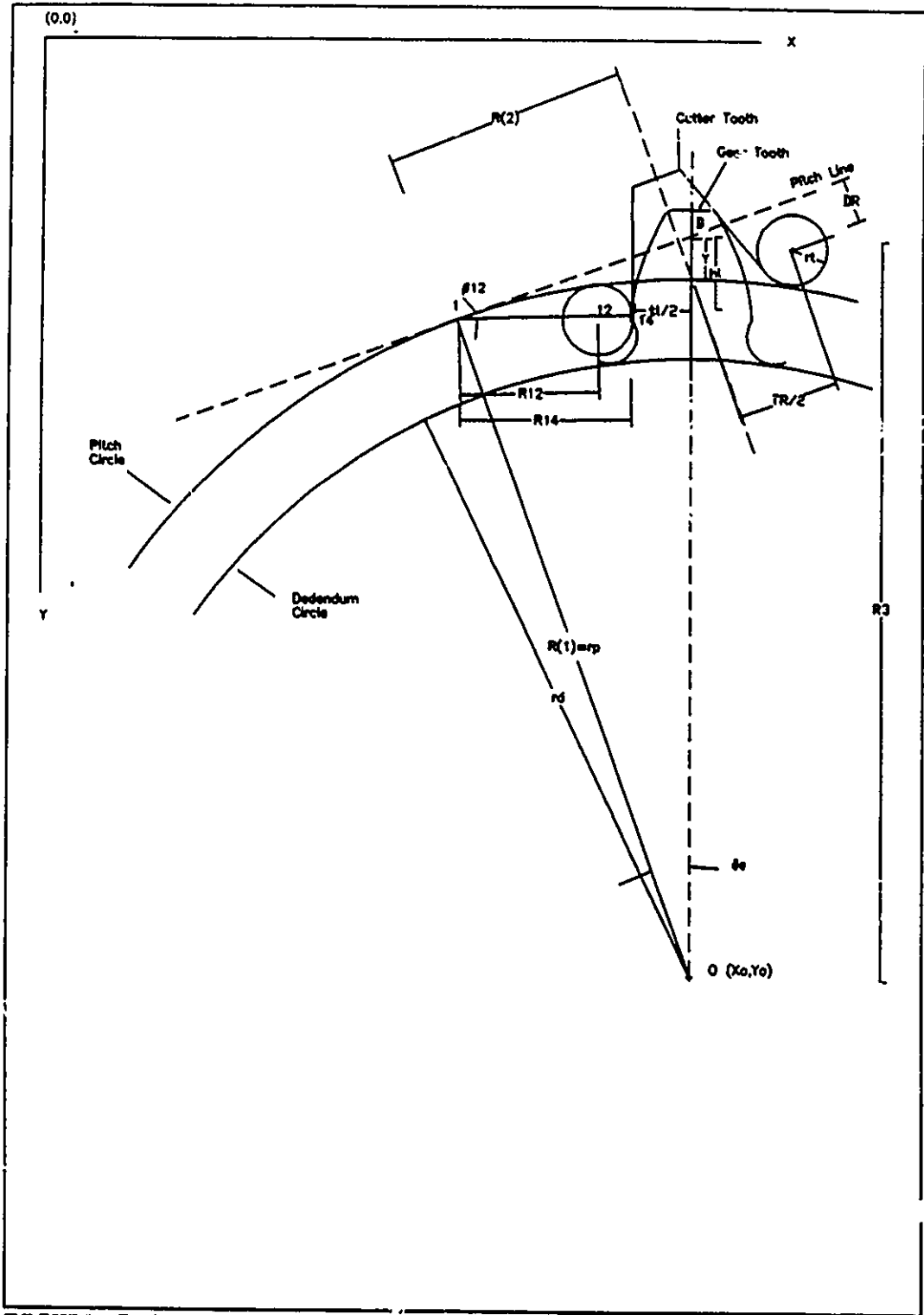
FIGURE 5.2: INSTANTANEOUS TOOTH CUTTER AND LOCALISED DIMENSIONS OF A GEAR TOOTH

45

where TR/2 = Distance between the centre of the cutter
tip radius and the tooth space axis of the
rack.

R(2) = Distance between point 1 and the tooth space
axis of the rack.

Determine the distance of the centre of the cutter tip.

$$R12 = \frac{DR}{\sin(\beta_{12})} \quad ---------- (5.6)$$

Determine the distance of the trochoid point.

$$R14 = R12 + r_t$$

Based on this R14 distance, the coordinates of trochoid
point 14 is determined in FIGS.EXT software and then tooth
thickness at the weakest section of the trochoid contour is
determined as:

$$t_j = 2 * [x(14) - x(o)] \quad ---------- (5.7)$$

(ii) Load Height:

Load position on the tooth axis is located by the radius
R3 as shown in **Figure 5.2**. In case of the Broghamer and Dolan
tooth models, the load position is recorded as the distance Y
either above or below the pitch circle of the tooth. Therefore
load height is determined from the centre of the gear as
follows.

$$R3 = R(1) + Y \quad ---------- (5.8)$$

$$h_l = R3 - [Y(O) - Y(14)] \quad ---------- (5.9)$$

46

(iii) Radius Of Trochoid Contour:

Figure 5.3 shows the procedure to determine the instantaneous centre of the trochoid contour of the gear tooth. While the gear tooth profile is being generated by the rack the gear blank rotates at constant angular velocity (ω). The point 12, centre of tip radius, is thought of as a point located at the distance "R12" from the point 1. Hence the loci of points 12 and 14 represent the trochoid contours which are parallel and the distance between each corresponding locus of the trochoid contours is equal to the tip radius. Velocity vectors of the points 1 and 12 are always parallel and opposite in direction for any locus of the trochoid contour. Hence the instantaneous centre is determined by locating the intersection point of the line connecting the points 1 and 12, and the line joining the extremities of these velocity vectors. The distance "R16" of this intersection point is obtained as follows.

$$\frac{R16}{R12} = \frac{R(1)\sin(\beta_{12})}{R12+R(1)\sin(\beta_{12})} \quad \text{------------} (5.10)$$

$$\therefore R16 = \frac{R12 * R(1)\sin(\beta_{12})}{R12+R(1)\sin(\beta_{12})}$$

47
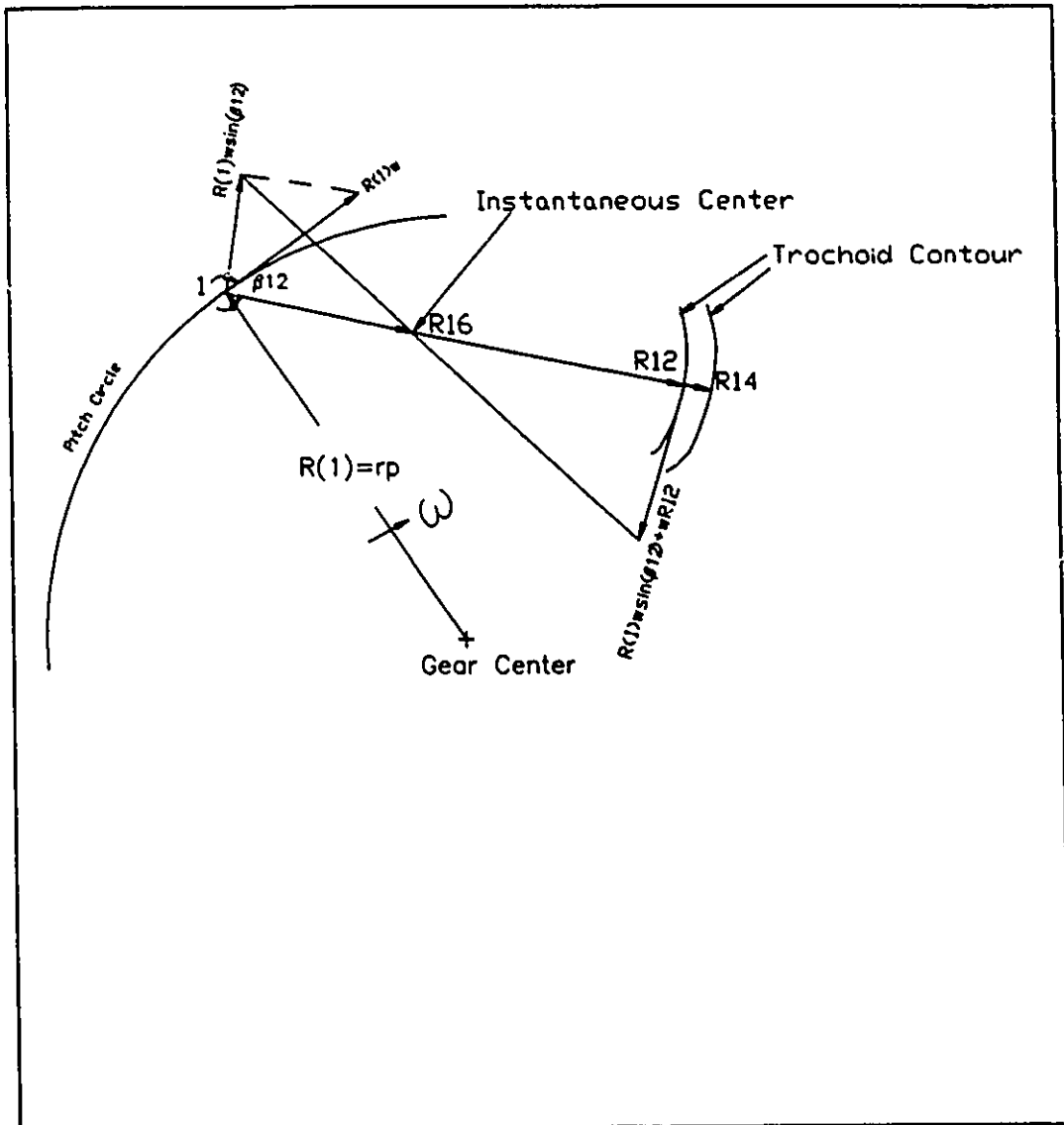
FIGURE 5.3: DETERMINATION OF RADIUS OF THE TROCHOID CONTOUR

$$r = R14 - R16 \quad \text{-----------} \quad (5.11)$$

Similarly the value of the tooth thickness, load height and the radius of the trochoid contour corresponding to any locus of the root profile can be determined. These values of tooth thickness and load height are used to calculate the nominal tensile stress (σ_t) by using equation 2.3 at various locations of the trochoid profile. Then maximum value of the nominal tensile stress is sought from these values of the nominal tensile stress, calculated at the various locations of the trochoid profile. Thus the maximum value of the nominal tensile stress and its location is determined. The tooth section corresponding to this location is defined as the theoretical weakest section. It should be noted that this load height(h_l) represents the location of the theoretical weakest section and the load height(h) determined by Broghamer and Dolan represents the location of the Lewis weakest section. Thus comparison of the values of the load heights for each case of the tooth models 4 to 11 indicates the difference in the location of the theoretical weakest section and the Lewis weakest section.

5.3 Results/Discussion:

5.3.1 Graphical And Analytical Tooth Layout For AGMA Tooth Model:

The error in the values of the tooth thickness at the tip and the base circle of the AGMA tooth model generated by the graphical method and FIGS.EXT software is tabulated in **Table 5.1.** The tooth cutter dimensions such as addendum and dedendum, pressure angle, pitch tooth thickness and the number teeth in gear are the same for these layouts. Since the difference in tooth thickness is small, it can be inferred that both the methods are consistent, and that FIGS.EXT software produces accurate dimensions of the tooth.

5.3.2 Graphical And Analytical Lewis Form Factor For AGMA Tooth Model:

The Lewis form factor for the AGMA tooth loaded at the tooth tip as determined by the graphical method and FIGS.EXT software is compared with that obtained from AGMA in **Table 5.2.** Since these values of the Lewis form factors are identical, it can be assumed that the procedure used to determine the Lewis x-factor in FIGS.EXT software is correct.

50

TABLE 5.1:   GRAPHICAL AND ANALYTICAL TOOTH THICKNESS FOR AGMA TOOTH MODEL.

Tooth thickness	Graphical measurement in.	Analytical calculation in.	Error per cent
T_t	0.798	0.795	0.38
T_b	2.070	2.074	-0.19

TABLE 5.2:   LEWIS FORM FACTOR FOR AGMA TOOTH MODEL.

Lewis form factor	AGMA [1.2]	FIGS.EXT software	Graphical
Y_f	0.308	0.308	0.308

5.3.3 Lewis x-factor And Dimensions Of The Lewis Weakest Section For Tooth Models.

The error in the values of the Lewis x-factor and the dimensions of the Lewis weakest section for tooth models 3 to 11 as determined by FIGS.EXT software and Broghamer and Dolan can be found in **Table A-5.1**. The error in the values of load height and tooth thickness is in no case greater than 10 per cent for each case of the all standard and non standard proportion tooth models except the tooth model 3. These errors are logical because Broghamer and Dolan measured these values from the graphical layout of each tooth model. These errors are positive and negative which provide the evidence for graphical errors.

The errors in the values of the Lewis x-factor as shown in **Table A-5.1** are less than 10 percent for each case of the all tooth models except the six cases of model 3 and four cases of the model 10. The errors are in the range of 12 to 20 per cent for these cases of the models 3 and 10. In calculating these errors, it is assumed that the Lewis x-factor determined by FIGS.EXT software is accurate.

5.3.3.1 Tooth Thickness For Model 3, 6 and 10.

The values of the tooth thickness at the tip and the base determined by the graphical method, analytical tooth thickness

53

relation and FIGS.EXT software, and their errors in percent are cited in **Table 5.3**. In calculating these errors, it is assumed that the tooth thickness as determined from the analytical tooth thickness relation is correct. The similar values of tooth thickness for these models indicate that layouts for these models are correct and also that FIGS.EXT generates the correct tooth layout.

5.3.3.2 Graphical Lewis x-factor And Dimensions Of The Lewis Weakest Section For Model 3, 6 and 10.

The comparison of the load height(h), tooth thickness(t) and Lewis x-factor for models 3, 6 and 10 determined by the graphical method and Broghamer and Dolan with those obtained from the FIGS.EXT software is shown in **Table 5.4**.

For each case of the model 3, the error in the values of the load height, tooth thickness and the Lewis x-factor as determined by the graphical method and FIGS.EXT software is less than the error of the same dimensions (h,t, Lewis x-factor) as obtained by graphical method and Broghamer and Dolan. This indicates that FIGS.EXT software and the graphical method are consistent and that FIGS.EXT software reports good values for tooth dimensions. The greater error in the values of these dimensions as determined by Broghamer and Dolan signals that FIGS.EXT software has not produced the geometry

TABLE 5.3:   TOOTH THICKNESS FOR MODEL 3, 6 and 10.

Tooth thickness	Theoretical equations in.	Graphical in.	Error per cent	FIGS in.	Error per cent
Model 3					
T_t	0.222	0.219	-1.35	0.222	0.0
T_b	0.412	0.422	2.43	0.412	0.0
Model 6					
T_t	0.173	0.175	1.16	0.173	0.0
T_b	0.430	0.440	2.33	0.430	0.0
Model 10					
T_t	0.236	0.250	5.93	0.236	0.0
T_b	0.432	0.434	0.46	0.432	0.0

TABLE 5.4: LEWIS X-FACTOR AND DIMENSIONS OF THE LEWIS WEAKEST SECTION FOR MODEL 3, 6 AND 10.

Model	Case	Dim	FIGS in.	Graphical method in.	Error per cent	B & D in.	Error per cent
3	4	h	0.757	0.741	-2.11	0.845	11.62
		t/2	0.421	0.418	-0.71	0.399	-5.23
		X	0.234	0.236	0.85	0.188	-19.66
	5	h	0.592	0.633	6.93	0.652	10.14
		t/2	0.428	0.438	2.34	0.406	-5.14
		X	0.309	0.302	-2.27	0.253	-18.12
	6	h	0.435	0.463	6.44	0.479	10.11
		t/2	0.443	0.453	2.26	0.421	-4.97
		X	0.450	0.443	-1.56	0.370	-17.78
6	1	h	0.725	0.731	0.83	0.728	0.41
		t/2	0.459	0.457	-0.44	0.461	0.44
		X	0.290	0.289	-0.34	0.292	0.69
	2	h	0.597	0.610	2.18	0.596	-0.17
		t/2	0.467	0.466	-0.21	0.461	-1.28
		X	0.365	0.356	-2.47	0.357	-2.19
	3	h	0.476	0.472	-0.84	0.472	-0.84
		t/2	0.480	0.475	-1.04	0.492	2.50
		X	0.483	0.476	-1.45	0.462	-4.35
	4	h	0.363	0.355	-2.20	0.341	-6.06
		t/2	0.502	0.488	-2.79	0.456	-9.16
		X	0.693	0.711	2.60	0.710	2.45
10	9	h	0.633	0.645	1.90	0.685	8.21
		t/2	0.906	0.885	-2.32	0.862	-4.86
		X	0.268	0.266	-0.75	0.229	-14.55

56

TABLE 5.4 (CONTINUED)

Model	Case	Dim.	FIGS in.	Graphical in.	Error per cent	B & D in.	Error per cent
10	10	h	0.633	0.645	1.90	0.685	8.21
		t/2	0.459	0.464	1.09	0.438	-4.58
		X	0.332	0.333	-0.30	0.279	-15.86
	11	h	0.503	0.505	0.40	0.544	8.15
		t/2	0.467	0.464	-0.64	0.443	-5.14
		X	0.433	0.425	-1.85	0.361	-16.63
	12	h	0.377	0.345	-8.49	0.398	5.57
		t/2	0.480	0.458	-4.58	0.447	-6.88
		X	0.610	0.609	-0.16	0.501	-17.87

of model 3 as described by Broghamer and Dolan. Hence model 3 is omitted from the further analysis of stress concentration of the gear tooth.

In each case of the standard proportion 20" pressure angle tooth model 6, the error in the values of the load height, tooth thickness and Lewis x-factor determined by the graphical method and FIGS.EXT software is not greater than 3 per cent. While the difference in the values of the Lewis x-factor determined by Broghamer and Dolan and FIGS.EXT software is also not greater than 4.5 per cent. This small error indicates that FIGS.EXT software accurately generates the layout and determines the correct values of the dimensions.

The error in the values of the Lewis x-factor for each case of the model 10 determined by the graphical method and FIGS.EXT software is not only less than 1.75 percent, but the error in the values of the load height and the tooth thickness is also consistently less than 4 percent in each case except the case 12. The values of the Lewis x-factor determined by Broghamer and Dolan and FIGS.EXT software are in error in the range of 14 to 18 per cent. Therefore once again, FIGS.EXT software and the graphical method have proved their consistency in determining the Lewis x-factor and the dimensions of the Lewis weakest section.

Since the error in the Lewis x-factor determined by Broghamer and Dolan, and FIGS.EXT software for the standard

proportion tooth models 8 and 9 as shown in **Table A-5.1** is within 10 per cent, it is assumed that the values of the load height, tooth thickness and the Lewis x-factor determined by FIGS.EXT software for the model 10 are correct and this tooth model is considered in stress concentration analysis for the gear tooth.

Figure 5.4(a) shows variation of the tooth thickness with the distance Y for the model 3 and 6. The tooth thickness, determined at the Lewis weakest section by the graphical method, Broghamer and Dolan, and FIGS.EXT software, increases as the intersection of the line of action and the tooth axis moves farther from the addendum circle.

Figure 5.4(b) indicates the variation of the load height with the distance Y. The load height, determined by the graphical method, Broghamer and Dolan and FIGS.EXT software, decreases as the intersection of the line of action and the tooth axis moves farther from the addendum circle.

Thus the variation in the dimensions of the Lewis weakest section determined by FIGS.EXT software, graphical method and Broghamer and Dolan are similar.

5.3.4   FIGS.EXT Software Capabilities:

FIGS.EXT software consistency with the graphical method for generating the tooth layout and determining the accurate
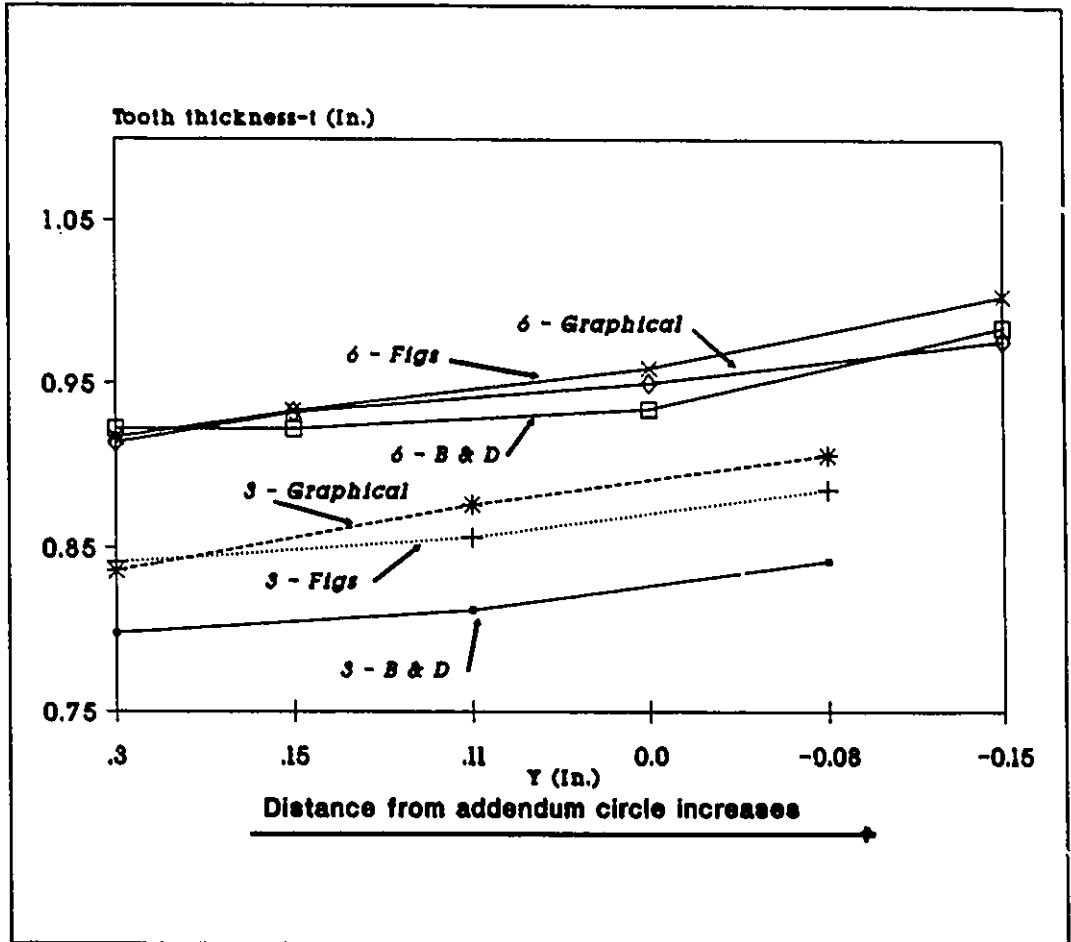
FIGURE 5.4(a): TOOTH THICKNESS VARIATION FOR TOOTH
MODEL 3 AND 6
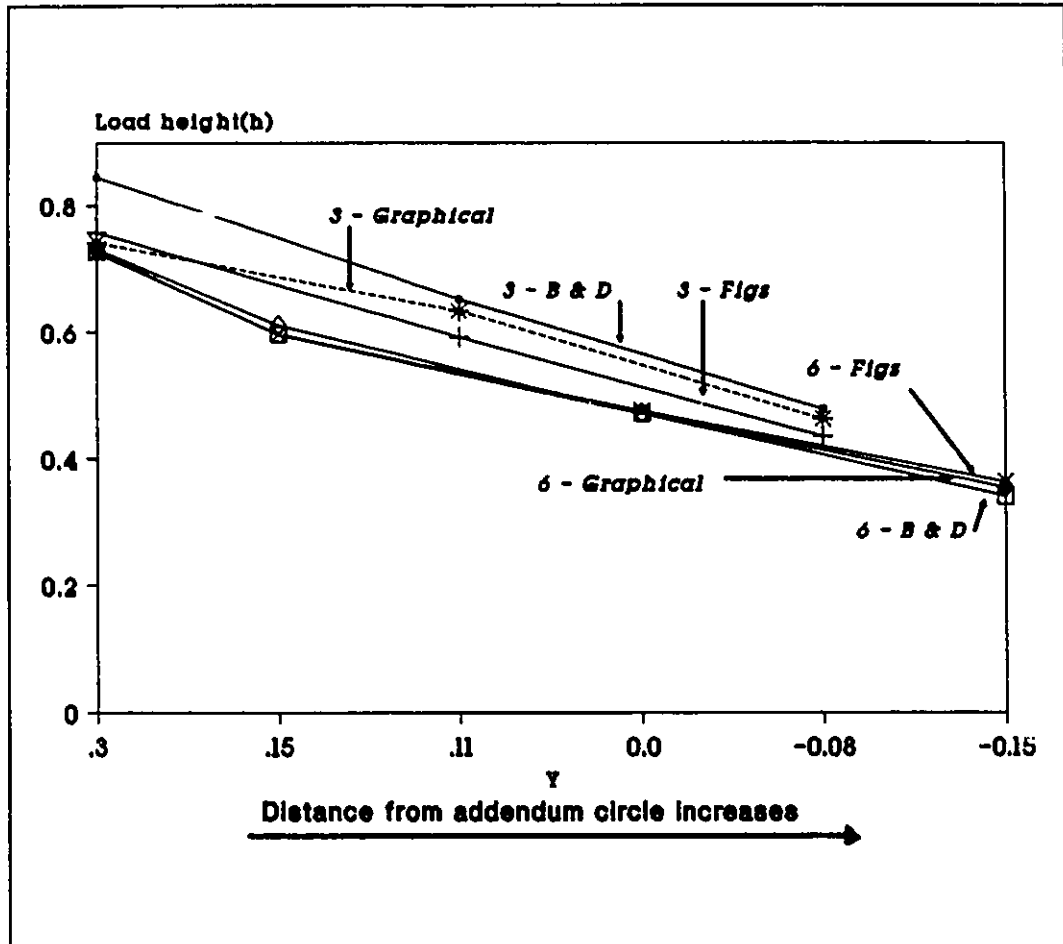
FIGURE 5.4(b): LOAD HEIGHT VARIATION FOR MODEL 3 AND 6

61

Lewis x-factor for models 6 to 11 as shown in **Table A-5.1,** indicates that FIGS.EXT software can be used for standard proportion tooth models. Since FIGS.EXT software can determine the Lewis x-factor for tooth models 4 and 5 as shown in **Table A-5.1** within 10 per cent error, it can also be used for non standard proportion tooth models.

Table A-5.2 shows the comparison of the Lewis form factor determined by FIGS.EXT software and AGMA for the tooth models having the number of teeth in range of 12 to 300. These identical Lewis form factors reveal that FIGS.EXT software can be undoubtly used for a varying number of teeth and size of the gear. This comparison also shows that FIGS.EXT software can also be used for the load at the tip of the tooth.

It is interesting to note how FIGS.EXT software has accurately determined the values of the load angle (**Table A-5.1**) for each case of the tooth models 4 to 11. The concept for variation in the value of load angle corresponding to the position of the load on tooth axis is derived from the equation 5.4. It should be recalled that the position of load is given in terms of the distance Y measured from the pitch circle. For positive value of Y (Load position is above the pitch circle), the value of the load angle is always greater than the value of the respective pressure angle. The load angle and the pressure angle are identical corresponding to zero value of Y (Load position at the pitch circle). While in case of the negative value of Y (load position below the pitch

62

circle), value of the load angle is always less than the value of respective pressure angle.

Examining values of the load angle determined by Broghamer and Dolan for each case of the model 3 to 10 having value of Y equal to zero, it reveals that these values are <u>never</u> equal to the respective pressure angles. With reference to these cases, FIGS.EXT software has determined the correct values of the load angle. Broghamer and Dolan identified incorrect values of the load angle as 20° and 14.5° corresponding to the negative values of Y in each case of the model 8 and 11 respectively. FIGS.EXT software has determined 18.78° and 12.72° for these cases. Thus for each case of the models 4 to 11, the correct value of the load angle is determined by FIGS.EXT software.

5.3.5 Maximum Nominal Tensile Stress And Dimensions Of The Theoretical Weakest Section.

The value of the localised radius of the trochoid contour, load height, tooth thickness and maximum nominal tensile stress corresponding to the theoretical weakest section for each case of the tooth models 4 to 11 are cited in **Table A-5.1.** These values are compared with the values of the load height and tooth thickness corresponding to the Lewis weakest section to determine the difference P_h and P_t as shown in **Table A-5.1** for each case of the tooth models. Distance

63

between the location of the theoretical weakest section and the Lewis weakest section is recorded in **Table A-5.1** under column headed "C". It should be noted that the localised dimensions of the model 3 are not considered in this analysis.

The value of the load height(h_l) corresponding to the theoretical weakest section is always bigger than that of the Lewis weakest section in each case of the tooth models. The maximum distance between the location of the theoretical weakest section and the Lewis weakest section is found to be 0.01". In only 2.4 percent of the cases are these sections found at the same location. This indicates that the location of the theoretical weakest section is always lower on the root profile than the location of the Lewis weakest section. The reason, that this theoretical weakest section is found lower on the root profile, is that the direct compressive stress produced by the axial component of the load is considered, while determining the theoretical weakest section.

In the photoelasticity experiments, the location of the actual weakest section corresponding to the maximum tensile stress is also found slightly lower than that of the Lewis weakest section but unfortunately the maximum distance between the actual weakest section and the Lewis weakest section distance was not recorded. Thus exact location of the actual weakest section is not known. Therefore it is difficult to say that the location discrepancy between the Lewis weakest section and the actual weakest section is completely

64

eliminated and the location of the theoretical weakest section is the location of the actual weakest section.

Tooth thickness of the theoretical weakest section is larger than that of the Lewis weakest section for each case of these models in range of 0.0 to 8.0 per cent. The reason for this increased tooth thickness is that the location of the theoretical weakest section is lower on the root profile.

A comparison of the localised radius of the trochoid contour and the minimum trochoid radius shows that the former radius is always bigger than the latter radius, in a range of 2.8 to 63.9 per cent for these models.

6   BENDING STRESS CONCENTRATION AS A FUNCTION OF
            LOCALISED VARIABLES.

6.1 Purpose:

The purpose of making the bending stress concentration factor dependent on the localised variables is:

(1) To determine the bending stress concentration factors(K and K_c) considering the nominal tooth stresses calculated at the theoretical weakest section.

(2) To develop the single equation of the bending stress concentration factor in terms of the localised dimensions of the theoretical weakest section.

6.2 Methodology

.

6.2.1   Bending Stress Concentration Factors For 20° And 14.5° Pressure Angle Teeth

The experimental value of the maximum tensile stress and the maximum compressive stress for each case of the tooth models 3 to 11 in **Table A-5.1**, shows the value of the resultant stress due to the bending stress and the direct compressive stress produced at the actual weakest section. Therefore bending stress concentration factors(K and K_c) for

gear teeth should be defined as the ratio of the maximum tooth stress to the nominal tooth stress determined at the theoretical weakest section. The value of the bending stress concentration factors for each case of the tooth models are calculated by using the equation 2.5 and 2.9 and listed **in Table A-5.1.**

Stress concentration is a localised phenomenon and bending stress concentration factor should be dependent on the localised dimensions of the theoretical weakest section instead of the Lewis weakest section and the minimum trochoid radius of the root profile. Hence the equations - 6.1 for 20° and 6.2 for 14.5° pressure angle teeth, are developed by performing multiple log linear regression using localised dimensions of each respective case of the tooth models. These equations are:

For 20° pressure angle teeth.

$$K=1.18 \left(\frac{t_l}{r_l}\right)^{0.24} \left(\frac{t_l}{h_l}\right)^{0.23} \text{-----------} (6.1)$$

For 14.5° pressure angle teeth.

$$K=1.29 \left(\frac{t_l}{r_l}\right)^{0.27} \left(\frac{t_l}{h_l}\right)^{0.22} \text{------------} (6.2)$$

Where t_l, h_l and r_l are the localised tooth dimensions.

67

In order to carry out the statistical analysis of these equations, parameters such as average error, standard deviation and range of 3σ limits obtained in determining the maximum tensile stress, are calculated in the same manner as that explained in section 4.2.3. Broghamer and Dolan data for ratios of t/h and t/r_t is plotted against the experimental stress concentration factor as determined at the Lewis weakest section by the equation 2.5.

6.2.2 Bending Stress Concentration Factors - Independent Of The Pressure Angle.

If bending stress concentration is dependent on the theoretical weakest section, then why should it not be independent of the pressure angle?

The answer to this question is explained from the variation in the radius of the trochoid contour and tooth thickness of the generated contour for 14.5° and 20° pressure angle teeth. The tooth thickness at the weakest section for 14.5° pressure angle teeth is smaller than that of the corresponding 20° pressure angle teeth. However the localised radius of the trochoid contour is larger in 14.5° pressure angle teeth than that of the corresponding 20° pressure angle teeth. This fact can also be seen by comparing the values of the tooth thickness and the localised radius of the trochoid contour for corresponding tooth models (6 & 9), (7 & 10) and

68

(8 & 11) of 14.5° and 20° pressure angle teeth in **Table A-5.1.**
When bending stress concentration factors are made dependent
on the localised radius of the trochoid contour and tooth
thickness, then it should not be dependent on the
pressure angle. Based on this concept, a log linear equation,
for bending stress concentration factor using the dimensions
of the theoretical weakest section of all tooth models 4 to
11, is developed in the same fashion as described in section
4.2.2. The equation is:

$$K=1.31 \left(\frac{t_1}{r_1}\right)^{0.22} \left(\frac{t_1}{h_1}\right)^{0.22} \text{------------(6.3)}$$

Average error, standard deviation, accuracy and range for
3σ limits of the error obtained in determining the maximum
tensile stress by this equation are computed and compared with
those determined for Broghamer and Dolan equations as well as
equations 6.1 and 6.2.

6.3   Results/discussion:

6.3.1   Bending Stress Concentration Factors:

Bending stress concentration factors(tensile) and bending
stress concentration factors(compressive) based on the
dimensions of the theoretical weakest section are found in the
range of 1.50 to 2.77 and 1.61 to 3.39 respectively.
Compressive bending stress concentration factors are computed

TABLE 6.1: RANGE FOR BENDING STRESS CONCENTRATION
FACTORS BASED ON LEWIS WEAKEST SECTION
AND THEORETICAL WEAKEST SECTION.

Stress concentration factor		Lewis weakest section	Theoretical weakest section	Difference Percent
K_c	Max	3.75	3.39	-9.60
	Min	1.66	1.61	-3.01
K	Max	2.47	2.77	12.15
	Min	1.51	1.50	-0.66

only to prove that the higher stresses are developed on the compressive side of the tooth even if direct compressive stress is considered. Comparison of the maximum and minimum values of these stress concentration factors with those determined by Broghamer and Dolan is made in **Table 6.1**. It shows that the difference in the values of bending stress concentration factors (tensile) and bending stress concentration factors (compressive) is in the range of 0.66% to 12.15% compared to those determined by Broghamer and Dolan. This difference is due to correction in the values of the load angle and converting these bending stress concentration factors dependent on the theoretical weakest section for each case of the tooth model.

Figure 6.1 shows a plot of equation 6.3. The value of the tensile bending stress concentration factor K increases with general increase of t_1/h_1 and t_1/r_1 ratios. This equation comes from a best fit to the experimental results of Broghamer and Dolan, and smooths out the extremes as found in **Figures 6.2 and 6.3**. **Figures 6.2 and 6.3** show the plots of Broghamer and Dolan data (t/h and t/r_f) and experimental stress concentration factor (Exp K).

The extremes of these figures show possible errors of Broghamer and Dolan results.
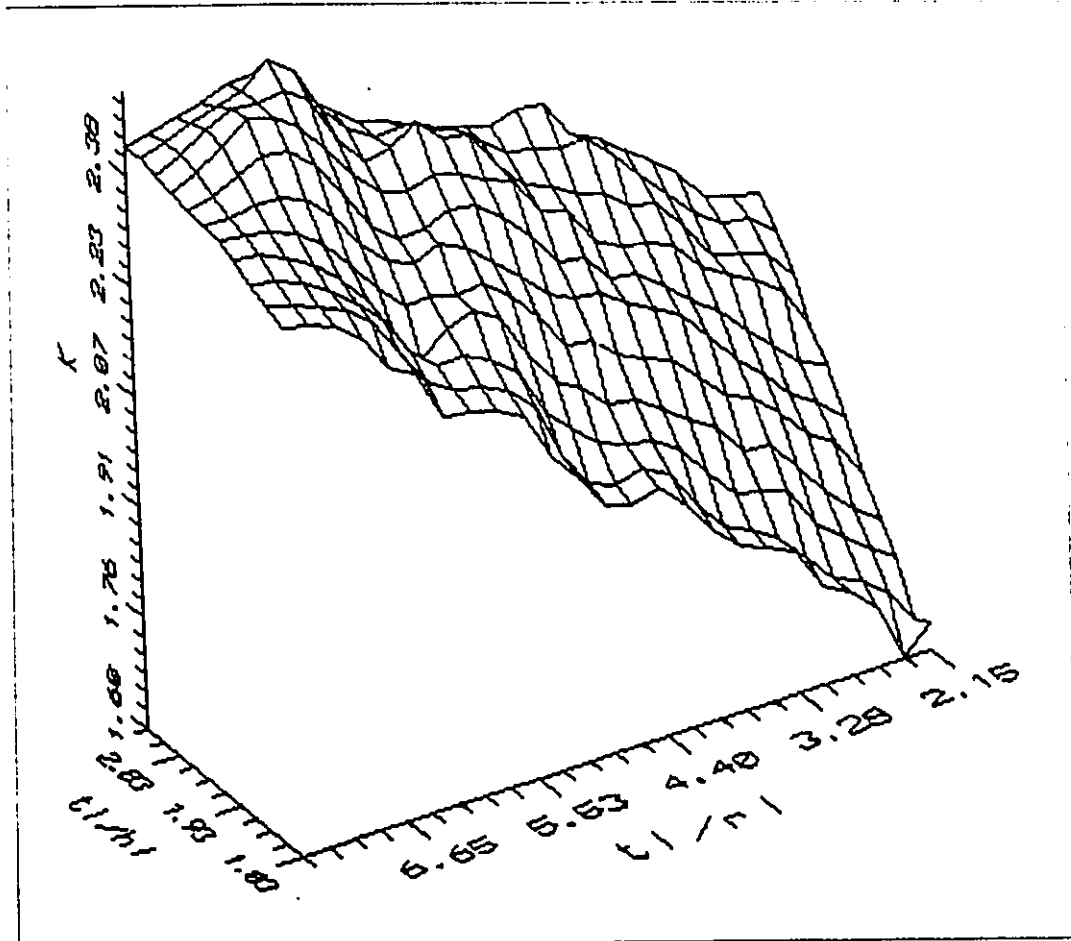
FIGURE 6.1: VARIATION OF STRESS CONCENTRATION FACTOR WITH RATIO OF t_1/r_1 AND t_1/h_1 [EQUATION 6.3]
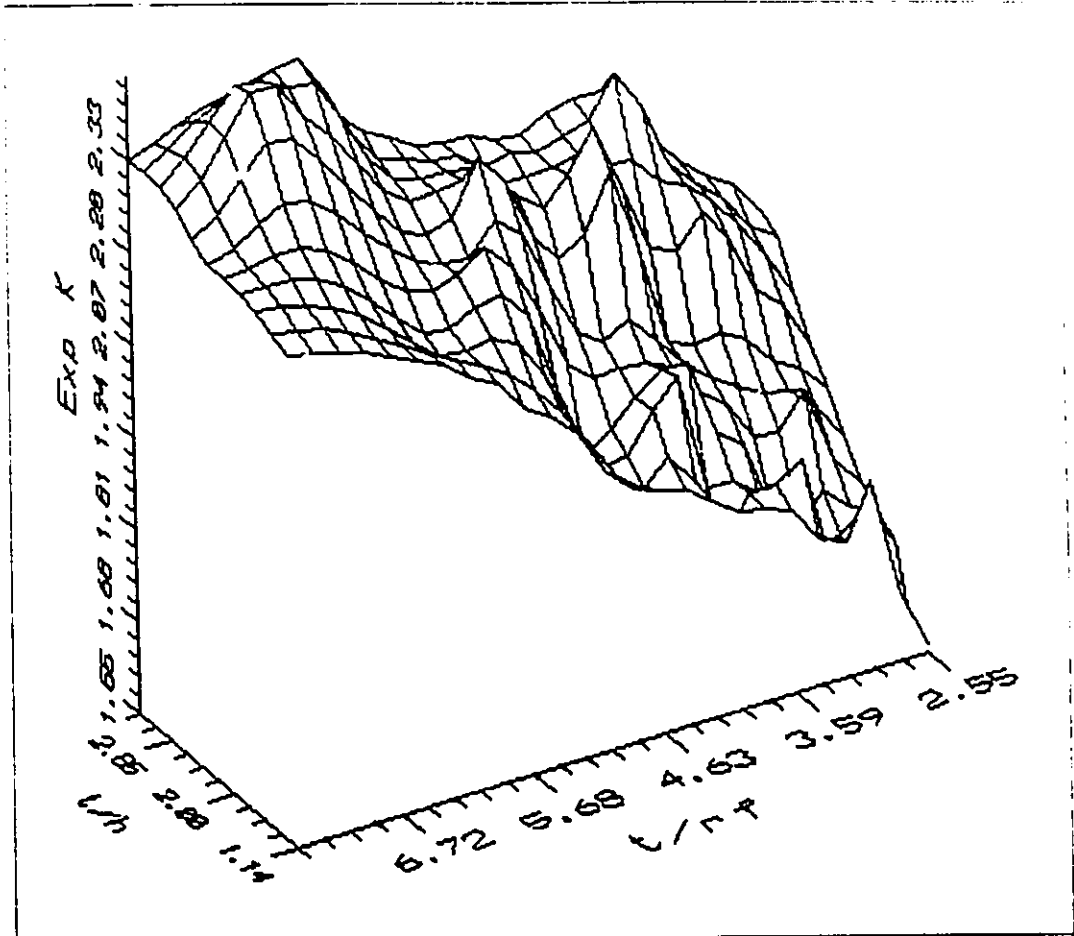
FIGURE 6.2: VARIATION OF STRESS CONCENTRATION FACTOR WITH
RATIOS t/r_f AND t/h FOR 20° PRESSURE ANGLE
TEETH [TABLE A-5.1]
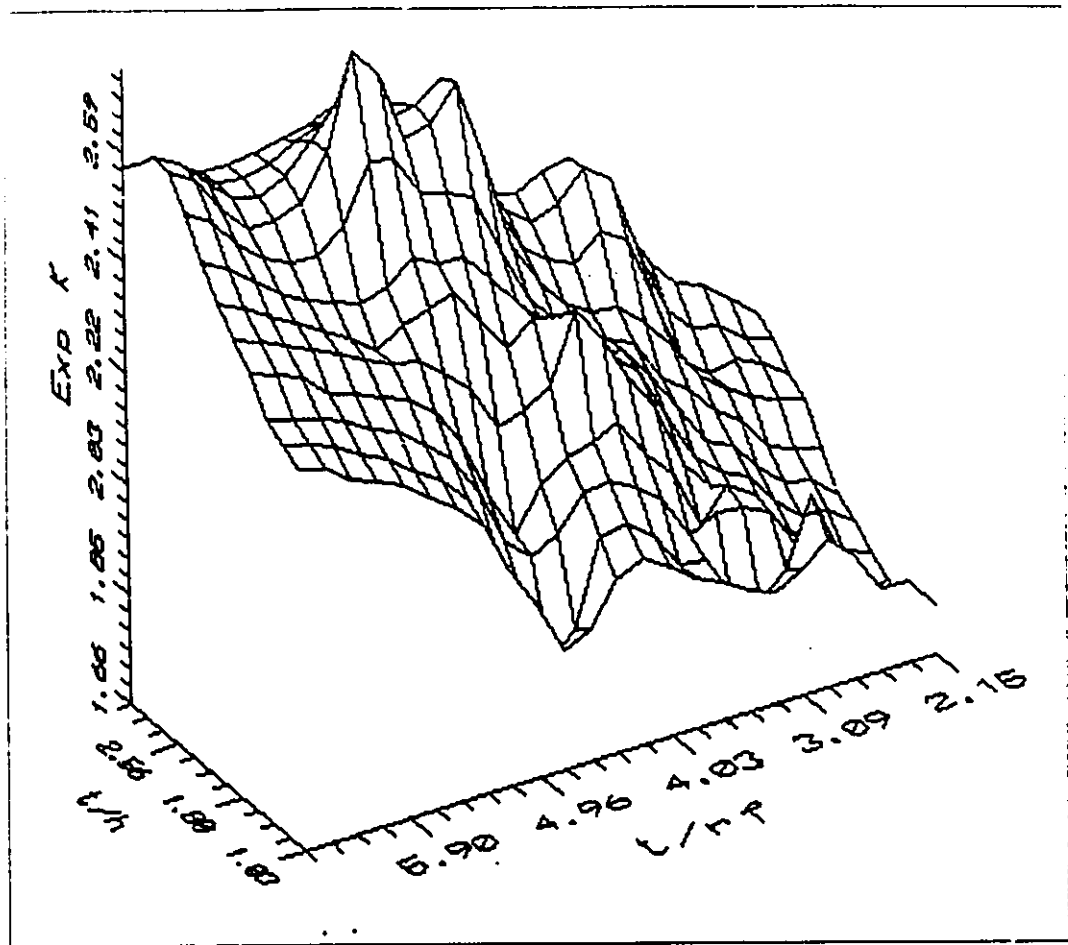
FIGURE 6.3: VARIATION OF STRESS CONCENTRATION FACTOR WITH
RATIOS t/r_f AND t/h FOR 14.5° PRESSURE ANGLE
TEETH [TABLE A-5.1]

6.3.2   Statistical Analysis Of Equations For Gear Tooth Stress Concentration.

Table 6.2 shows the comparison of statistical parameters of the Broghamer and Dolan equations, and the equations based on the dimensions of the theoretical weakest section. It is found that the average error of all the log linear equations is approximately the same however the spread(σ) is larger for these equations.

The single equation 6.3 shows that bending stress concentration factors are dependent only on localised tooth dimensions and these stress concentration factors are now independent of following variables.

(1) Manufacturing method, for example generating and forming method. As long as the ratios of t_i/h_i and t_i/r_i fall in specified limits(page 102), this equation can be used to determine bending stress concentration for the gear teeth.

(2) Type of tooth profile, for example involute, circular or cycloidal tooth profile. Stress concentration depends on the geometry where it occurs in root profile of the gear teeth and hence the stress concentration does not depend on the geometry of the tooth profile where stress concentration does not occur.

The average error and standard deviation of the single equation are -0.28 per cent and 7.51 per cent respectively. The standard deviation of the error for the single equation is

TABLE 6.2:   STATISTICAL PARAMETERS FOR EQUATIONS OF BENDING STRESS CONCENTRATION FACTOR.

Equations	Basis	ϕ deg.	μ per cent	σ per cent	Range-3σ per cent
Broghamer & Dolan	Lewis weakest section & minimum trochoid radius	14.5	-0.11	2.22	-6.77 to 6.55
		20	-0.49	2.25	-7.24 to 6.26
Log Linear	Theoretical weakest section & localised trochoid radius	14.5	0.75	6.71	-19.38 to 20.88
		20	0.19	5.48	-16.24 to 16.63
Single equation	Theoretical weakest section & localised trochoid radius	-	-0.28	7.51	-22.81 to 22.25

76

slightly increased compared to that of the equation for 14.5 pressure angle teeth (separate equations). The maximum error between the values of the maximum tensile stress as determined by the single equation and experimental tensile stress is 17.5 per cent.

7 DETERMINATION OF MAXIMUM TENSILE STRESS AND ITS LOCATION FOR THE SPUR GEAR TEETH.

7.1 Purpose:

The purpose of determining the maximum tensile stress and its location is to present the general solution of the bending stress concentration for the gear tooth.

7.2 Methodology:

7.2.1 Maximum Tensile Stress And Its Location.

The value of maximum tensile stress (M_{bs}) for each of the tooth models 4 to 11 is determined as follow.

$$M_{bs}=K*\sigma_t$$

$$M_{bs}=K(S_1-S_a)$$

$$M_{bs}=[1.31(\frac{t_1}{r_1})^{0.22}(\frac{t_1}{h_1})^{0.22}](S_1-S_a)$$

$$M_{bs}=1.31(\frac{t_1}{r_1})^{0.22}(\frac{t_1}{h_1})^{0.22}(\frac{6P_{ts}h_1}{Ft_1^2}-\frac{P_a}{Ft_1}) \ ----- (7.1)$$

It is assumed that stress concentration factor is the same for bending and direct compressive stress in determining the maximum tensile stress because the explicite experimental

78

value for either stress explicitly is not available. Equation 7.1 shows that the maximum tensile stress depends upon the tooth load and the localised dimensions of the theoretical weakest section. This maximum tensile stress for each case of the tooth models is plotted against the ratios of t_i/r_i and t_i/h_i. Furthermore the location of the maximum tensile stress is also determined from the free end of the tooth for each case of the tooth models. This distance can be found under the column headed "L" in **Table A-5.1.** Thus a general solution for the gear tooth models 4 to 11 is obtained.

7.3 Results/Discussion:

7.3.1 Variation Of Maximum Tensile Stress With Respect To Localised Dimensions Of the Gear Teeth

Figure 7.1 represents equation 6.3 multiplied by the nominal tensile stress at the theoretical weakest section in the form of M_{ba}. It indicates that the maximum tensile stress increases with the genral decrease of t_i/h_i and t_i/r_i ratios. As equation 6.3 is derived for a best fit of the experimental data of **Figure** 7.2 and **Figure** 7.3, the results are somewhat smoother. **Figures** 7.2 **and** 7.3 suggest possible experimental errors. Hence it is assumed that the spikes in **Figure** 7.1 are a result of experimental errors in Broghamer and Dolan data.
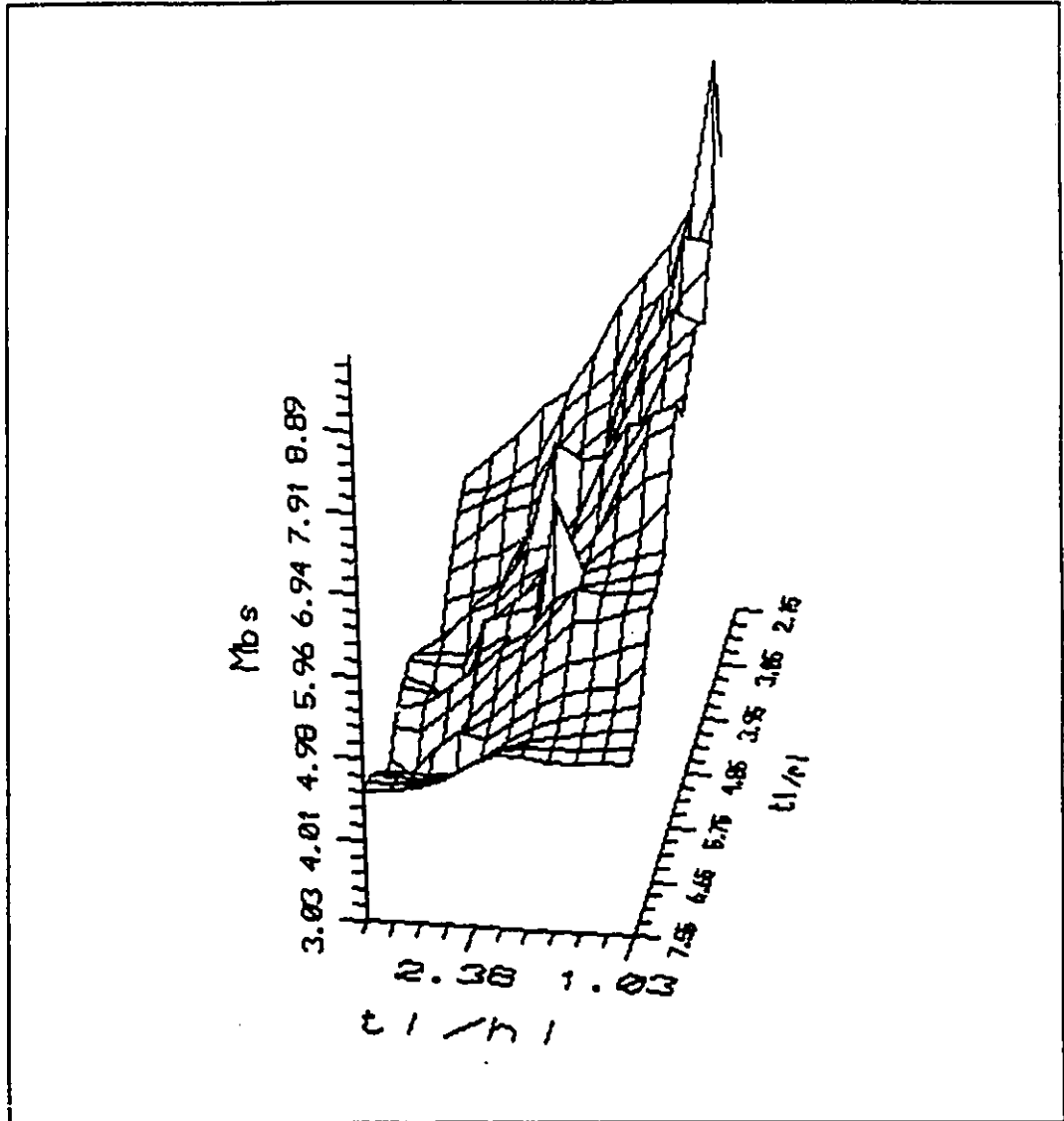
FIGURE 7.1: MAXIMUM TENSILE STRESS FOR THE SPUR GEAR TEETH
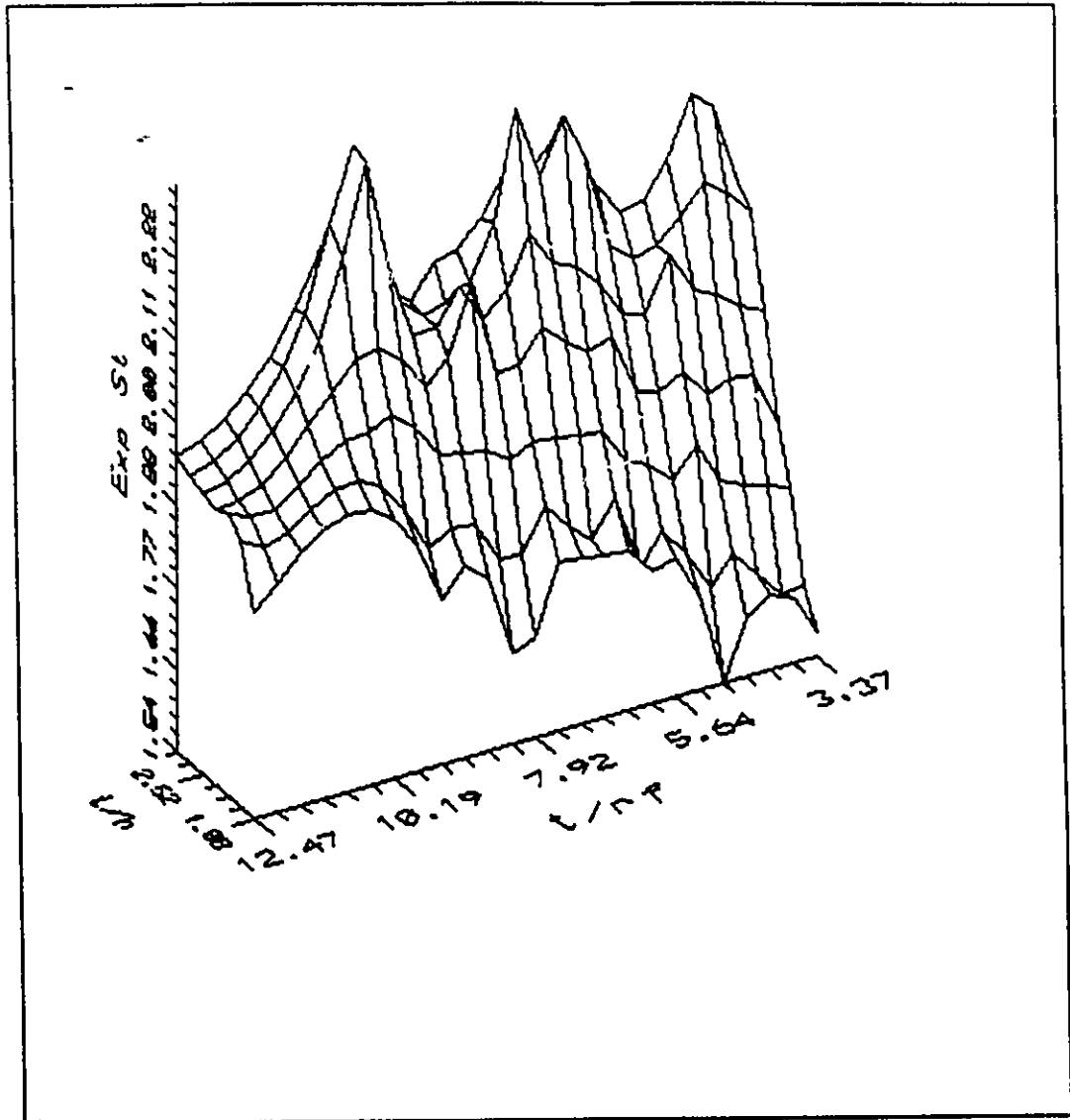
FIGURE 7.2: VARIATION IN EXPERIMENTAL MAXIMUM TENSILE
STRESS WITH t/r_t AND t/h RATIOS FOR 20°
PRESSURE ANGLE TEETH

---

[1] Data for t, h and r_t are given in **Table A-5.1**
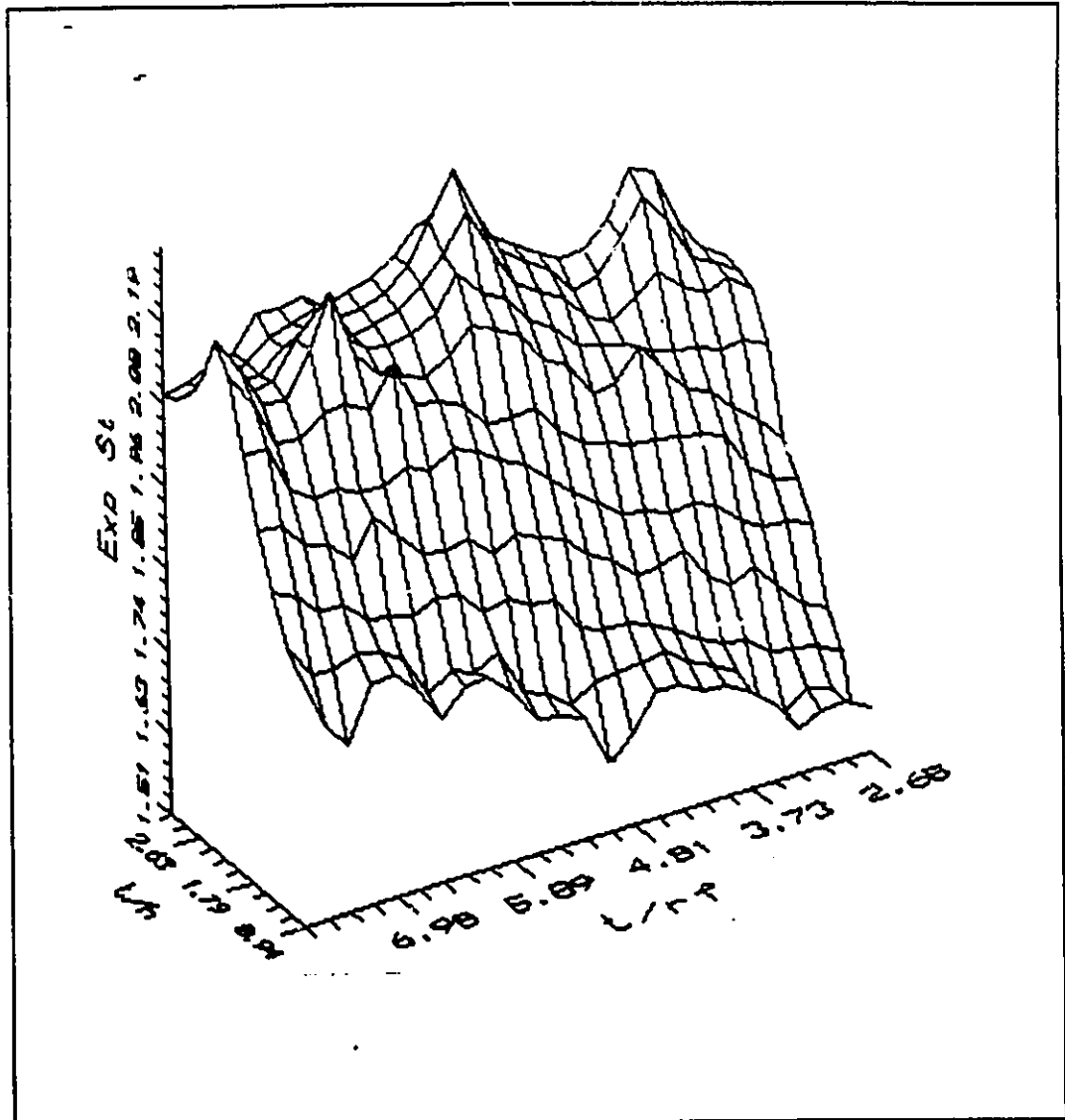
FIGURE 7.3: VARIATION IN EXPERIMENTAL MAXIMUM TENSILE STRESS WITH RATIOS OF t/r^f AND t/h FOR 14.5° PRESSURE ANGLE TEETH

---

[2] Data for t, h and r_f are given in **Table A-5.1**

8   THE GENERAL SOLUTION OF THE STRESS CONCENTRATION FOR BEAM BENDING.

8.1   Purpose:

The purpose is to determine if equation 7.1 can be used to accurately predict the magnitude and location of the bending stress in a cantilever beam.

8.2   Methodology:

Maximum tensile stress, developed in Broghamers photoelastic experiments for the conventionalised gear tooth models, is found **slightly larger** than that of the standard gear tooth models of similar proportion, if direct compressive stress is considered in the gear tooth stress concentration. This conclusion provided a direction that if loading condition and localised geometry(t_i/r_i and t_i/h_i) of the proportionate cantilver beam, defined as below, are similar to the gear tooth cases, the maximum tensile stress and its location for these "proportionate" cantilever beams should be estimated by the euqation 7.1. Based on this concept, an attempt was made here to determine the maximum tensile stress and its location for these proportionate cantilever beams by two procedures- One uses finite element analysis and second uses the equation 7.1.

These proportionate cantilver beams are of unit width and the distance of the load position from the fixed end of the cantileve: beam is identical to the distance of the load position from the dedendum circle in the respective tooth case. The value of the fillet radius is also equal to the value of the localised radius of the trochoid contour of the corresponding tooth case. In order be to consistent with the corresponding gear tooth case for load direction, the load was applied at an angle equal to the load angle of the corresponding tooth case in these conventionalised models instead of applying only perpendicular load to the cantilever surface, in the same fashion as Broghamer and Dolan did during the experiments. The methodology to compare the general solutions obtained from the two procedures is as follows.

(1)   Six tip loaded cantilever beam models, three of them subjected to tensile load and the rest of them subjected to bending load, are analyzed by the finite element technique to determine the maximum tensile stress developed in their filleted section. This value of the maximum tensile stress is then compared with the theoretical maximum tensile stress determined by using the stress concentration factors taken from reference [1.3]. Thus this comparison ensures the accuracy of the finite element analysis(FEA) to determine the maximum tensile stress for these kinds of models.

(2)   Four proportionate cantilever beam models, similar
        to cases 5, 6, 7 and 8 of the model 6, are defined
        and analyzed to determine the maximum tensile stress
        and its location by FEA. This value of the maximum
        tensile stress and its location is compared with
        that obtained from the equation 7.1 for each case.
        In order to minimize the statistical error of
        equation 7.1 in this comparison, only the above
        cases with less than 5 per cent error in the values
        of the maximum tensile stress determined by this
        equation and the experimental maximum tensile stress
        are selected for this verification.

8.2.1   Finite Element Analysis(FEA):

Dimensions of the cantilever beam models are listed in
Table 8.1. **Figure 8.1** shows the cantilever beam models and
their loading condition. These models are generated in
ALGOR -finite element software that performs the static stress
analysis. **Figures 8.2(a) to (f)** indicate the FEA models of
these cantilever beams. The value of the maximum tensile
stress is compared with the reference value [1.3] of the
stress obtained as follows to determine the error in these
values of the maximum tensile stress. The error is calculated
by the equation 4.1.

TABLE 8.1 : DIMENSIONS OF CANTILEVER BEAMS.

Model	Loading condition	r_c in.	d_c in.	D_c in.	l_c in.	t_c in.
1	Tensile Load	0.4	1.5	2.25	1.2	0.04
2		0.3	2.0	2.62	4.0	0.04
3		0.5	2.0	3.0	1.2	0.04
4	Bending Load	0.3	2.0	2.6	4.0	0.05
5		0.4	2.0	2.6	4.0	0.05
6		0.4	2.66	2.6	4.0	0.05
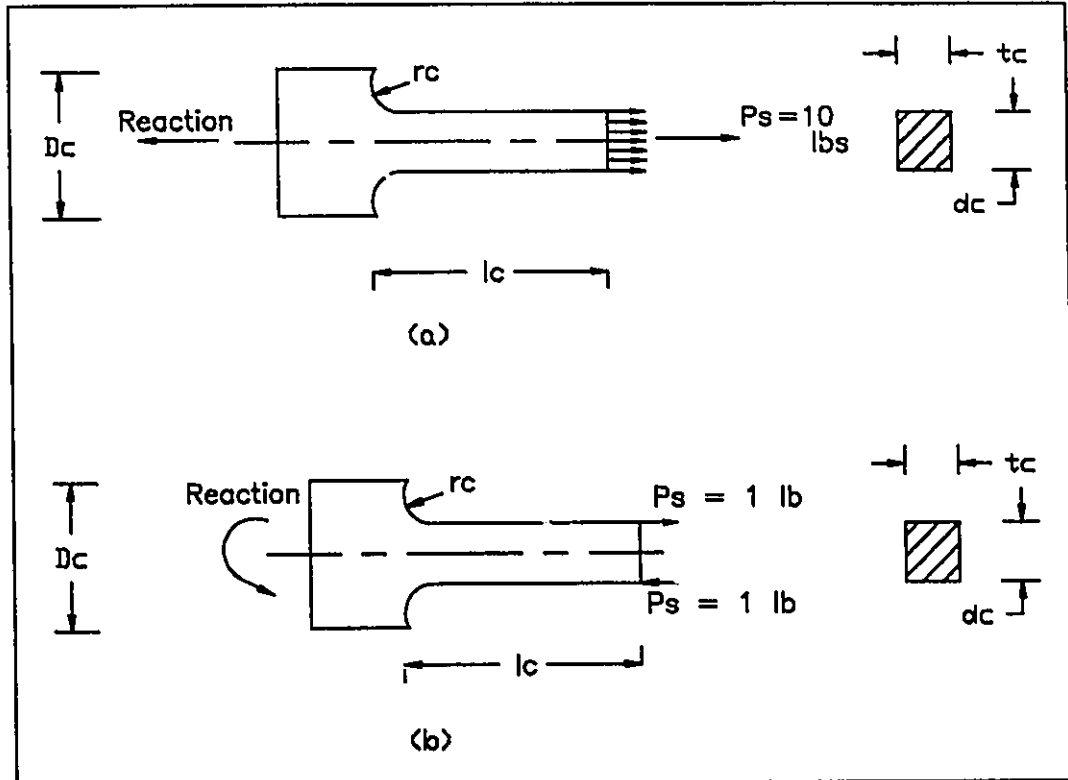
FIGURE 8.1: CANTILEVER BEAM
    (a) SUBJECTED TO TENSILE LOAD
    (b) SUBJECTED TO BENDING LOAD
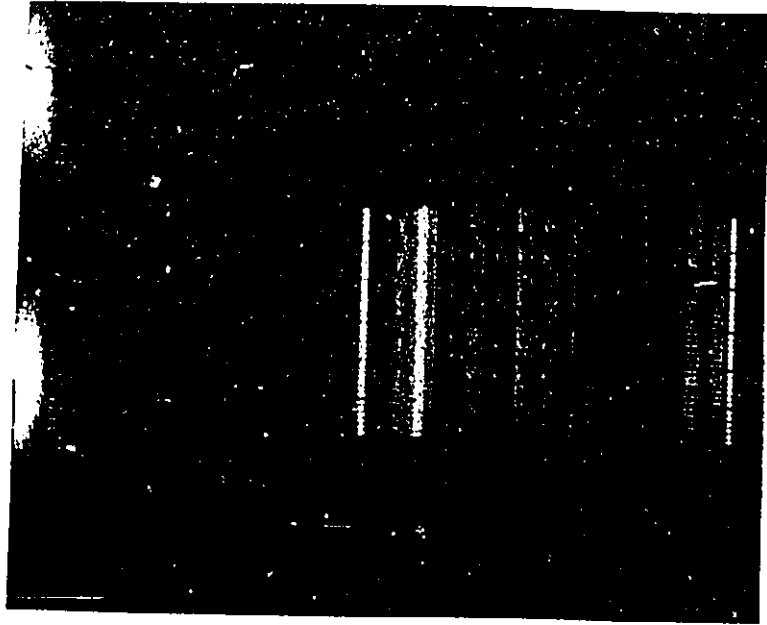
FIGURE 8.2(a): FEA - CANTILEVER BEAM MODEL 1
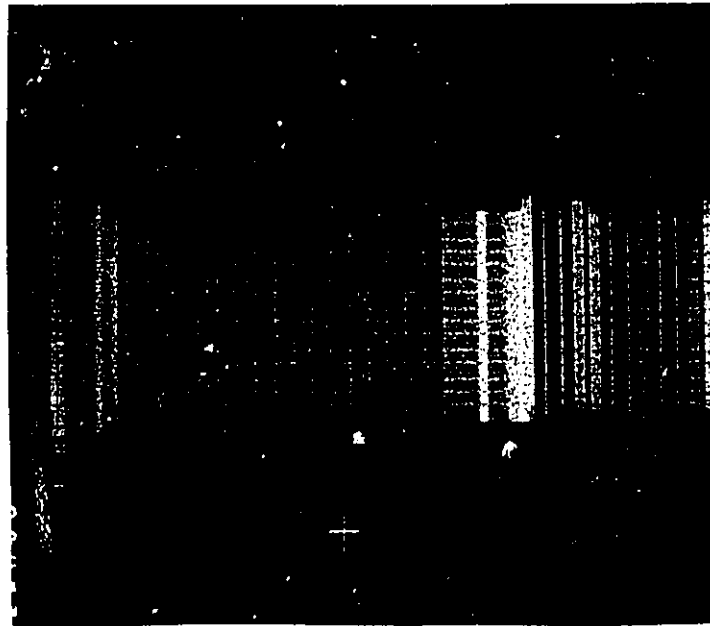
FIGURE 8.2(b): FEA CANTILEVER BEAM MODEL 2
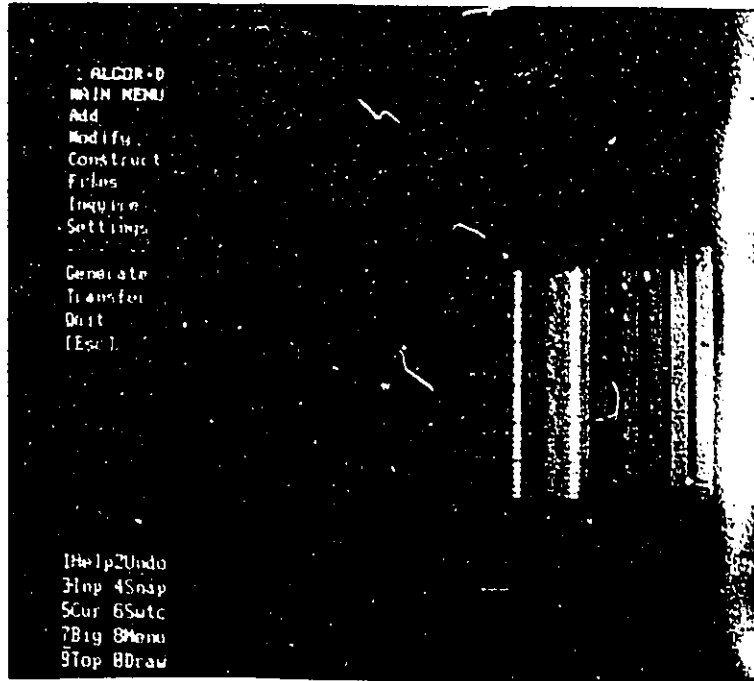
FIGURE 8.2(c): FEA - CANTILEVER BEAM MODEL 3
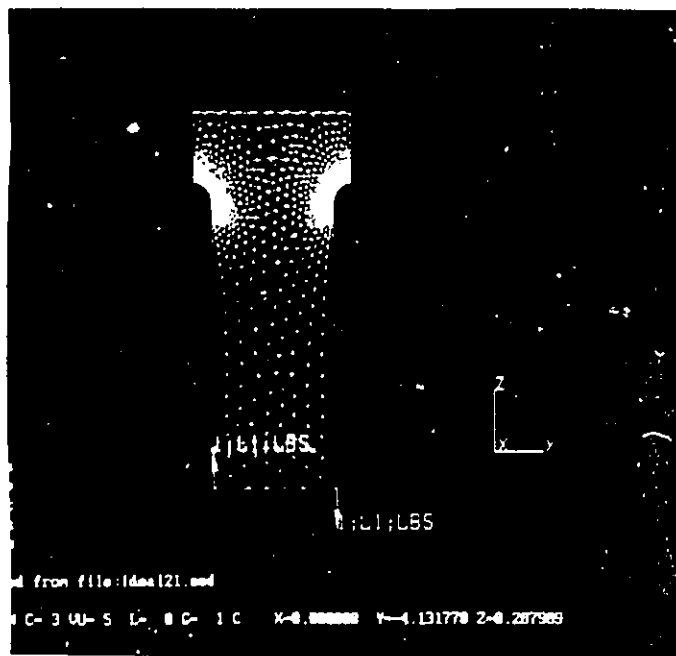
FIGURE 8.2(d): FEA CANTILEVER BEAM MODEL 4
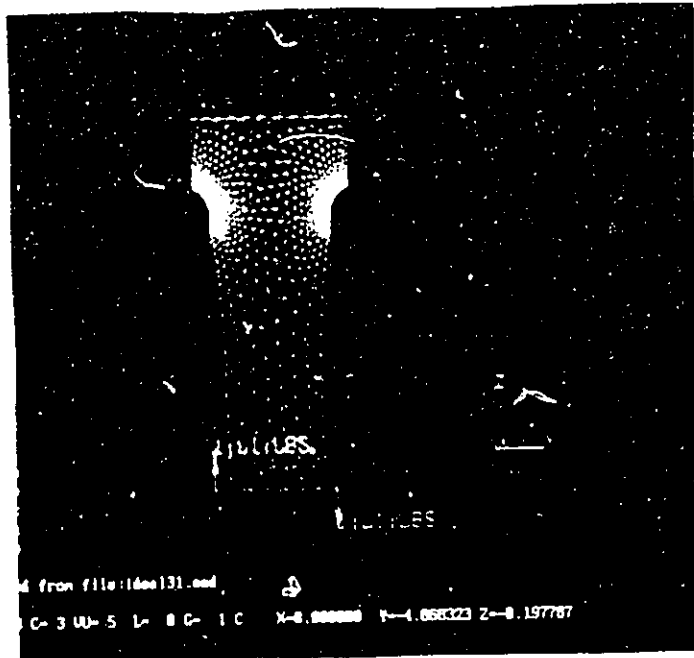
FIGURE 8.2(e): FEA - CANTILEVER BEAM MODEL 5
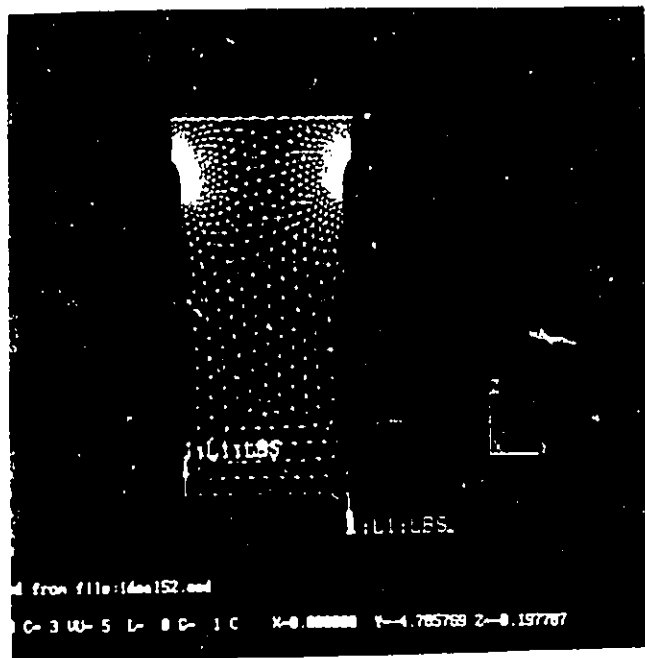
FIGURE 8.2(f): FEA CANTILEVER BEAM MODEL 6

$$S_t = \sigma_t * K_b \ \text{------------} (8.1)$$

Where σ_t = $P_3 / t_r * d$. ------- For tensile load

$= P_3 * d_i * (d_i/2) / t_r * (d_i^3/12)$ ---- For bending load

K_b = Stress concentration factors taken from
reference [1.3].

8.2.2 Maximum Tensile Stress And Its Location Of The Proportionate Cantilever Beam.

Table 8.2 shows the dimensions of the proportionate cantilever beam models. **Figure 8.3** shows the proportionate cantilever beam. These proportionate cantilever beams are modelled and analyzed in Algor software in the same fashion as used for cantilever beams to determine the maximum tensile stress(FEA), its corresponding section thickness(t_n) and load height(h_a). These values of the maximum tensile stress is then compared with the values of the maximum tensile stress of the corresponding cases 5, 6, 7 and 8 of the tooth model 6 as determined by the equation 7.1.

8.3 Results/Discussions:

8.3.1 Maximum Tensile Stress Of The Cantilever Beam - Finite Element Analysis.

Table 8.3 indicates the maximum tensile stress for

91

TABLE 8.2 : DIMENSIONS OF PROPORTIONATE CANTILEVER BEAMS

Model	r_c in.	d_c in.	ϕ_1 deg.	l_c in.	D_c in.	b_c in.
1	0.327	0.826	27.56	1.078	1.378	0.878
2	0.299	0.826	24.17	1.078	1.412	0.728
3	0.267	0.826	20.00	1.078	1.354	0.578
4	0.234	0.826	14.36	1.078	1.28	0.428
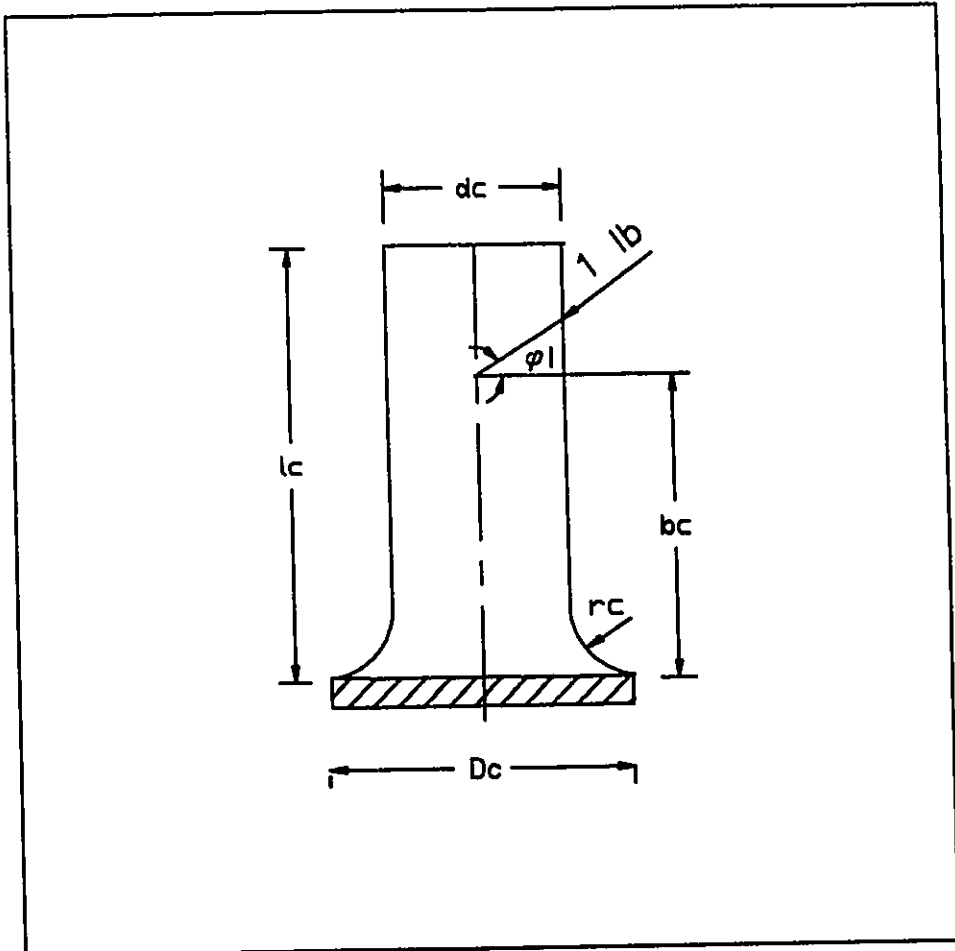
FIGURE 8.3: PROPORTIONATE CANTILEVER BEAM

TABLE 8.3: MAXIMUM TENSILE STRESS FOR CANTILEVER BEAMS

Model	Type of Load	K_b [1.3]	σ_t psi	Maximum tensile stress(S_t)		
				Theoretical $\sigma_t * K_b$ psi	FEA psi	P_{st} per cent
1	Tensile Load	1.65	166.67	275.00	258.65	-5.95
2		1.70	125.00	212.50	206.48	-2.87
3		1.65	125.00	206.25	191.08	-7.36
4	Bending load	1.62	60.00	97.20	92.38	-4.95
5		1.57	60.00	94.20	86.45	-8.23
6		1.52	45.11	68.57	62.40	-8.99
					Absolute Average Error:	6.00%

the cantilever beams as determined from the finite element analysis. **Figures 8.4(a) to (f)** show the stress contours obtained in the finite element analysis for these models. The maximum tensile stress obtained by FEA for each case of the cantilever models is less than the maximum tensile stress determined from the equation 8.1 in the range of 2.87 to 8.99 per cent. Hence it can be implied that this method of finite elements determines the magnitude of the maximum tensile stress with an absolute average error of about 6.0 per cent compared to that value of the reference[1.3]

8.3.2 Maximum Tensile Stress And Its Location In The Proportionate Cantilever Beam.

A comparison of the maximum tensile stress and its location for the proportionate cantilever beams determined by the finite element analysis and the equation 7.1 for their corresponding gear tooth cases is shown in **Table 8.4**. Maximum tensile stress as determined by the finite element analysis for each proportionate cantilever beam is smaller than that of the corresponding gear tooth case(equation 7.1). However the value of ratios t_c/r_c and t_c/h_c falls in the specified range of the localised tooth dimensions of the gear teeth as shown in **Table 8.5**, the difference in the values of the maximum tensile stress as determined from the FEA and the equation 7.1 for the proportionate cantilever beam is in the range of 6 to 21 per
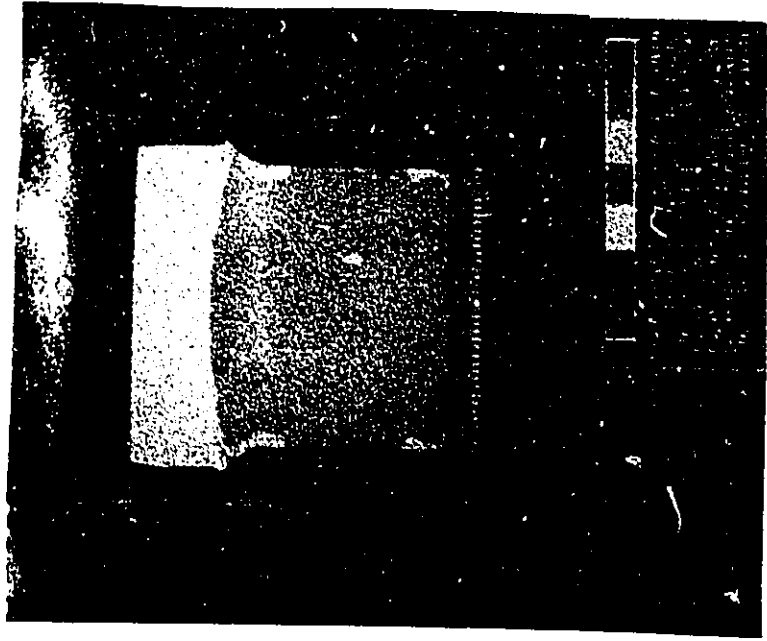
FIGURE 8.4(a): FEA – STRESSES FOR CANTILEVER BEAM MODEL 1

FIGURE 8.4(b): FEA STRESSES FOR CANTILEVER BEAM MODEL 2
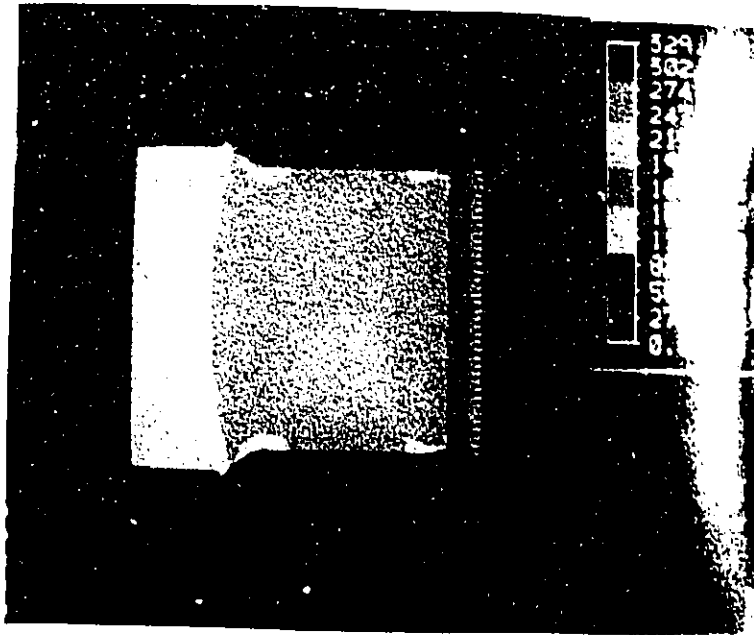
FIGURE 8.4(c): FEA - STRESSES FOR CANTILEVER BEAM MODEL 3
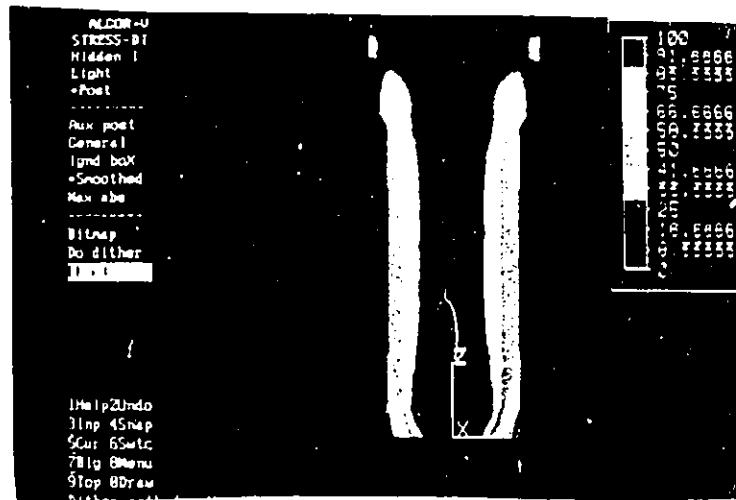
FIGURE 8.4(d): FEA STRESSES FOR CANTILEVER BEAM MODEL 4
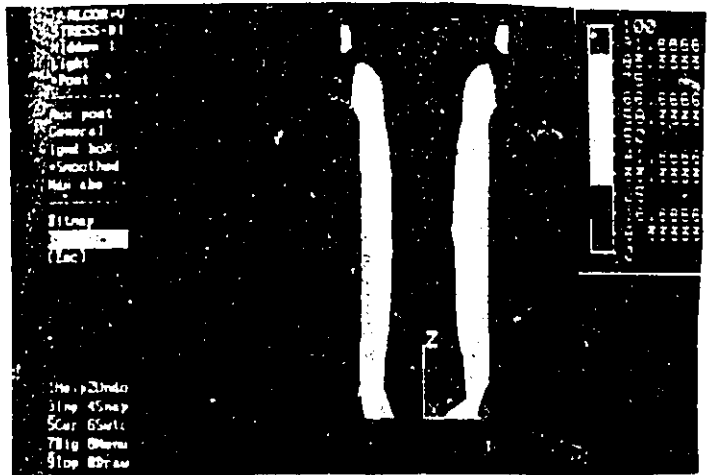
FIGURE 8.4(e): FEA - STRESSES FOR CANTILEVER BEAM MODEL 5
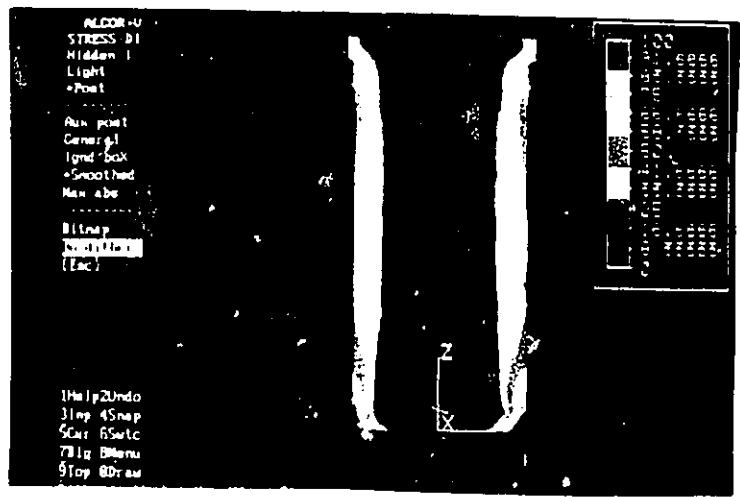
FIGURE 8.4(f): FEA STRESSES FOR CANTILEVER BEAM MODEL 6

TABLE 8.4: MAXIMUM TENSILE STRESS AND ITS LOCATION FOR PROPORTIONATE CANTILEVER BEAMS.

Model	Maximum tensile stress(S_t)			Location from free end		
	Eqn. 7.1 psi	FEA psi	P_{st} per cent	Eqn. 7.1 in.	FEA in.	P_{ds} per cent
1	7.43	6.98	-6.06	0.963	0.833	-13.50
2	6.55	5.21	-20.46	0.980	0.869	-11.33
3	5.58	4.64	-16.85	1.005	0.900	-10.45
4	4.56	4.25	-6.80	1.036	0.951	-8.21

TABLE 8.5: LOCALISED DIMENSIONS OF THE PROPORTIONATE CANTILEVER BEAMS

Model	t_s in.	r_c in.	h_s in.	t_s/r_c	t_s/h_s
1	0.846	0.327	0.633	2.59	1.34
2	0.854	0.299	0.519	2.86	1.65
3	0.858	0.267	0.400	3.21	2.15
4	0.880	0.234	0.303	3.76	2.32

cent. The contribution of statistical error and FEA error is not greater than 6 per cent compared to this large difference obtained in maximum tensile stress. Hence it can be suggested that the equation 7.1 **overestimates** the maximum tensile stress of the proportionate cantilever beam.

The location of the maximum tensile stress from the free end of the cantilever beam determined by the finite element analysis is found higher on the root profile than that of equation 7.1 in the range of 8.00 to 14.00 per cent. The location of the stress concentration is normally not specified with the value of the stress concentration factor in any stress concentration reference for beams. Hence these locations for the proportionate cantilever beams cannot be compared with any reference except for the locations of the corresponding gear tooth cases. The importance of this difference in the locations of the proportionate cantilever beams and the corresponding gear tooth cases depends upon how accurately any method (photoelasticity) of stress analysis can determine the location of the stress concentration. Even in the photoelasticity method of stress analysis, this method only identifies the general region of the stress concentration in any machine element and not the exact location in that region. Based on this fact of the stress analysis, the equation 7.1 estimates the location of the stress concentration, **reasonably close** to that determined by the finite element analysis in the proportionate cantilever beams.

9. CONCLUSIONS

9.1 Bending stress concentration factor and its equation for spur gear teeth.

9.1.1 Statistical model for the equation of the bending stress concentration.

The comparison of the statistical parameters of the Broghamer equation and the log linear equation for 20° and 14.5° pressure angle teeth showed that the log linear equations are statistically better as shown in **Table 4.1**. The improved accuracy of the log linear equations provided the strong base to use this statistical model to fit the experimental data with the localised dimensions of the theoretical weakest section.

9.1.2 Gear tooth layouts and their localised variables for the bending stress concentration factor.

The comparison of the tip tooth thickness and the base tooth thickness as determined by FIGS.EXT software and the analytical involutometry equations for AGMA tooth models as well as the tooth models 3, 6 and 10 as shown in **Table 5.1 and Table 5.3** respectively, indicates that FIGS.EXT software is capable of producing the correct involute tooth layout. Lewis

factors determined by FIGS.EXT software for standard proportion AGMA tooth models having a number of teeth in a range of 12 to 300 are identical to that used by AGMA as shown in **Table A-5.3** indicates that FIGS.EXT software does not only generate the correct root profile, but also correctly determines the required dimensions of the gear tooth to calculate the Lewis factors.

The error less than 10 per cent in the dimensions of the Lewis weakest section as determined by FIGS.EXT software and Broghamer and Dolan for each case of the tooth models 4 to 11 as shown in **Table A-5.1**, and the consistency of FIGS.EXT software with the graphical method to generate the layout and to determine the Lewis x-factor for tooth models 6 and 10 as shown in **Table 5.4**, provided the confidence to use the FIGS.EXT software for standard and non standard gear teeth. Since the reason for large discrepancy in the dimensions of the Lewis weakest section for model 3 is unknown, this model was removed from the bending stress concentration analysis of the gear teeth.

A larger tooth thickness and load height corresponding to the theoretical weakest section than those corresponding to the Lewis weakest section for each case of the tooth models 4 to 11 shows that the theoretical weakest section is indeed lower on the root profile than the Lewis weakest section. As expected, the localised radius as determined by FIGS.EXT software of the trochoid contour of the generated gear tooth

103

models is always larger than the minimum radius of the fillet.

9.1.3   Equations for bending stress concentration factors:

The statistical parameters for bending stress concentration factor (tensile) using localised tooth dimensions for 20° and 14.5° pressure angle teeth are:

For 20° pressure angle teeth :

$$K = 1.18 \left(\frac{t_1}{r_1}\right)^{0.26} \left(\frac{t_1}{h_1}\right)^{0.23}$$

Average Error = 0.192%

Standard Deviation = 5.48%

Maximum Error (Accuracy) = 11.09%

For 14.5° pressure angle teeth :

$$K = 1.29 \left(\frac{t_1}{r_1}\right)^{0.27} \left(\frac{t_1}{h_1}\right)^{0.22}$$

Average Error = 0.749%

Standard Deviation = 6.71%

Maximum Error (Accuracy) = 17.71%

The statistical comparison of these equations with Broghamer and Dolan equations using minimum fillet radius as shown in **Table 6.2** reveals the fact that the average error is less than 1 per cent and standard deviation is less than 6.75 per cent

for these log linear equations. The maximum error is markedly increased.

The comparison of the statistical parameters of the single equation for stress concentration based on localised tooth dimensions with that of the separate equations for 20" and 14.5° pressure angle teeth using localised tooth dimensions as shown in **Table 6.2**, shows that the standard deviation of the single equation is only slightly increased. Hence the single equation of the bending stress concentration factor(tensile) for spur gear teeth having the following range of t_1/r_1 and t_1/h_1 ratios is recommended.

$$1.028 < \frac{t_1}{h_1} < 3.281 \ ----------(9.1)$$

$$2.153 < \frac{t_1}{r_1} < 7.551 \ -----------(9.2)$$

The recommended single equation is :

$$K = 1.31 \left(\frac{t_1}{r_1}\right)^{0.22} \left(\frac{t_1}{h_1}\right)^{0.22} \ -----------(9.3)$$

Average Error = -0.28% and

Standard Deviation = 7.51%

Maximum Error(Accuracy)=17.28%

Since this equation is dependent only on the localised tooth dimensions, it becomes independent of the manufacturing method and type of the tooth profile.

105

9.2 The General Solution Of The Bending Stress Concentration:

9.2.1 For the spur gear teeth:

The spikes and variation of the maximum tensile stress $(M_{b\cdots})$ with respect to t_1/r_1 ratio as shown in **Figure 7.1**, and an overestimation of the maximum tensile stress by the single equation for the proportionate cantilever beams as cited in **Table 8.4** indicated that the experimental values of the maximum tensile stress for the gear teeth could be in error.

From the comparison of the load height corresponding to the theoretical weakest section and the Lewis weakest section, it can be concluded that location of the theoretical weakest section is <u>closer</u> to the location of the actual weakest section found in the photoelasticity experiments.

9.2.2 For the proportionate cantilever beams:

The comparison of the maximum tensile stress as determined from equation 7.1 and the finite element analysis as shown in **Table 8.4** indicated that this equation overestimates the maximum tensile stress for the proportionate cantilever beams. This equation also predicts reasonably accurately the location of the maximum tensile stress for the

proportionate cantilever beams.

10. RECOMMENDATIONS

10.1 Separating stress concentration factor for tangential and axial components of the tooth load for spur gear teeth.

In order to precisely determine the stress concentration factors for spur gear teeth, it is recommended to separately determine the stress concentration produced by the tangential and axial components of the tooth load as follows.

Maximum tensile stress(S_t) as developed by normal load(P) and maximum tensile stress(S_o) as developed by tangential load (P_{ta}) should be experimentally determined for tooth models 4 to 11. Stress concentration factor(K_o) for each case of these tooth models should be calculated as follows.

$$K_o = \frac{S_o}{S_l} \quad \text{-----------} (10.1)$$

Substituting this stress concentration factor(K_o) and maximum tensile stress(S_t) in the equation 10.2 and then solving this equation for stress concentration factor(K_d) to determine the stress concentration produced by the axial component of the tooth load for each case of the tooth models.

$$K_d = \frac{S_t - K_o(S_l)}{S_a} \quad \text{--------------} (10.2)$$

10.2 General solution of the Stress Concentration For The Cantilever Beam:

Since Broghamer and Dolan did not compare the experimentally determined location of the maximum tensile stress for the cantilever beam with that of the corresponding gear tooth, it is recommended that proportionate cantilever beam models similar to tooth models 4 to 11 should be experimentally examined to determine the location of the maximum tensile stress and then this location should be compared with that obtained from the single equation. This comparison will provide the experimental authenticity to use this equation to determine the general solution of the cantilever beam.

LIST OF REFERENCES

1   J. E. Shigley., C. R. Mischke., **Mechanical Engineering Design**. Mcgraw-Hill Book Company.

    1.1 Fifth Edition, Chapter 14, PG 587.

    1.2 Fourth Edition, Chapter 13, PG 598.

    1.3 Fifth Edition, Appendix, PG 587.

        *   Figure A-15-5 for tensile load.

        *   Figure A-15-6 for bending load.

2   E. L. Broghamer., T. J. Dolan., **A Photoelastic Study Of Stresses In Gear Tooth Fillets**., University of Illinois., Bulletin series 335.

    2.1 Equation Number (2), (3), (4) and (5) of PG 18 and 19.

    2.2 Equation Number (6) and (7) of PG 25.

    2.3 Appendix C, Table 2, PG 41.

3   Raymond J. Drago., **Fundamentals Of Gear Design.** Butterworth Publishers, Chapter 14, PG 89, Figure 4.5.

4   S. Timoshenko and R. V. Baud., **The Strength Of Gear Teeth**., The journal of the American Society of Mechanical Engineers., Volume 48., Number 11., 1926.

5   M. A. Jacobson., **Bending Stress In Spur Gears**., Proceedings o4f The Institution of Mechanical Engineers., Volume 169., 1955.

6   R. B. Haywood., **Tensile Fillet Stresses In Loaded**

Projections., Proceedings o4f The Institution of Mechanical Engineers., Volume 159., 1948.

7   H. E. Merritt., **Gear Tooth Stresses And Rating Formulae.**, Proceedings o4f The Institution of Mechanical Engineers., Volume 166., 1952.

8   AGMA Standard 220.02., **Strength Of Spur Gear Teeth.**, 1966.

9   Toshio and Norihisa ARAI. **Stress Distribution Along The Fillet Curve Of Gears.**, Bulletin Of Japan Society Of Mechanical Engineers., Volume 17, Number 104, 1974.

10   Akira Ishibashi and Shiro Kido., **Bending Stress and Load Capacity of Gears.**, Bulletin Of Japan Society Of Mechanical Engineers., Volume 12, Number 51, 1969.

APPENDIX A

No.	Model	Case	Phi	a	b	rp	T	N	Y	rt	ft	rf	Pr	Figs	B & D		Figs (h)	B (h)
1	3	1	14.5	0.500	0.594	6	0.785	24	0.300	0.247	---	0.253	---	---	25.50	---	0.723	0.
2		2							0.110	0.247	---	0.253	---	---	16.33	---	0.561	0
3		3							-0.080	0.247	---	0.253	---	---	10.67	---	0.412	0
4		4							0.300	0.149	---	0.161	---	---	25.50	---	0.757	0
5		5							0.110	0.149	---	0.161	---	---	16.33	---	0.592	0
6		6							-0.080	0.149	---	0.161	---	---	10.67	---	0.435	0
7	4	1	14.5	0.675	0.419	6	0.883	24	0.495	0.260	0.296	0.285	10.47	26.57	24.67	-7.15	0.768	0.
8		2							0.315	0.260	0.286	0.265	7.34	23.10	21.33	-7.64	0.609	0
9		3							0.115	0.260	0.275	0.265	3.64	18.21	15.67	-13.95	0.443	0
10		4							0.495	0.150	0.247	0.162	34.41	26.57	24.67	-7.15	0.818	0
11		5							0.315	0.150	0.222	0.162	27.03	23.10	21.33	-7.64	0.651	0
12		6							0.115	0.150	0.197	0.162	17.77	18.21	15.67	-13.95	0.475	0
13	5	1	14.5	0.705	0.389	6	0.918	24	0.505	0.265	0.287	0.270	5.92	26.76	25.50	-4.71	0.754	0.
14		2							0.325	0.265	0.328	0.270	17.68	23.37	23.67	1.28	0.595	0.
15		3							0.135	0.265	0.274	0.270	1.46	18.77	17.33	-7.67	0.439	0
16		4							0.505	0.152	0.208	0.163	21.63	26.76	25.50	-4.71	0.804	0.
17		5							0.325	0.152	0.207	0.163	21.28	23.37	23.67	1.28	0.639	0
18		6							0.135	0.152	0.188	0.163	12.37	18.77	17.33	-7.67	0.471	0
19	9	1	14.5	0.500	0.578	5	0.785	20	0.300	0.303	0.392	0.317	19.13	24.03	20.00	-16.77	0.695	0
20		2							0.150	0.303	0.372	0.317	14.78	19.96	18.50	-7.31	0.569	0
21		3							0.000	0.303	0.354	0.317	10.45	14.50	16.33	12.62	0.452	0
22		4							-0.150	0.303	0.339	0.317	6.49	3.54	9.00	154.24	0.343	0
23		5							0.300	0.129	0.342	0.166	51.48	24.03	20.00	-16.77	0.752	0
24		6							0.150	0.129	0.311	0.166	46.62	19.96	18.50	-7.31	0.620	0
25		7							0.000	0.129	0.273	0.166	39.19	14.50	16.33	12.62	0.493	0
26		8							-0.150	0.129	0.233	0.166	28.76	3.54	9.00	154.24	0.371	0
27		9							0.300	0.062	0.335	0.111	67.01	24.03	20.00	-16.77	0.773	0
28		10							0.150	0.062	0.295	0.111	62.54	19.96	18.50	-7.31	0.640	0
29		11							0.000	0.062	0.253	0.111	56.32	14.50	16.33	12.62	0.510	0
30		12							-0.150	0.062	0.205	0.111	46.10	3.54	9.00	154.24	0.385	0
31	10	1	14.5	0.500	0.578	10	0.785	40	0.300	0.267	0.382	0.276	23.78	19.96	18.00	-9.82	0.698	0
32		2							0.150	0.267	0.336	0.276	17.86	17.48	17.50	0.11	0.571	0
33		3							0.000	0.267	0.311	0.276	11.25	14.50	17.00	17.24	0.451	0
34		4							-0.150	0.267	0.295	0.276	8.44	10.61	11.33	6.79	0.339	0
35		5							0.300	0.152	0.323	0.170	47.37	19.96	18.00	-9.82	0.748	0
36		6							0.150	0.152	0.285	0.170	40.35	17.48	17.50	0.11	0.616	0
37		7							0.000	0.152	0.248	0.170	30.89	14.50	17.00	17.24	0.488	0
38		8							-0.150	0.152	0.211	0.170	19.43	10.61	11.33	6.79	0.366	0
39		9							0.300	0.111	0.318	0.132	58.49	19.96	18.00	-9.82	0.765	0
40		10							0.150	0.111	0.271	0.132	51.29	17.48	17.50	0.11	0.633	0
41		11							0.000	0.111	0.225	0.132	41.33	14.50	17.00	17.24	0.503	0
42		12							-0.150	0.111	0.183	0.132	27.87	10.61	11.33	6.79	0.377	0
43	11	1	14.5	0.500	0.578	20	0.785	80	0.300	0.285	0.347	0.290	16.43	17.48	15.67	-10.35	0.888	0
44		2							0.150	0.285	0.328	0.290	11.04	16.07	15.33	-4.60	0.562	0
45		3							0.000	0.285	0.309	0.290	6.15	14.50	14.50	0.00	0.442	0
46		4							-0.150	0.285	0.298	0.290	2.68	12.72	14.50	13.99	0.332	0
47		5							0.300	0.180	0.298	0.188	38.91	17.48	15.67	-10.35	0.741	0
48		6							0.150	0.180	0.259	0.188	27.41	16.07	15.33	-4.60	0.609	0
49		7							0.000	0.180	0.231	0.188	18.61	14.50	14.50	0.00	0.481	0
50		8							-0.150	0.180	0.208	0.188	9.62	12.72	14.50	13.99	0.359	0
51		9							0.300	0.109	0.273	0.126	53.85	17.48	15.67	-10.35	0.777	0
52		10							0.150	0.109	0.227	0.126	44.49	16.07	18.33	-4.60	0.643	0
53		11							0.000	0.109	0.181	0.126	30.39	14.50	14.50	0.00	0.510	0.
54		12							-0.150	0.109	0.153	0.126	17.85	12.72	14.50	13.99	0.379	0
55	6	1	20.0	0.500	0.578	5	0.785	20	0.300	0.256	0.361	0.274	24.10	27.56	28.00	1.60	0.725	0
56		2							0.150	0.256	0.343	0.274	20.12	24.17	22.67	-6.21	0.597	0
57		3							0.000	0.256	0.320	0.274	14.37	20.00	21.33	6.65	0.476	0
58		4							-0.150	0.256	0.300	0.274	8.67	14.36	15.00	4.46	0.363	0
59		5							0.300	0.155	0.327	0.189	42.20	27.56	28.00	1.60	0.759	0
60		6							0.150	0.155	0.299	0.189	36.79	24.17	22.67	-6.21	0.628	0
61		7							0.000	0.155	0.267	0.189	29.21	20.00	21.33	6.65	0.501	0
62		8							-0.150	0.155	0.234	0.189	19.23	14.36	15.00	4.46	0.380	0
63		9							0.300	0.062	0.304	0.110	63.82	27.56	28.00	1.60	0.790	0
64		10							0.150	0.062	0.272	0.110	59.56	24.17	22.67	-6.21	0.656	0
65		11							0.000	0.062	0.228	0.110	51.75	20.00	21.33	6.65	0.525	0
66		12							-0.150	0.062	0.184	0.110	40.22	14.36	15.00	4.46	0.398	0
67	7	1	20.0	0.500	0.578	10	0.785	40	0.300	0.267	0.349	0.277	20.63	24.17	22.67	-6.21	0.709	0
68		2							0.150	0.267	0.323	0.277	14.24	22.21	20.33	-8.46	0.582	0
69		3							0.000	0.267	0.308	0.277	10.06	20.00	18.50	-7.50	0.461	0
70		4							-0.150	0.267	0.292	0.277	5.14	17.45	17.50	0.29	0.348	0
71		5							0.300	0.152	0.303	0.170	43.89	24.17	22.67	-6.21	0.759	0
72		6							0.150	0.152	0.260	0.170	34.62	22.21	20.33	-8.46	0.627	0
73		7							0.000	0.152	0.233	0.170	27.04	20.00	18.50	-7.50	0.499	0
74		8							-0.150	0.152	0.202	0.170	15.84	17.45	17.50	0.29	0.375	0
75		9							0.300	0.085	0.279	0.106	62.01	24.17	22.67	-6.21	0.789	0
76		10							0.150	0.085	0.240	0.106	55.83	22.21	20.33	-8.46	0.654	0
77		11							0.000	0.085	0.192	0.106	44.79	20.00	18.50	-7.50	0.522	0
78		12							-0.150	0.085	0.157	0.106	32.48	17.45	17.50	0.29	0.393	0
79	8	1	20.0	0.500	0.578	20	0.785	80	0.300	0.270	0.327	0.275	15.90	22.21	22.50	1.31	0.705	0
80		2							0.150	0.270	0.306	0.275	10.13	21.14	21.33	0.90	0.577	0
81		3							0.000	0.270	0.294	0.275	6.48	20.00	20.67	3.35	0.456	0
82		4							-0.150	0.270	0.283	0.275	2.83	18.78	20.00	6.50	0.343	0
83		5							0.300	0.149	0.263	0.158	39.92	22.21	22.50	1.31	0.786	0
84		6							0.150	0.149	0.226	0.158	30.09	21.14	21.33	0.90	0.632	0
85		7							0.000	0.149	0.199	0.158	20.60	20.00	20.67	3.35	0.502	0
86		8							-0.150	0.149	0.178	0.158	11.24	18.78	20.00	8.50	0.375	0
87		9							0.300	0.078	0.233	0.090	61.37	22.21	22.50	1.31	0.803	0
88		10							0.150	0.076	0.164	0.090	51.09	21.14	21.33	0.90	0.665	0
89		11							0.000	0.078	0.147	0.090	38.78	20.00	20.67	3.35	0.530	0

h	Ph	t	t	Pt	x	x	Pz	hi	C	g	PH	Si	So	Si	SigmaT	SigmaC	K	Kc	Mbs	L
B & D			Figs	B & D		Figs	B & D													
0.767	6.09	0.855	0.824	-3.63	0.253	0.221	-12.45	---	---	---	---	8.52	10.38	---	---	---	---	---	---	---
0.614	9.45	0.874	0.854	-2.29	0.340	0.297	-12.77	---	---	---	---	7.34	8.88	---	---	---	---	---	---	---
0.431	4.61	0.912	0.868	-4.82	0.505	0.437	-13.41	---	---	---	---	5.90	7.00	---	---	---	---	---	---	---
0.845	11.62	0.841	0.798	-5.11	0.234	0.188	-19.34	---	---	---	---	10.01	12.70	---	---	---	---	---	---	---
0.652	10.14	0.856	0.812	-5.14	0.309	0.253	-18.30	---	---	---	---	9.04	11.02	---	---	---	---	---	---	---
0.479	10.11	0.885	0.842	-4.88	0.450	0.370	-17.80	---	---	---	---	7.35	8.82	---	---	---	---	---	---	---
0.797	3.78	0.949	0.934	-1.53	0.293	0.274	-6.56	0.772	0.004	0.951	0.264	7.19	9.16	4.11	4.11	5.05	1.75	1.81	7.29	0.952
0.629	3.28	0.963	0.955	-0.87	0.381	0.362	-4.86	0.612	0.003	0.966	0.270	5.87	7.51	3.21	3.21	4.03	1.83	1.87	6.08	0.972
0.434	-2.03	0.996	0.967	-2.93	0.560	0.539	-3.82	0.447	0.004	1.001	0.482	4.95	6.10	2.23	2.23	2.85	2.22	2.14	4.64	1.007
0.845	3.55	0.943	0.903	-4.24	0.272	0.241	-11.45	0.818	0.002	0.945	0.212	8.48	10.60	4.44	4.44	5.39	1.91	1.97	8.08	0.998
0.647	-0.61	0.954	0.908	-4.82	0.350	0.319	-8.85	0.654	0.003	0.956	0.210	7.23	9.08	3.54	3.54	4.36	2.04	2.08	6.95	1.014
0.488	2.74	0.974	0.944	-3.08	0.499	0.457	-8.57	0.478	0.003	0.977	0.308	6.01	7.14	2.53	2.53	3.17	2.37	2.25	5.52	1.038
0.790	4.77	0.980	1.024	4.49	0.318	0.332	4.21	0.758	0.004	0.984	0.408	6.06	7.81	3.74	3.74	4.65	1.62	1.68	6.81	0.958
0.639	7.39	0.995	1.048	5.01	0.418	0.430	2.68	0.578	-0.017	1.008	1.002	5.10	6.82	2.74	2.74	3.53	1.86	1.93	5.42	0.958
0.472	7.52	1.030	1.069	3.79	0.604	0.605	0.19	0.446	0.007	1.034	-2.524	4.51	5.72	2.19	2.03	2.83	2.06	2.02	4.31	1.016
0.867	7.84	0.978	1.010	3.27	0.297	0.294	-1.10	0.828	0.022	0.977	-0.102	7.40	9.49	4.18	4.18	5.10	1.77	1.86	7.77	1.026
0.690	7.98	0.989	1.015	2.63	0.383	0.373	-2.46	0.642	0.003	0.991	0.202	6.30	8.07	3.20	3.20	4.00	1.97	2.02	6.50	1.021
0.509	8.07	1.010	1.030	1.98	0.541	0.521	-3.76	0.478	0.005	1.014	0.396	5.45	6.71	2.31	2.31	2.95	2.36	2.28	5.18	1.048
0.718	3.31	0.842	0.840	-0.24	0.255	0.246	-3.66	0.697	0.002	0.844	0.238	8.08	9.90	4.88	4.88	5.84	1.68	1.69	7.90	0.897
0.568	-0.18	0.859	0.859	0.00	0.324	0.325	0.18	0.573	0.004	0.862	0.349	6.65	8.35	3.95	3.95	4.74	1.68	1.76	6.81	0.923
0.448	-0.88	0.886	0.871	-1.81	0.434	0.422	-2.72	0.454	0.002	0.889	0.339	5.54	7.60	3.06	3.06	3.62	1.81	2.10	5.69	0.954
0.331	-3.50	0.935	0.900	-3.85	0.639	0.612	-4.19	0.345	0.002	0.938	0.214	4.50	6.45	2.28	2.28	2.41	1.97	2.67	4.65	0.995
0.801	8.52	0.810	0.828	2.22	0.218	0.214	-1.90	0.758	0.006	0.810	0.000	10.32	13.12	5.83	5.83	6.83	1.77	1.92	9.30	0.958
0.641	3.39	0.821	0.834	1.58	0.272	0.271	-0.19	0.622	0.002	0.823	0.244	8.80	11.33	4.76	4.76	5.59	1.85	2.03	8.23	0.973
0.507	2.84	0.838	0.840	0.24	0.356	0.348	-2.30	0.495	0.002	0.840	0.239	7.52	9.66	3.78	3.78	4.37	1.99	2.21	7.12	0.995
0.371	0.00	0.867	0.855	-1.38	0.507	0.493	-2.75	0.373	0.002	0.868	0.115	6.22	8.00	2.89	2.89	3.04	2.15	2.64	6.08	1.023
0.840	8.67	0.798	0.828	3.76	0.206	0.204	-0.93	0.776	0.003	0.798	0.000	11.20	14.00	6.17	8.17	7.19	1.82	1.95	9.81	0.976
0.674	5.31	0.806	0.834	3.47	0.254	0.258	1.67	0.643	0.003	0.808	0.248	9.50	12.05	5.13	5.13	5.98	1.85	2.02	8.82	0.993
0.541	8.08	0.821	0.850	3.53	0.330	0.334	1.05	0.512	0.002	0.822	0.122	8.09	10.20	4.10	4.10	4.71	1.97	2.17	7.71	1.011
0.408	5.97	0.844	0.862	2.13	0.463	0.455	-1.57	0.385	0.000	0.844	0.000	7.00	8.69	3.16	3.16	3.31	2.21	2.63	6.72	1.035
0.716	2.58	0.907	0.894	-1.43	0.295	0.279	-5.29	0.707	0.004	0.909	0.221	7.35	8.46	4.42	4.42	5.17	1.88	1.64	7.49	0.902
0.572	0.18	0.924	0.911	-1.41	0.374	0.363	-2.96	0.574	0.003	0.927	0.325	6.35	7.65	3.50	3.50	4.15	1.81	1.84	6.37	0.924
0.471	4.43	0.951	0.944	-0.74	0.501	0.473	-5.65	0.458	0.007	0.955	0.421	5.12	6.42	2.65	2.63	3.18	1.93	2.02	5.20	0.958
0.344	1.47	0.999	0.977	-2.20	0.736	0.694	-5.75	0.343	0.004	1.004	0.501	4.32	5.73	1.82	1.82	2.19	2.37	2.62	3.95	0.993
0.794	8.15	0.906	0.888	-1.99	0.274	0.248	-9.50	0.752	0.004	0.909	0.331	9.20	11.05	4.76	4.76	5.51	1.93	2.01	8.18	0.952
0.638	3.57	0.919	0.894	-2.72	0.343	0.313	-8.63	0.619	0.003	0.921	0.218	7.73	9.45	3.85	3.85	4.50	2.01	2.10	7.12	0.969
0.518	5.74	0.937	0.916	-2.24	0.450	0.407	-9.62	0.491	0.003	0.940	0.320	6.45	8.67	2.96	2.96	3.49	2.18	2.48	6.01	0.991
0.393	7.38	0.968	0.927	-4.24	0.640	0.547	-14.59	0.368	0.002	0.972	0.413	5.61	7.53	2.11	2.11	2.49	2.68	3.03	4.79	1.018
0.812	8.14	0.906	0.862	-4.86	0.268	0.229	-14.72	0.768	0.003	0.907	0.110	10.01	12.27	4.89	4.89	5.64	2.05	2.18	8.35	0.969
0.685	8.21	0.917	0.875	-4.58	0.332	0.279	-15.86	0.635	0.002	0.919	0.218	8.52	10.80	3.98	3.98	4.63	2.14	2.33	7.40	0.985
0.544	8.15	0.933	0.886	-5.04	0.433	0.361	-16.62	0.506	0.003	0.936	0.322	7.27	9.50	3.09	3.09	3.62	2.35	2.62	6.34	1.006
0.398	5.57	0.959	0.893	-6.88	0.610	0.501	-17.87	0.380	0.003	0.964	0.521	6.15	8.38	2.22	2.22	2.60	2.77	3.22	5.15	1.030
0.707	2.76	0.945	0.944	-0.11	0.325	0.315	-2.89	0.690	0.002	0.947	0.212	6.87	8.28	4.09	4.09	4.72	1.68	1.75	7.18	0.890
0.584	3.91	0.964	0.960	-0.41	0.413	0.395	-4.56	0.584	0.002	0.966	0.207	5.90	7.44	3.20	3.20	3.77	1.84	1.97	5.99	0.914
0.460	4.07	0.994	0.988	-0.60	0.559	0.531	-5.07	0.446	0.004	0.998	0.402	4.76	6.74	2.35	2.35	2.85	2.03	2.38	4.75	0.948
0.328	-1.81	1.048	0.994	-5.15	0.827	0.758	-8.38	0.336	0.004	1.055	0.668	3.67	5.78	1.56	1.56	1.98	2.38	2.92	3.47	0.986
0.744	0.40	0.958	0.926	-3.34	0.310	0.288	-6.95	0.743	0.002	0.960	0.209	8.00	9.85	4.30	4.30	4.93	1.86	2.00	7.72	0.943
0.635	4.27	0.972	0.949	-2.37	0.388	0.355	-8.58	0.612	0.003	0.974	0.206	7.08	9.10	3.44	3.44	4.00	2.06	2.27	6.67	0.962
0.493	2.49	0.991	0.960	-3.13	0.510	0.467	-8.44	0.483	0.002	0.999	0.838	5.88	8.36	2.56	2.58	3.06	2.30	2.73	5.49	0.983
0.359	0.00	1.025	0.989	-3.51	0.732	0.681	-6.90	0.361	0.002	1.029	0.390	4.59	7.16	1.78	1.78	2.21	2.58	3.24	4.18	1.011
0.803	3.35	0.967	0.954	-1.34	0.301	0.283	-5.82	0.779	0.002	0.968	0.103	8.65	10.73	4.45	4.45	5.07	1.94	2.12	8.07	0.979
0.657	2.18	0.978	0.960	-1.84	0.372	0.351	-5.70	0.643	0.000	0.978	0.000	7.50	9.64	3.59	3.60	4.16	2.09	2.32	7.12	0.993
0.522	2.35	0.922	0.972	5.42	0.482	0.452	-5.12	0.513	0.003	0.995	7.918	6.35	8.70	2.76	2.76	3.26	2.30	2.67	6.88	1.013
0.393	3.89	1.015	0.988	-2.66	0.680	0.621	-8.62	0.381	0.002	1.017	0.197	5.12	7.73	1.94	1.94	2.37	2.64	3.26	4.78	1.031
0.728	0.41	0.917	0.922	0.55	0.290	0.292	0.68	0.730	0.005	0.921	0.436	6.12	8.04	4.08	4.08	5.08	1.50	1.58	6.91	0.930
0.596	-0.17	0.933	0.922	-1.18	0.365	0.357	-2.18	0.599	-0.002	0.935	0.214	5.75	7.43	3.31	3.31	4.19	1.74	1.77	5.97	0.949
0.472	-0.84	0.959	0.934	-2.61	0.483	0.462	-4.34	0.480	0.004	0.963	0.417	4.81	6.32	2.56	2.56	3.27	1.88	1.93	4.98	0.980
0.341	-6.06	1.003	0.984	-1.89	0.693	0.710	2.46	0.369	0.006	1.012	0.897	3.92	5.21	1.85	1.85	2.34	2.12	2.23	3.95	1.019
0.797	5.01	0.912	0.912	0.00	0.274	0.261	-4.77	0.763	0.004	0.914	0.219	7.12	9.85	4.35	4.35	5.36	1.64	1.84	7.43	0.963
0.650	3.50	0.924	0.917	-0.75	0.340	0.323	-4.84	0.630	0.002	0.926	0.216	6.50	8.93	3.58	3.58	4.46	1.82	2.00	6.55	0.980
0.505	0.80	0.944	0.922	-2.33	0.445	0.421	-5.36	0.505	0.004	0.947	0.318	5.50	7.80	2.81	2.81	3.54	1.95	2.25	5.58	1.005
0.379	-0.26	0.976	0.928	-4.92	0.627	0.568	-9.36	0.386	0.006	0.983	0.717	4.72	7.00	2.07	2.07	2.57	2.28	2.72	4.56	1.036
0.826	4.56	0.905	0.894	-1.22	0.259	0.242	-6.67	0.794	0.004	0.907	0.221	8.40	13.15	4.62	4.62	5.64	1.82	2.33	7.93	0.994
0.677	3.20	0.915	0.900	-1.64	0.319	0.299	-6.25	0.658	0.002	0.916	0.109	7.40	11.58	3.85	3.85	4.74	1.92	2.44	7.07	1.008
0.538	2.48	0.930	0.911	-2.04	0.412	0.386	-6.36	0.528	0.003	0.933	0.323	6.25	9.82	3.05	3.05	3.79	2.05	2.59	6.18	1.028
0.405	1.78	0.954	0.916	-3.98	0.572	0.518	-9.40	0.402	0.004	0.959	0.524	5.25	8.46	2.28	2.28	2.60	2.30	3.02	5.20	1.052
0.711	0.28	0.994	1.018	2.41	0.348	0.364	4.59	0.714	0.005	0.996	0.201	5.35	7.01	3.53	3.53	4.35	1.52	1.61	6.25	0.914
0.577	-0.86	1.010	1.028	1.78	0.438	0.458	4.49	0.592	0.010	1.019	0.891	4.75	6.53	2.80	2.80	3.54	.70	1.85	5.31	0.942
0.451	-2.17	1.039	1.043	0.38	0.585	0.603	3.01	0.465	0.004	1.043	0.385	3.92	5.77	2.08	2.08	2.74	1.88	2.11	4.25	0.965
0.333	-4.58	1.088	1.078	-0.92	0.848	0.872	2.89	0.356	0.007	1.100	1.103	3.22	5.34	1.41	1.41	1.98	2.28	2.73	3.17	1.006
0.757	-0.26	1.007	1.015	0.79	0.334	0.340	1.86	0.763	0.004	1.009	0.199	6.30	8.95	3.70	3.70	4.0	1.70	1.99	6.70	0.963
0.615	-1.91	1.020	1.028	0.78	0.415	0.430	3.56	0.634	0.007	1.026	0.588	5.34	8.00	2.98	2.98	3.7	1.79	2.15	5.86	0.984
0.494	-1.00	1.040	1.044	0.38	0.542	0.552	1.79	0.502	0.003	1.043	0.288	4.51	6.95	2.27	2.27	2.93	1.98	2.37	4.86	1.002
0.362	-3.47	1.072	1.067	-0.47	0.766	0.786	2.63	0.380	0.005	1.080	0.748	3.54	6.38	1.59	1.59	2.14	2.23	2.98	3.78	1.030
0.791	0.25	1.015	0.995	-1.97	0.326	0.313	-4.15	0.793	0.004	1.018	0.296	7.00	10.35	3.79	3.79	4.59	1.85	2.25	6.97	0.993
0.667	1.99	1.026	1.018	-0.78	0.402	0.388	-3.47	0.657	0.003	1.028	0.195	6.25	9.28	3.09	3.09	3.82	2.03	2.43	6.14	1.007
0.522	0.00	1.042	1.022	-1.92	0.520	0.500	-3.80	0.527	0.005	1.047	0.480	5.27	8.55	2.38	2.38	3.04	2.21	2.82	5.27	1.027
0.388	-1.27	1.066	1.040	-2.44	0.723	0.697	-3.59	0.396	0.003	1.070	0.375	4.20	7.35	1.70	1.70	2.26	2.47	3.25	4.22	1.048
0.744	5.53	1.033	1.078	4.36	0.378	0.390	3.19	0.709	0.004	1.036	0.290	5.17	6.84	3.30	3.30	4.03	1.58	1.70	6.06	0.909
0.602	4.33	1.052	1.084	3.04	0.480	0.488	1.77	0.585	0.004	1.059	0.665	4.40	6.23	2.58	2.58	3.26	1.71	1.91	5.05	0.935
0.460	0.88	1.082	1.090	0.74	0.642	0.646	0.60	0.481	0.005	1.087	0.462	3.60	5.68	1.89	1.89	2.51	1.91	2.26	3.97	0.961
0.383	5.83	1.134	1.147	1.15	0.937	0.906	-3.33	0.349	0.006	1.145	0.970	2.75	5.05	1.23	1.23	1.79	2.23	2.82	2.85	1.000
0.820	7.05	1.065	1.095	2.82	0.370	0.366	-1.25	0.789	0.003	1.067	0.188	5.95	8.53	3.40	3.40	4.11	1.75	2.08	6.51	0.969
0.658	4.11	1.077	1.105	2.60	0.459	0.464	1.11	0.636	0.004	1.080	0.279	5.09	7.78	2.72	2.72	3.39	1.87	2.30	5.64	0.988
0.527	4.98	1.096	1.113	1.55	0.598	0.588	-1.77	0.504	0.002	1.100	0.356	4.42	7.23	2.04	2.04	2.66	2.17	2.72	4.63	1.004
0.398	6.13	1.128	1.125	-0.09	0.845	0.795	-5.95	0.379	0.004	1.133	0.622	3.40	6.64	1.39	1.39	1.96	2.44	3.39	3.49	1.029
0.882	9.84	1.083	1.118	3.23	0.365	0.354	-2.98	0.805	0.002	1.085	0.185	8.50	10.72	3.45	3.45	4.15	1.88	2.59	8.78	1.005
0.719	8.12	1.092	1.118	2.38	0.448	0.435	-3.05	0.670	0.005	1.096	0.356	5.91	9.72	2.79	2.79	3.45	2.12	2.82	6.03	1.020
0.573	8.11	1.106	1.122	1.45	0.577	0.549	-4.81	0.534	0.004	1.110	0.362	4.86	8.65	2.14	2.14	2.75	2.28	3.14	5.12	1.034

TABLE A-5.2: CHARACTERISTIC AND PURPOSE OF TOOTH MODELS.

Group	Model number	Characteristic and purpose of the tooth models.
A	1 Standard Formed Teeth	* Load action line is perpendicular to the center line of the tooth and thereby only tangential load was applied in this group. Hence load angle is zero in all these cases. * Used to study the effects of the tangential load on the stress concentration.
B	2 Standard Formed Teeth	* Load action line is perpendicular to the tooth surface. * Used to study the effects of the radial component of a load on the stress concentration.
C	3,4 & 5 Non Standard Generated Teeth	* These tooth models were in the form of spur gears, but their design was based on bevel gears of varying addendum and dedendum. * Used to determine the effects of varying addendum and dedendum on the stress concentration.
D	6,7 & 8 Standard Generated Teeth	* This group has 20 degree pressure angle tooth models with varying number of teeth, Load position and tool tip radius. * Used to determine the effects of these variables on the stress concentration.
E	9,10 & 11 Standard Generated Teeth	* This group has 14.5 degree pressure angle tooth models with varying number of teeth, load position and tool tip radius. The proportion of these models are same as the models group D. * Used to determine the effects of these variables on the stress concentration.

(Contd)

TABLE A-5.2 (CONTINUED)

Group	Model number	Characteristic and purpose of the tooth models.
F	Conventionalised Gear Tooth Models.[2]	* This group has models in form of the short cantilever beam with the varying circular fillet radius and lcad position. * Used to determine the effects of each tooth variable on the stress concentration.

TABLE A-5.3:   LEWIS FORM FACTOR FOR VARYING NUMBER OF TEETH

Sr. No.	N	AGMA[1.2]	FIGS.EXT
		Y_f	
1	12	0.22960	0.22960
2	13	0.24317	0.24317
3	14	0.25530	0.25530
4	15	0.26622	0.26622
5	16	0.27610	0.27610
6	17	0.28508	0.28508
7	18	0.29327	0.29327
8	19	0.30078	0.30078
9	20	0.30769	0.30769
10	21	0.31406	0.31406
11	22	0.31997	0.31997
12	24	0.33056	0.33056
13	26	0.33979	0.33979
14	28	0.34790	0.34790
15	30	0.35510	0.35510
16	34	0.36731	0.36731
17	38	0.37727	0.37727
18	45	0.39093	0.39093
19	50	0.39860	0.39860
20	60	0.41047	0.41047
21	75	0.42283	0.42283
22	100	0.43574	0.43574
23	150	0.44930	0.44930
24	300	0.46364	0.46364

APPENDIX B

TABLE B-1: ERROR OF EQUATIONS FOR 14.5° AND 20° PRESSURE ANGLE TOOTH MODELS

Sr No	Model	Case	S_t psi	S_{ta} psi	P_{st} per cent	S_{ta} psi	P_{st} per cent
				Brog. & Dolan Equations.		Log linear Equations.	
Pressure angle 20°							
1		1	6.12	6.10	-0.33	6.15	0.49
2		2	5.75	5.68	-1.22	5.71	-0.70
3		3	4.81	4.78	-0.62	4.79	-0.42
4		4	3.92	3.79	-3.32	3.78	-3.57
5		5	7.12	6.96	-2.25	7.06	-0.84
6	6	6	6.50	6.40	-1.54	6.49	-0.15
7		7	5.50	5.39	-2.00	5.44	-1.09
8		8	4.72	4.72	0.00	4.74	0.42
9		9	8.40	7.91	**-5.83**	8.11	-3.45
10		10	7.40	7.30	-1.35	7.46	0.81
11		11	6.25	6.19	-0.96	6.31	0.96
12		12	5.25	5.44	3.62	5.51	4.95
13		1	5.35	5.50	2.80	5.55	3.74
14		2	4.75	4.81	1.26	4.84	1.89
15		3	3.92	4.03	2.81	4.03	2.81
16		4	3.22	3.08	-4.35	3.06	**-4.97**
17		5	6.30	6.17	-2.06	6.27	-0.48
18		6	5.34	5.38	0.75	5.45	2.06
19	7	7	4.51	4.59	1.77	4.64	2.88
20		8	3.54	3.57	0.85	3.58	1.13
21		9	7.00	6.99	-0.14	7.16	2.29

TABLE B-1: (CONTINUED)

S r N o	M o d e l	C a s e	S_t psi	S_{te} psi	P_{st} per cent	S_{te} psi	P_{st} per cent
				Brog. & Dolan Equations.		Log linear Equations.	
Pressure angle 20°							
22		10	6.25	6.16	-1.44	6.30	0.80
23		11	5.27	5.27	0.0	5.36	1.71
24		12	4.20	4.19	-0.24	4.23	0.71
25		1	5.17	5.21	0.77	5.26	1.74
26		2	4.40	4.50	2.27	4.53	2.95
27		3	3.60	3.69	2.50	3.69	2.50
28		4	2.75	2.84	3.27	2.83	2.91
29		5	5.95	5.86	-1.51	5.97	0.34
30	8	6	5.09	5.02	-1.38	5.10	0.20
31		7	4.42	4.26	-3.62	4.31	-2.49
32		8	3.40	3.41	0.29	3.43	0.88
33		9	6.50	6.44	-0.92	6.63	2.00
34		10	5.91	5.66	-4.23	5.81	-1.69
35		11	4.86	4.83	-0.62	4.93	1.44
Absolute Maximum Error					5.78%		4.98%
Average Error					-0.49%		0.66%
Pressure angle 14.5°							
36		1	8.52	8.52	0.00	8.37	-1.76
37		2	7.34	7.57	2.86	7.51	2.32
38	3	3	5.90	6.04	2.37	6.07	2.88
39		4	10.01	10.41	3.60	10.30	2.90
40		5	9.04	9.25	1.77	9.24	2.21
41		6	7.35	7.39	0.27	7.47	1.63

TABLE B-1: (CONTINUED)

S r N o	M o d e l	C a s e	S_t psi	S_{te} psi	P_{st} per cent	S_{te} psi	P_{st} per cent
				Brog. & Dolan Equations.		Log linear Equations.	
Pressure angle 14.5°							
42		1	7.19	7.21	0.28	7.13	-0.83
43		2	5.87	6.07	3.41	6.05	3.07
44	4	3	4.95	4.82	-2.63	4.85	-2.02
45		4	8.48	8.65	2.00	8.63	1.77
46		5	7.23	7.32	1.24	7.36	1.80
47		6	6.01	5.96	-0.83	6.05	0.67
48		1	6.06	6.11	0.83	6.06	0.00
49		2	5.10	5.12	0.39	5.12	0.39
50	5	3	4.51	4.27	-5.32	4.31	**-4.43**
51		4	7.40	7.31	-1.22	7.33	-0.95
52		5	6.30	6.25	-0.79	6.31	0.16
53		6	5.45	5.25	-3.67	5.34	-2.02
54		1	8.08	8.07	-0.12	7.91	-2.10
55		2	6.65	6.66	0.15	6.59	-0.90
56		3	5.54	5.60	1.08	5.59	0.90
57		4	4.50	4.63	2.89	4.66	3.56
58		5	10.32	9.99	-3.20	9.92	-3.88
59		6	8.80	8.53	-3.07	8.54	-2.95
60		7	7.52	7.27	-3.32	7.33	-2.53
61	9	8	6.22	6.10	-1.93	6.19	-0.48
62		9	11.20	11.09	-0.98	11.11	-0.80
63		10	9.50	9.50	0.00	9.59	0.95
64		11	8.09	8.05	-0.49	8.17	0.99

TABLE B-1: (CONTINUED)

Sr No	Model	Case	S_z psi	S_{te} psi	P_{st} per cent	S_{te} psi	P_{st} per cent
				Brog. & Dolan Equations.		Log linear Equations.	
Pressure angle 14.5°							
65	9	12	7.00	6.93	-1.00	7.08	1.14
66		1	7.35	7.64	3.95	7.54	2.59
67		2	6.35	6.32	-0.47	6.30	-0.79
68		3	5.12	5.20	1.56	5.22	1.95
69		4	4.32	4.17	-3.47	4.23	-2.08
70		5	9.20	9.04	-1.74	9.02	-1.96
71		6	7.73	7.68	-0.65	7.71	-0.26
72	10	7	6.45	6.36	-1.40	6.43	-0.31
73		8	5.61	5.45	-2.85	5.54	-1.25
74		9	10.01	10.05	0.40	10.06	0.50
75		10	8.52	8.74	2.58	8.80	3.29
76		11	7.27	7.29	0.28	7.39	1.65
77		12	6.15	6.10	-0.81	6.22	1.14
78		1	6.87	7.05	2.62	6.98	1.60
79		2	5.90	6.00	1.69	5.99	1.53
80		3	4.76	4.86	2.10	4.88	2.52
81		4	3.67	3.69	0.55	3.74	1.91
82		5	8.00	8.12	1.50	8.12	1.50
83		6	7.08	7.01	-0.99	7.04	-0.57
84	11	7	5.88	5.78	-1.70	5.84	-0.68
85		8	4.59	4.34	**-5.45**	4.43	-3.49
86		9	8.65	8.79	1.62	8.86	2.43
87		10	7.50	7.57	0.93	7.68	2.40

TABLE B-1: (CONTINUED)

S r N o	M o d e l	C a s e	S_t psi	S_{te} psi	P_{st} per cent	S_{te} psi	P_{st} per cent
				Brog. & Dolan Equations.		Log linear Equations.	
Pressure angle 14.5°							
88	11	11	6.35	6.35	0.00	6.47	1.89
89		12	5.12	5.01	-2.15	5.14	0.39
Absolute Maximum Error					5.42%		4.39%
Average Error					-0.11%		0.32%

APPENDIX C

GRAPHICAL METHOD TO GENERATE THE LAYOUT FOR AGMA TOOTH MODEL AND TO DETERMINE ITS LEWIS FORM FACTOR.

The graphical method is explained in four following sections.

(i) Generating The Tooth Layout

The principle of the graphical method to generate the tooth layout is same as that used in the generating method to manufacture the gears. Therefore it is important to know the basic principle of the generating method of producing the gear tooth. The principle is that if the dimensions of the generating rack of the tooth form are known, that tooth form can be generated. This generating rack has straight sided teeth, whose contour is used as the sharp cutting edges to remove the material from the gear blank. It reciprocates along the gear axis and is fed into the gear blank until the pitch circles are tangent. The gear blank rotates at constant angular velocity, while gear teeth are being generated. Thus the generating rack cuts the material as shown in **Figure C-1**.

Table C-1 shows the dimensions of the AGMA tooth model whose layout is graphically generated. The first step in generating the tooth layout is to prepare a template of the generating rack for the AGMA tooth model. This generating rack is shown in **Figure C-2**. The equipment needed to generate the tooth layout are listed in **Table C-2**. The following is the procedure, written with reference to **Figure C-3**, for cutting

124
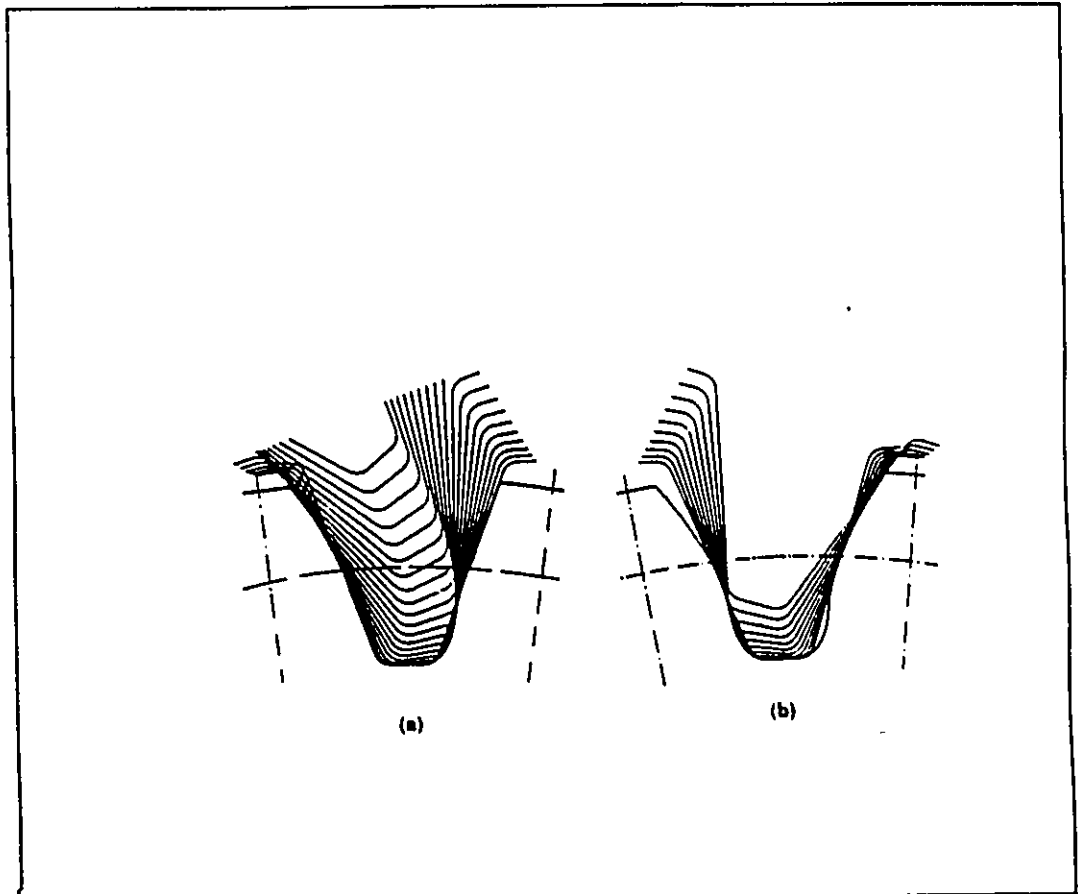
FIGURE C-1: GENERATING PROCESS
(a) CUTTER CUTS INVOLUTE SHAPE ON LEFT FLANK AS IT ENTERS.
(b) CUTTER CUTS INVOLUTE SHAPE ON RIGHT FLANK AS IT
    LEAVES.

125

TABLE C-1:   DIMENSIONS OF AGMA TOOTH MODEL.

Sr no.	m in.	N	ϕ deg.	a in.	b in.	r_t in.
1	1.18	20	20	1.18	1.48	0.354
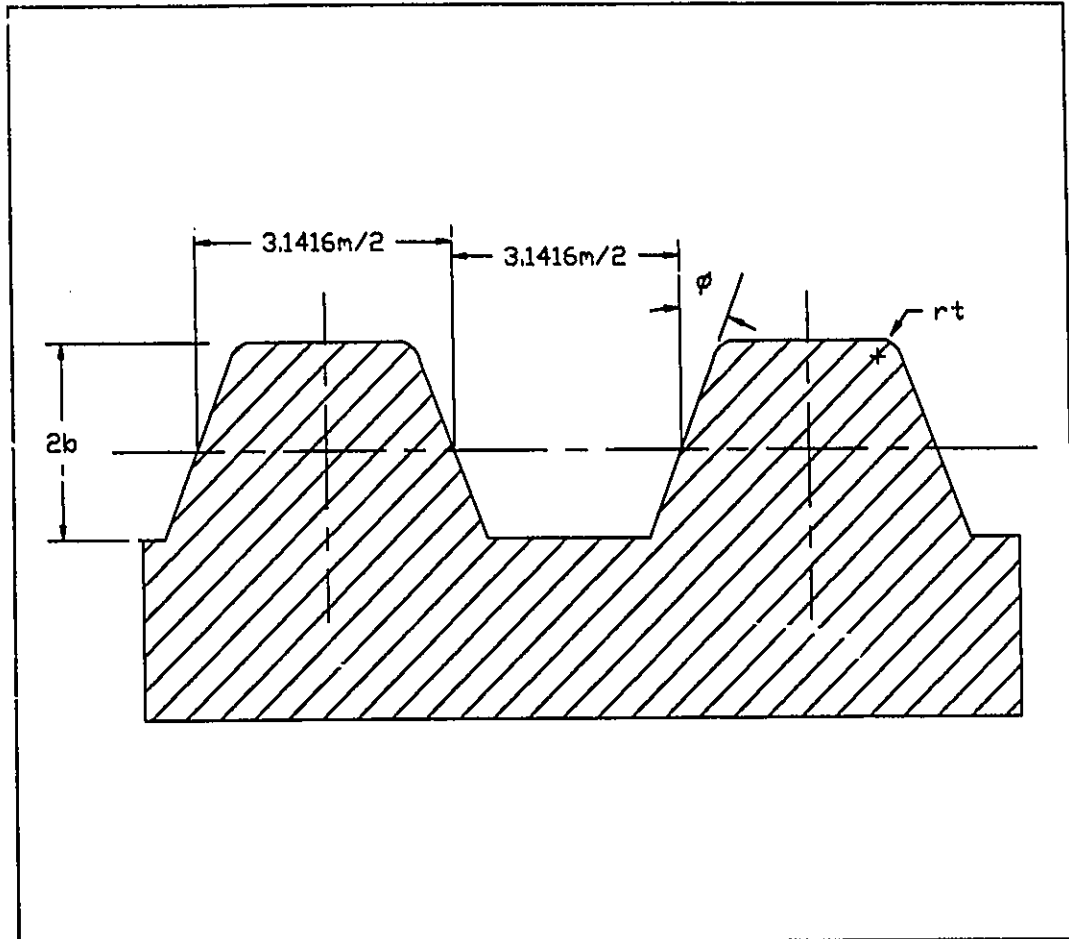
FIGURE C-2: GENERATING RACK FOR AGMA TOOTH MODEL

TABLE C-2 :   EQUIPMENT USED IN GRAPHICAL METHOD

Name Of Equipment	Qty	Size
Sheet of clear plastic	01	28" * 22"
Drawing paper (White)	01	28" * 22"
Engineering compass	01	15" radius
Sharp edge blade	01	-
Scale	01	Accuracy 1/64"
Sellotape	01	-
Set square	01	1 set
Divider	01	-
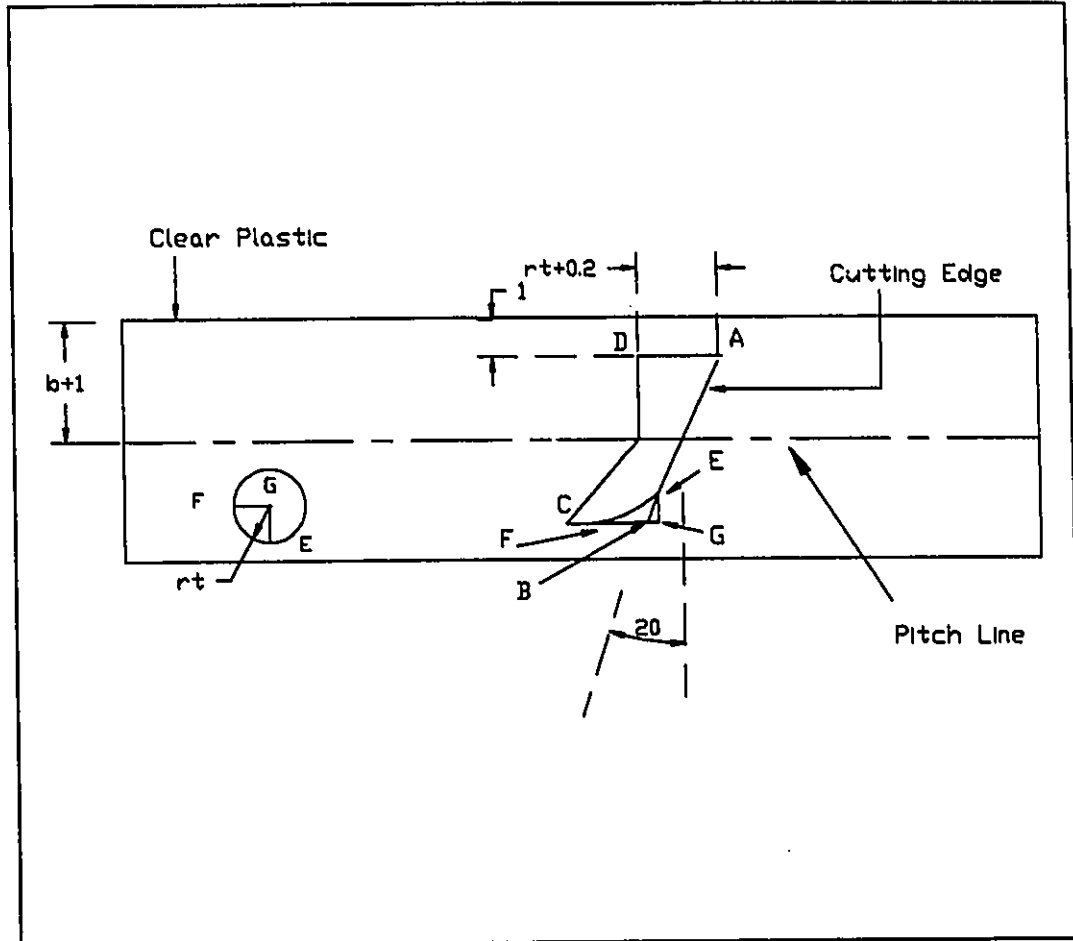
FIGURE C-3: DIMENSIONS OF A TEMPLATE FOR GENERATING RACK

the template for this model.

(1) A centre line is cut on the clear plastic with a sharp edge blade. This centre line is known as the pitch line of the generating rack. It is necessary to make sure that this pitch line should be slightly deep in the template so that it can be sensed by a finger tip, when the finger is moved on it.

(2) A line AB, at an angle equal to the pressure angle, is cut on the template. This line AB shows the cutting edge of the generating rack.

(3) Lines BC and AD, whose lengths must be atleast equal to the tool tip radius, are slightly cut on the template. The clear plastic of shape ABCD is deeply cut and then removed from the template.

(4) A circle of radius equal to the tool tip radius is slightly cut on the template. The tool tip radius in the shape of EFG is removed from the template and attached by a sellotape to the cutting edge of the template. It is essential to make sure that the point E and F of the tool tip radius are tangent to the cutting edge of the generating rack.

The second step is generating the tooth layout as shown in **Figure C-4**. A point O, near the lower edge of the drawing paper is selected as the centre of gear. The addendum circle, pitch circle, base circle and the dedendum circle of the tooth are drawn to scale from this centre. After constructing these circles, the pitch line of the template is kept on the pitch circle of the tooth in such a way that it is tangent to the

130

.
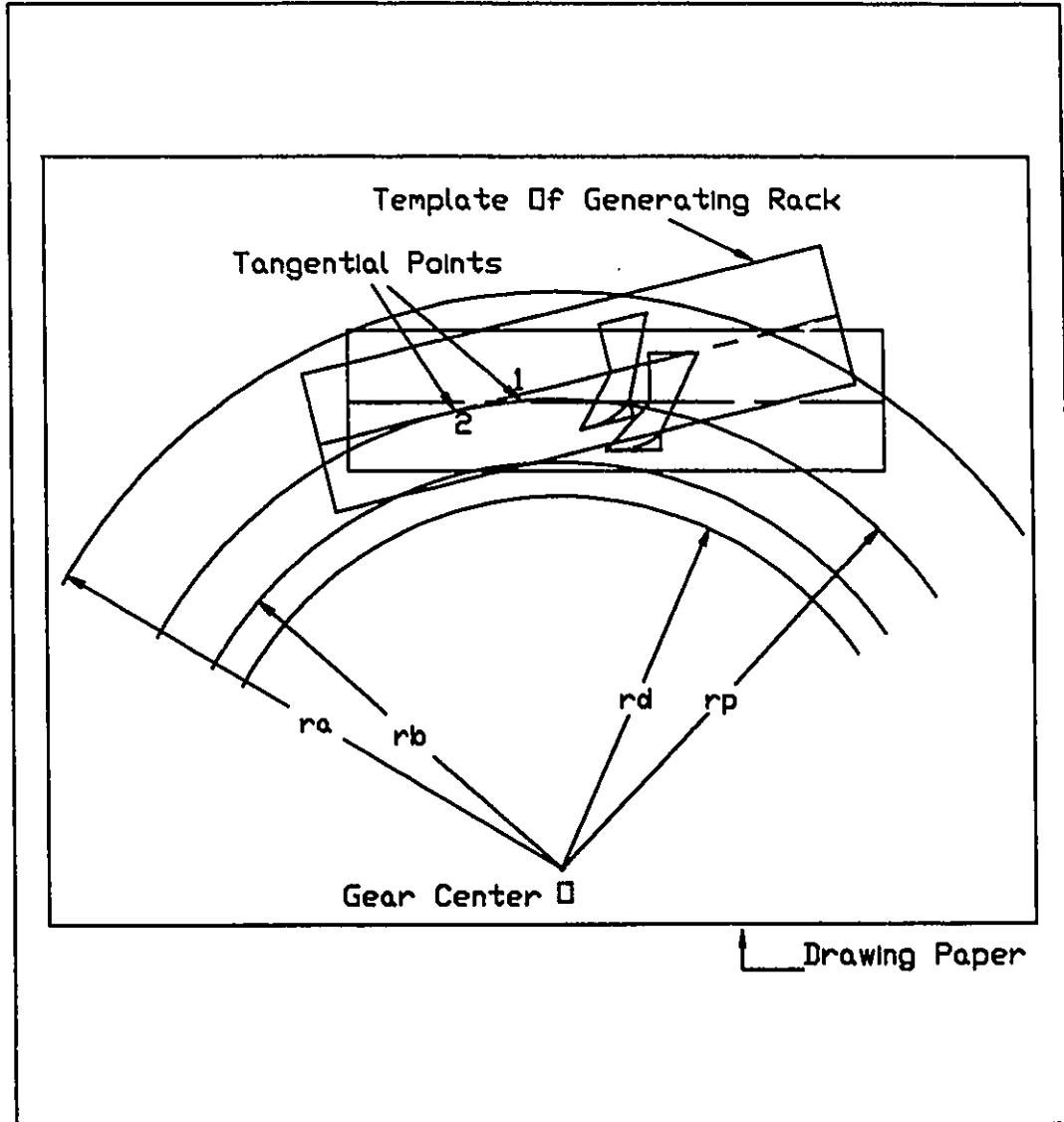
FIGURE C-4: CONSTRUCTION OF AN INVOLUTE TOOTH

pitch circle of the tooth at point 1. This point is marked on the drawing paper as well as on the template by poking the divider through the template. Holding the template in this position, a contour of the cutting edge of the template is drawn on the paper with a sharp pencil. Next the pitch line of the template is moved to the adjacent point 2 on the pitch circle of the tooth and is again made tangent to this point. Once again without displacing the template, the contour of the cutting edge is drawn in the same fashion as before. This process is continued until the root profile of the tooth layout becomes tangent to the dedendum circle.

(ii) Constructing The Tooth Axis:

In order to construct the tooth axis, the chordal tooth thickness for this model is determined by using the equation C-1. A line PQ, whose length is equal to this chordial tooth thickness, is drawn in the layout as shown in **Figure C-5**. The tooth axis OO_1 is then drawn passing through the point Q.

$$PQ = r_p * \sin\left(\frac{90}{N}\right) \quad ----------(C-1)$$

(iii) Constructing The Load Line:

The Lewis bending stress equation 2.1 is derived based on the assumption that the maximum load is exerted at the tip of tooth. Therefore the position of the load is assumed to be at the tip of the tooth for this AGMA tooth model in order to draw the load line. The load line for this model is constructed by drawing a line B_1B_2, tangent to the base circle
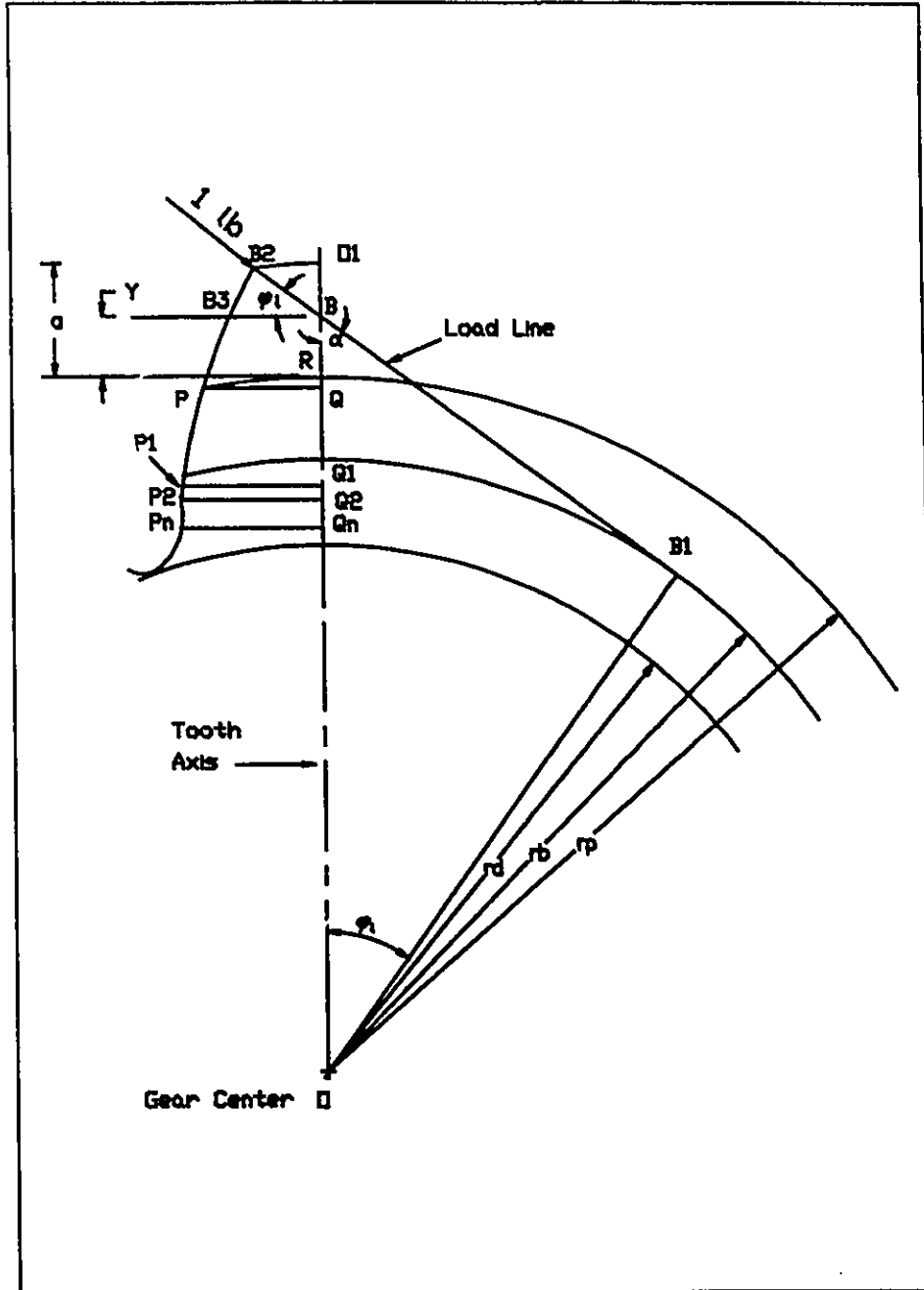
FIGURE C-5: CONSTRUCTION OF LOAD LINE AND TOOTH AXIS

from the tip of the tooth. Then the intersection of the load line and the tooth axis is located at the point B.

(iv) Determining The Lewis Form Factor For AGMA Tooth Model.

Lewis form factor(Y_i) is derived from the Lewis x-factor determined at the location of the Lewis weakest section. Therefore at first, it is necessary to determine the Lewis x-factor and the dimensions of the Lewis weakest section from the following Lewis equation of the bending stress.

$$S_1 = \frac{6 * P_{ta} * h}{F * t^2}$$

$$S_1 = \frac{3 * P_{ta}}{2 * F * ((\frac{t}{2})^2 / h)} \quad \text{----------} (C-2)$$

Investigating the equation C-2, it can be observed that, for constant loading condition (magnitude and direction) and face width of a gear tooth, the Lewis bending stress is dependent only on the $(t/2)^2/h$ - ratio of the dimensions of the Lewis weakest section. This ratio is called x-factor. This equation also indicates that the Lewis bending stress is maximum, when the value of this x-factor is minimum. This minimum value of the x-factor is called Lewis x-factor. Hence the tooth section corresponding to the location, where this Lewis x-factor is found in the root profile, should be the weakest section of the tooth. This weakest section is called Lewis weakest section. Using this theory of minimum x-factor, the Lewis weakest section for AGMA tooth model is graphically determined by the method as described below.

134

Points such as Q_1, Q_2 .... Q_n are arbitrarily selected on the tooth axis between the base circle and the dedendum circle as shown in **Figure C-5**. These points represent the locations where the tooth thickness and the load height are to be measured. Perpendiculars to the tooth axis such as P_1Q_1, P_2Q_2.........P_nQ_n are then drawn from each location by using a set square. Since the distance of each location from the point B and the length of each perpendicular represent the load height and the half tooth thickness respectively for each location, this load height and half tooth thickness are then measured. Thus dimensions required to determine the x-factor at each location are obtained. **Figure C-6** shows the involute tooth layout generated by this graphical method and **Table C-3** indicates the values of the load height and half tooth thickness measured at each shown location in the tooth layout. The following shows an equation to calculate the x-factor at various locations.

$$X = \frac{(\frac{t}{2})^2}{h} \text{------------(C-3)}$$

The minimum value of the x-factor (Lewis x-factor) is then sought from these x-factors, calculated at various locations of the tooth profile.

Based on this Lewis x-factor, the Lewis form factor for AGMA tooth model is determined by using equation C-4 and this value of Lewis form factor is compared with that given by AGMA.

135
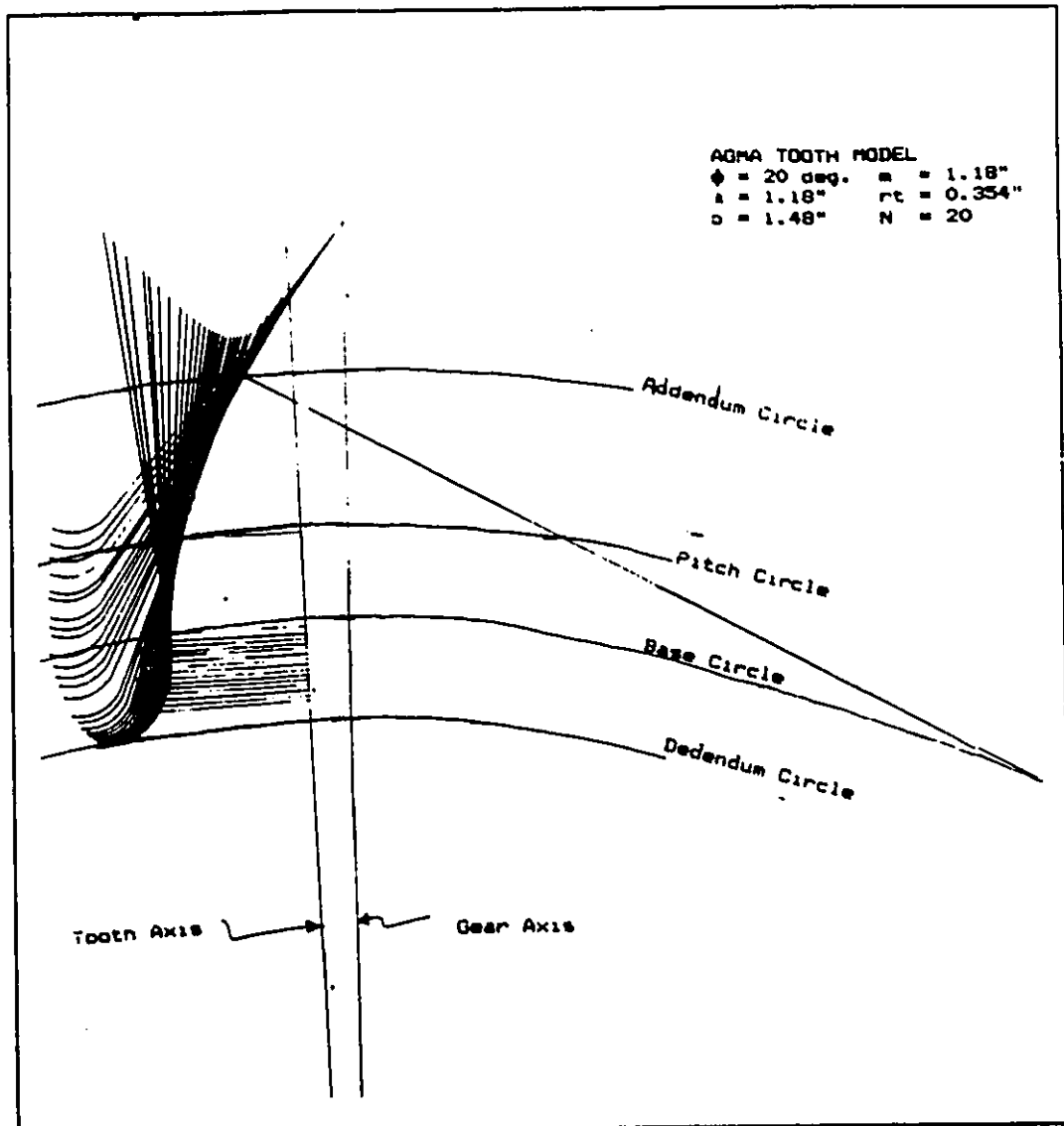
FIGURE C-6: GRAPHICAL INVOLUTE TOOTH LAYOUT FOR AGMA TOOTH MODEL.

TABLE C-3: GRAPHICAL LOAD HEIGHT, HALF TOOTH
THICKNESS AND LEWIS X-FACTOR AT
VARIOUS LOCATIONS FOR AGMA TOOTH MODEL

Sr. No.	h in.	t/2 in.	$X=(t/2)^2/h$ in.
1	1.7716	1.0391	0.6094
2	1.8811	1.0391	0.5962
3	1.8504	1.0430	0.5879
4	1.8898	1.0391	0.5713
5	1.9291	1.0469	0.5681
6	1.9685	1.0469	0.5567
7	2.0078	1.0546	0.5540
8	2.0472	1.0625	0.5514
9	2.0866	1.0664	0.5450
10	2.1260	1.0781	0.5467
11	2.1654	1.0938	0.5525
12	2.2047	1.1094	0.5582

$$Y = \frac{2 * X * P_d}{3} \quad \text{----------}\ (C-4)$$

APPENDIX D

ANALYTICAL METHOD TO DETERMINE INVOLUTE TOOTH THICKNESS

In standard proportion gear tooth design, the value of the tooth thickness at the pitch circle, pitch radius and involute of the pressure angle is generally known to determine the tooth thickness constant (C_i). The equation to determine this tooth thickness constant is written in section 1.3.6

In order to determine the tooth thickness at some other points such as point I located at any radius r as shown in **Figure 1.4** on the involute profile of the tooth, the tooth thickness constant is equated to the sum of the half tooth thickness angle (β) and the involute of pressure angle ($Inv(\phi)$) corresponding to this point I.

$$C_i = \beta + Inv(\phi)$$

Substituting the value of angle beta and solving for T_r, tooth thickness at the radius r can be determined as follows.

$$T_r = 2r * (C_i - Inv(\phi))$$

$$T_r = 2r * [C_i - \tan(\arccos(\frac{r_b}{r})) + \arccos(\frac{r_b}{r})] \quad \text{---- (D-1)}$$

Subsequently, tooth thickness at the tip and the base is determined by using the value of r_a and r_b in place of r in equation D-1.

APPENDIX E

141

```
C                    GETSCO20 - PROGRAM LISTINGS
C     THIS PROGRAM READS THE BROGHAMER AND DOLAN DATA, SUCH AS
C     MINIMUM FILLET RADIUS(RF), LOAD HEIGHT(H), TOOTH
C     THICKNESS(T) AND EXPERIMENTAL TENSILE STRESS(ST), OF 35
C     CASES OF THE TOOTH MODEL 6 TO 8 FROM THE DATA FILE
C     (GETSCO20.DAT), AND DETERMINES THE VARIABLES
C     (K, T/RF & T/H) FOR EACH CASE. THE VALUES OF THESE
C     VARIABLES ARE ADDED TO OBTAIN THE MATRIX A(3,3) AND
C     ARRAY B(3) DEFINED AS BELOW. THIS MATRIX AND ARRAY IS
C     THEN SOLVED BY GAUSSIAN ELIMINATION TO DETERMINE THE
C     CONSTANTS-C1, C2 AND C3 FOR THE LOG LINEAR EQUATION OF
C     20 PRESSURE ANGLE TEETH.
C     *****************************************************************
C     *                      LIST OF VARIABLES                       *
C     *****************************************************************
C     RF    - MINIMUM FILLET RADIUS
C     H     - LOAD HEIGHT AS DETERMINED BY BROGHAMER AND DOLAN
C      T     - TOOTH THICKNESS AS DETERMINED BY BROGHAMER AND
C             DOLAN
C     ST    - EXPERIMENTAL MAXIMUM TENSILE STRESS AS DETERMINED
C              BY BROGHAMER AND DOLAN.
C     AL    - LOAD ANGLE AS DETERMINED BY BROGHAMER AND DOLAN
C     LOAD  - APPLIED LOAD ON THE GEAR TOOTH DURING EXPERIMENTS
C     WIDTH - WIDTH OF THE GEAR TOOTH
C     SL    - BENDING STRESS OF THE GEAR TOOTH
C     SA    - DIRECT COMPRESSIVE STRESS OF THE GEAR TOOTH
```

```
C      NSTRES - NOMINAL TENSILE STRESS OF THE GEAR TOOTH
C      K       - BENDING STRESS CONCENTRATION FACTOR FOR TENSILE
C                  FILLET=ST/NSTRES
C      A(3,3)   - MATRIX DEFINED AS FOLLOWS FOR THE EQUATION 4.3
C                  (PAGE- NUMBER 30)
C
C                  | N         X1S        X2S |
C
C      A(3,3) =    | X1S       QS         PS  |    =
C
C                  | X2S       PS         RS  |
C
C
C
```

$$
A(3,3) =
\begin{vmatrix}
35 & \sum_{i=1}^{N} LOG(t/r_t) & \sum_{i=1}^{N} LOG(t/h) \\
\sum_{i=1}^{N} LOG(t/r_t) & \sum_{i=1}^{N} LOG(t/r_t)^2 & \sum_{i=1}^{N} \{LOG(t/r_t) * LOG(t/h)\} \\
\sum_{i=1}^{N} LOG(t/h) & \sum_{i=1}^{N} \{LOG(t/r_t) * LOG(t/h)\} & \sum_{i=1}^{N} LOG(t/h)^2
\end{vmatrix}
$$

```
C
C
C
C
C
```

```
C     B(3)      - ARRAY DEFINED AS FOLLOWS FOR THE EQUATION 4.3
C                 (PAGE NUMBER 30)
C
```
$$
B(3) = \begin{vmatrix} YS \\ \\ R1KS \\ \\ R2KS \end{vmatrix} = \begin{vmatrix} \sum\limits_{i=1}^{N} LOG(K) \\ \sum\limits_{i=1}^{N} LOG(K)*LOG(t/r_i) \\ \sum\limits_{i=1}^{N} LOG(K)*LOG(t/h) \end{vmatrix}
$$
```
C
C     IROW      - NUMBER OF ROWS.
C     ICOL      - NUMBER OF COLUMNS
C     PIVOT     - PIVOTED ELEMENT OF THE EQUATION MATRIX
C     ************************************************************
C     *              DECLARATION OF STATEMENTS                  *
C     ************************************************************
      REAL RF(35),H(35),T(35),SL(35),ST(35),K(35),AL(35),
     +  A(3,3),B(3),DET,PIVOT,FACTOR,NSTRES(35),SA(35)
      INTEGER WIDTH
C     ************************************************************
C     * OPEN UP AND READ IN DATA FROM FILE (GETSCO20.DAT)       *
C     ************************************************************
      OPEN(UNIT=11,FILE='GETSCO20.DAT',STATUS='OLD')
      OPEN(UNIT=10,FILE='EQN20.OUT',STATUS='NEW')
```

```
        READ(11,4)(RF(I),I=1,35)

        READ(11,4)(H(I),I=1,35)

        READ(11,4)(T(I),I=1,35)

        READ(11,6)(ST(I),I=1,35)

        READ(11,7)(AL(I),I=1,35)

8       FORMAT(12(I2,1X)/12(I2,1X)/11(I2,1X))

9       FORMAT(12(F4.2,1X)/12(F4.2,1X)/11(F4.2,1X))

4       FORMAT(12(F5.3,1X)/12(F5.3,1X)/11(F5.3,1X))

7       FORMAT(11(F6.3,1X)/11(F6.3,1X)/11(F6.3,1X)/3(F6.3,1X))

6       FORMAT(12(F4.2,1X)/12(F4.2,1X)/11(F4.2,1X))

5       FORMAT(12(F5.2,1X)/12(F5.2,1X)/12(F5.2,1X))

C       ****************************************************

C       * ASSIGNING THE VALUE FOR LOAD AND WIDTH OF THE GEAR  *

C       * TOOTH                                              *

C       ****************************************************

        PI=3.1416

        LOAD=1

        WIDTH=1

C       ****************************************************

C       * INITIALIZATION OF ELEMENTS OF THE MATRIX-A(3,3) AND  *

C       * ARRAY B(3)                                         *

C       ****************************************************

        X1S=0.0

        X2S=0.0

        YS=0.0

        PS=0.0
```

```
      QS=0.0

      RS=0.0

      R1KS=0.0

      R2KS=0.0
C     ********************************************************
C     * DETERMINATICN OF ELEMENTS OF THE MATRIX-A(3,3) AND   *
C     * ARRAY B(3)                                           *
C     ********************************************************
      DO 11 I=1,35
            SL(I)=6.0*LOAD*COS((AL(I)*PI/180))*H(I)
     +      /(WIDTH*(T(I)**2))
            SA(I)=LOAD*SIN((AL(I)*PI/180))/(WIDTH*T(I))
            NSTRES(I)=SL(I)-SA(I)
            K(I)= ST(I)/NSTRES(I)
            X1S=X1S+ALOG10(T(I)/RF(I))
            X2S=X2S+ALOG10(T(I)/H(I))
            YS=YS+ALOG10(K(I))
            PS=PS+(ALOG10(T(I)/RF(I))*ALOG10(T(I)/H(I)))
            QS=QS+((ALOG1C(T(I)/RF(I)))**2)
            RS=RS+((ALOG10(T(I)/H(I)))**2)
            R1KS=R1KS+(ALOG10(K(I))*ALOG10(T(I)/RF(I)))
            R2KS=R2KS+(ALOG10(K(I))*ALOG10(T(I)/H(I)))
11          CONTINUE
```

```
C     *******************************************************
C     * ASSIGNING VALUES TO ELEMENTS OF THE MATRIX A(3,3) AND*
C     * ARRAY B(3)                                           *
C     *******************************************************
      A(1,1)=35.0
      A(1,2)=X1S
      A(1,3)=X2S
      A(2,1)=X1S
      A(2,2)=QS
      A(2,3)=PS
      A(3,1)=X2S
      A(3,2)=PS
      A(3,3)=RS
      B(1)=YS
      B(2)=R1KS
      B(3)=R2KS
C     *******************************************************
C     * WRITING MATRIX-A(3,3) AND ARRAY-B(3) FOR 20 DEG.    *
C     * PRESSURE ANGLE TEETH TO THE FILE (EQN20.OUT).       *
C     *******************************************************
      WRITE(10,40)
40    FORMAT('0','MATRIX A(3,3)',T53,'ARRAY B(3)')
      DO 26 I=1,3
      WRITE(10,27)(A(I,J),J=1,3),B(I)
27    FORMAT('0 ',5X,(3(F10.7,5X)), T54,F10.7)
26    CONTINUE
```

```
C       *******************************************************
C       * DETERMINING THE CONSTANTS-C1, C2 AND C3 FOR LOG    *
C       * LINEAR EQUATION BY GAUSSIAN ELIMINATION FOR 20 DEG. *
C       * PRESSURE ANGLE TEETH                                *
C       *******************************************************
C       * PIVOTING THE ELEMENT OF MATRIX A(3,3)              *
C       *******************************************************
        DET=1.0
        DO 30 IPV=1,3
              PIVOT=A(IPV,IPV)
              DET=DET*PIVOT
C       *******************************************************
C       * NORMALIZING THE PIVOTED ROW.                       *
C       *******************************************************
              DO 31 J=1,3
                    A(IPV,J)=A(IPV,J)/PIVOT
31            CONTINUE
              B(IPV)=B(IPV)/PIVOT
C       *******************************************************
C       * ELIMINATION OF NON PIVOTED ROWS.                   *
C       *******************************************************
              DO 32 IROW=1,3
                    IF(IROW .NE.IPV) THEN
                          FACTOR=A(IROW,IPV)/A(IPV,IPV)
                    DO 33 ICOL=1,3
```

```
        A(IROW,ICOL)=A(IROW,ICOL)-(FACTOR*A(IPV,ICOL))

33      CONTINUE

        B(IROW) = B(IROW) - (FACTOR * B(IPV))

            ENDIF

32      CONTINUE

30      CONTINUE

C       ****************************************************
C       * WRITING CONSTANTS-C1, C2 & C3 TO THE FILE (EQN20.OUT)*
C       * FOR 20 DEG. PRESSURE ANGLE TEETH                  *
C       ****************************************************
        WRITE(10,35)(B(I),I=1,3)

35      FORMAT('0 ','LOGC1=',F6.3,5X,'C2=',F6.3,5X,'C3=',F6.3)

        C1=10**(B(1))

        WRITE(10,36) C1

36      FORMAT('0','C1=',F6.3)

        CLOSE(10)

        CLOSE(11)

        STOP

        END
```

```
C                       GETSCO14.5 - PROGRAM LISTINGS

C    THIS PROGRAM READS THE BROGHAMER AND DOLAN DATA, SUCH AS

C    MINIMUM FILLET RADIUS(RF), LOAD HEIGHT(H), TOOTH

C    THICKNESS(T) AND EXPERIMENTAL TENSILE STRESS(ST), OF 54

C    CASES OF THE TOOTH MODEL[2] 3 to 5 and 9 to 11  FROM THE

C    DATA FILE (GETSCO14.DAT), AND DETERMINES THE VARIABLES

C    (K, T/RF & T/H) FOR EACH CASE. THE VALUES OF THESE

C    VARIABLES ARE ADDED TO OBTAIN THE MATRIX A(3,3) AND

C    ARRAY B(3) DEFINED AS BELOW. THIS MATRIX AND ARRAY IS

C    THEN SOLVED BY GAUSSIAN ELIMINATION TO DETERMINE THE

C    CONSTANTS-C1, C2 AND C3 FOR THE LOG LINEAR EQUATION OF

C    14.5 PRESSURE ANGLE TEETH.

C    *****************************************************

C    *                  LIST OF VARIABLES                *

C    *****************************************************

C    RF   - MINIMUM FILLET RADIUS

C    H    - LOAD HEIGHT AS DETERMINED BY BROGHAMER AND DOLAN

C    T    - TOOTH THICKNESS AS DETERMINED BY BROGHAMER AND

C             DOLAN

C    ST   - EXPERIMENTAL MAXIMUM TENSILE STRESS OF THE GEAR

C             TOOTH AS DETERMINED BY BROGHAMER AND DOLAN

C    AL   - LOAD ANGLE AS DETERMINED BY BROGHAMER AND DOLAN

C    LOAD - APPLIED LOAD ON THE GEAR TOOTH DURING EXPERIMENTS

C    WIDTH - WIDTH OF THE GEAR TOOTH

C    SL   - BENDING STRESS OF THE GEAR TOOTH

C    SA   - DIRECT COMPRESSIVE STRESS OF THE GEAR TOOTH
```

150

```
C      NSTRES - NOMINAL TENSILE STRESS OF THE GEAR TOOTH

C      K       - BENDING STRESS CONCENTRATION FACTOR FOR TENSILE

C                  FILLET=ST/NSTRES

C      A(3,3)  - MATRIX DEFINED AS FOLLOWS FOR THE EQUATION 4.3

C                  (PAGE- NUMBER 30)

C

C                  | N          X1S         X2S  |

C

C      A(3,3) =    | X1S        QS          PS   |        =

C

C                  | X2S        PS          RS   |

C
```

```
C

C

C

C

C
```

151

```
C     B(3)     - ARRAY DEFINED AS FOLLOWS FOR THE EQUATION 4.3
C                  (PAGE NUMBER 30)
C
```

$$
B(3) = \begin{vmatrix} YS \\ R1KS \\ R2KS \end{vmatrix} = \begin{vmatrix} \sum_{i=1}^{N} LOG(K) \\ \sum_{i=1}^{N} LOG(K)*LOG(t/r_i) \\ \sum_{i=1}^{N} LOG(K)*LOG(t/h) \end{vmatrix}
$$

```
C
C     IROW     - NUMBER OF ROWS.
C     ICOL     - NUMBER OF COLUMNS
C     PIVOT    - PIVOTED ELEMENT OF THE EQUATION MATRIX
C     ********************************************************
C     *            DECLARATION OF STATEMENTS                *
C     ********************************************************
      REAL RF(54),H(54),T(54),SL(54),ST(54),K(54),AL(54),
   +  A(3,3), B(3),DET,PIVOT, FACTOR,NSTRES(54), SA(54),
      INTEGER WIDTH
C     ********************************************************
C     * OPEN UP AND READ IN DATA FROM FILE (GETSCO14.DAT)   *
C     ********************************************************
      OPEN(UNIT=11,FILE='GETSCO14.DAT',STATUS='OLD')
      OPEN(UNIT=10,FILE='EQN14.OUT',STATUS='NEW')
```

```
      READ(11,4)(RF(I),I=1,54)

      READ(11,5)(H(I),I=1,54)

      READ(11,5)(T(I),I=1,54)

      READ(11,6)(ST(I),I=1,54)

      READ(11,7)(AL(I),I=1,54)

4     FORMAT(11(F6.4,1X)/11(F6.4,1X)/11(F6.4,1X)/11(F6.4,1X)

+     /11(F6.4,1X)/5(F6.4,1X))

5     FORMAT(12(F5.3,1X)/12(F5.3,1X)/12(F5.3,1X)/12(F5.3,1X)

+     /12(F5.3,1X))

7     FORMAT(11(F6.3,1X)/11(F6.3,1X)/11(F6.3,1X)/11(F6.3,1X)

+     /11(F6.3,1X)/5(F6.3,1X))

6     FORMAT(12(F5.2,1X)/12(F5.2,1X)/12(F5.2,1X)/12(F5.2,1X)

+     /12(F5.2,1X))C

C     ********************************************************

C     * ASSIGNING THE VALUE FOR LOAD AND WIDTH OF THE GEAR  *

C     * TOOTH CASES                                         *

C     ********************************************************

      PI=3.1416

      LOAD=1

      WIDTH=1

C     ********************************************************

C     * INITIALIZATION OF ELEMENTS OF THE MATRIX-A(3,3) AND *

C     * ARRAY B(3)                                          *

C     ********************************************************

      X1S=0.0

      X2S=0.0
```

153

```fortran
      YS=0.0
      PS=0.0
      QS=0.0
      RS=0.0
      R1KS=0.0
      R2KS=0.0
C     *******************************************************
C     * DETERMINATION OF ELEMENTS OF THE MATRIX-A(3,3) AND   *
C     * ARRAY B(3)                                           *
C     ******************************************************
      DO 11 I=1,54
          SL(I)=6.0*LOAD*COS((AL(I)*PI/180))*H(I)
     +    /(WIDTH*(T(I)**2))
          SA(I)=LOAD*SIN((AL(I)*PI/180))/(WIDTH*T(I))
          NSTRES(I)=SL(I)-SA(I)
          K(I)= ST(I)/NSTRES(I)
          X1S=X1S+ALOG10(T(I)/RF(I))
          X2S=X2S+ALOG10(T(I)/H(I))
          YS=YS+ALOG10(K(I))
          PS=PS+(ALOG10(T(I)/RF(I))*ALOG10(T(I)/H(I)))
          QS=QS+((ALOG10(T(I)/RF(I)))**2)
          RS=RS+((ALOG10(T(I)/H(I)))**2)
          R1KS=R1KS+(ALOG10(K(I))*ALOG10(T(I)/RF(I)))
          R2KS=R2KS+(ALOG10(K(I))*ALOG10(T(I)/H(I)))
11    CONTINUE
```

154

```
C      *************************************************************
C      * ASSIGNING VALUES TO ELEMENTS OF THE MATRIX A(3,3) AND*
C      * ARRAY B(3)
C      *************************************************************
       A(1,1)=35.0
       A(1,2)=X1S
       A(1,3)=X2S
       A(2,1)=X1S
       A(2,2)=QS
       A(2,3)=PS
       A(3,1)=X2S
       A(3,2)=PS
       A(3,3)=RS
       B(1)=YS
       B(2)=R1KS
       B(3)=R2KS
C      *************************************************************
C      * WRITING MATRIX-A(3,3) AND ARRAY-B(3) FOR 14.5 DEG.   *
C      * PRESSURE ANGLE TEETH TO THE FILE (EQN14.OUT).        *
C      *************************************************************
       WRITE(10,40)
40     FORMAT('0','MATRIX A(3,3)',T53,'ARRAY B(3)')
       DO 26 I=1,3
          WRITE(10,27)(A(I,J),J=1,3),B(I)
27        FORMAT('0 ',5X,(3(F10.7,5X)), T54,F10.7)
26     CONTINUE
```

155

```
C     ********************************************************
C     * DETERMINING THE CONSTANTS-C1, C2 AND C3 FOR LOG       *
C     * LINEAR EQUATION BY GAUSSIAN ELIMINATION FOR 14.5 DEG. *
C     * PRESSURE ANGLE TEETH                                  *
C     ********************************************************
C     * PIVOTING THE ELEMENT OF MATRIX A(3,3)                 *
C     ********************************************************
      DET=1.0
      DO 30 IPV=1,3
              PIVOT=A(IPV,IPV)
              DET=DET*PIVOT
C     ********************************************************
C     * NORMALIZING THE PIVOTED ROW.                          *
C     ********************************************************
      DO 31 J=1,3
              A(IPV,J)=A(IPV,J)/PIVOT
31    CONTINUE
              B(IPV)=B(IPV)/PIVOT
C     ********************************************************
C     * ELIMINATION OF NON PIVOTED ROWS.                      *
C     ********************************************************
      DO 32 IROW=1,3
              IF(IROW .NE.IPV) THEN
                      FACTOR=A(IROW,IPV)/A(IPV,IPV)
      DO 33 ICOL=1,3
        A(IROW,ICOL)=A(IROW,ICOL)-(FACTOR*A(IPV,ICOL))
```

```fortran
33      CONTINUE
            B(IROW) = B(IROW) - (FACTOR * B(IPV))
                ENDIF
32    CONTINUE
30    CONTINUE
C     ************************************************************
C     * WRITING CONSTANTS-C1, C2 & C3 TO THE FILE (EQN14.OUT)*
C     * FOR 14.5 DEG. PRESSURE ANGLE TEETH                  '
C     ************************************************************
      WRITE(10,35)(B(I),I=1,3)
35    FORMAT('0 ','LOGC1=',F6.3,5X,'C2=',F6.3,5X,'C3=',F6.3)
      C1=10**(B(1))
      WRITE(10,36) C1
36    FORMAT('0','C1=',F6.3)
      CLOSE(10)
      CLOSE(11)
      STOP
      END
```

DATA FILES FOR GETSCO20 AND GETSCO14.5 PROGRAMMES

Data File for 20 deg. pressure angle teeth.

****

VALUES OF RF (Minimum Fillet Radius):

0.274 0.274 0.274 0.274 0.189 0.189 0.189 0.189 0.110 0.110

0.110 0.110 0.277 0.277 0.277 0.277 0.170 0.170 0.170 0.170

0.106 0.106 0.106 0.106 0.275 0.275 0.275 0.275 0.158 0.158

0.158 0.158 0.090 0.090 0.090

VALUES OF H (Load Height Measured At Lewis Weakest Section):

0.728 0.596 0.472 0.341 0.797 0.650 0.505 0.379 0.826 0.677

0.538 0.405 0.711 0.577 0.451 0.333 0.757 0.615 0.494 0.362

0.791 0.667 0.522 0.388 0.744 0.602 0.460 0.363 0.820 0.658

0.527 0.398 0.882 0.719 0.573

VALUES OF T (Tooth Thickness Measured At Lewis Weakest Section):

0.922 0.922 0.934 0.984 0.912 0.917 0.922 0.928 0.894 0.900

0.911 0.916 1.018 1.028 1.043 1.078 1.015 1.028 1.044 1.067

0.995 1.018 1.022 1.040 1.078 1.084 1.090 1.147 1.095 1.101

1.113 1.125 1.118 1.118 1.122

VALUES OF ST (Maximum Experimental Tensile Stress):

6.12 5.75 4.81 3.92 7.12 6.50 5.50 4.72 8.40 7.40 6.25 5.25

5.35 4.75 3.92 3.22 6.30 5.34 4.51 3.54 7.00 6.25 5.27 4.20

5.17 4.40 3.60 2.75 5.95 5.09 4.42 3.40 6.50 5.91 4.86

VALUES OF AL (Load Angles):

28.000 22.666 21.333 15.000 28.000 22.666 21.333 15.000 28.000

22.666 21.333 15.000 22.666 20.333 18.833 17.833 22.666 20.333

18.833 17.833 22.666 20.333 18.833 17.833 22.500 21.333 20.666

20.000 22.500 21.333 20.666 20.000 22.500 21.333 20.666

Data File for 14.5 deg. pressure angle teeth:

****

VALUES OF RF (Minimum Fillet Radius):

0.3170 0.3170 0.3170 0.3170 0.1660 0.1660 0.1660 0.1660 0.1105

0.1105 0.1105 0.1105 0.2760 0.2760 0.2760 0.2760 0.1700 0.1700

0.1700 0.1700 0.1320 0.1320 0.1320 0.1320 0.2900 0.2900 0.2900

0.2900 0.1880 0.1880 0.1880 0.1880 0.1260 0.1260 0.1260 0.1260

0.2530 0.2530 0.2530 0.1610 0.1610 0.1610 0.2650 0.2650 0.2650

0.1620 0.1620 0.1620 0.2700 0.2700 0.2700 0.1630 0.1630 0.1630

VALUES OF H (Load Height Measured at Lewis weakest Section):

0.718 0.568 0.448 0.331 0.801 0.641 0.507 0.371 0.840 0.674

0.541 0.408 0.716 0.572 0.471 0.344 0.794 0.638 0.516 0.393

0.812 0.685 0.544 0.398 0.707 0.584 0.460 0.326 0.741 0.635

0.493 0.359 0.803 0.657 0.522 0.393 0.767 0.614 0.431 0.845

0.652 0.479 0.797 0.629 0.434 0.845 0.647 0.488 0.790 0.639

0.472 0.867 0.690 0.509

VALUES OF T (Tooth Thickness Measured at Lewis Weakest Section):

0.840 0.859 0.870 0.900 0.828 0.834 0.840 0.855 0.828 0.834

0.850 0.862 0.894 0.911 0.944 0.977 0.888 0.894 0.916 0.927

0.862 0.875 0.886 0.893 0.944 0.960 0.988 0.994 0.926 0.949

0.960 0.989 0.954 0.960 0.972 0.988 0.824 0.854 0.868 0.798

0.812 0.842 0.934 0.955 0.967 0.903 0.908 0.944 1.024 1.048

1.069 1.010 1.015 1.030

VALUES OF ST (Maximum Experimental Tensile Stress):

08.08 06.65 05.54 04.50 10.32 08.80 07.52 06.22 11.20 09.50

08.09 07.00 07.35 06.35 05.12 04.23 09.20 07.73 06.45 05.61

10.01 08.52 07.27 06.15 06.87 05.30 04.76 03.67 08.00 07.08

05.88 04.59 08.65 07.50 06.35 05.12 08.52 07.34 05.90 10.01

09.04 07.35 07.19 05.87 04.95 08.48 07.23 06.01 06.06 05.10

04.51 07.40 06.30 05.45

VALUES OF AL (Load Angles)

20.000 18.500 16.333 09.000 20.000 18.500 16.333 09.000 20.000

18.500 16.333 09.000 18.000 17.500 17.000 11.333 18.000 17.500

17.000 11.333 18.000 17.500 17.000 11.333 15.666 15.333 14.500

14.500 15.666 16.333 14.500 14.500 15.666 15.333 14.500 14.500

25.500 16.333 10.666 25.500 16.333 10.666 24.666 21.333 15.666

24.666 21.333 15.666 25.833 23.666 17.333 25.833 23.666 17.333

VITA AUCTORIS

1961   Born in Bharuch, Gujrat, India

1979   Received Higher Secondary Diploma from The New Progressive High School, Mehsana, Gujrat, India.

1983   Received the degree of Bachelor of Engineering in Mechanical Engineering from University of Gujrat, Ahmedabad, Gujrat, India.

1988   Received Post Graduate Diploma in Computer Aided Engineering Management from George Brown College, Toronto, Ontario, Canada.

1992   Currently a candidate for the degree of Master of Applied Science In Mechanical Engineering at the University of Windsor, Ontario, Canada.